ADDIS ABABA UNIVERSITY

ADDIS ABABA INSTITUTE OF TECHNOLOGY

SCHOOL OF CHEMICAL AND BIO ENGINEERING

Extraction, Characterization, and Optimization of Cellulose Nanocrystals from Corncob

Getahun Esubalew Demewoz

A Thesis Submitted to Addis Ababa University, Institute of Technology, in Partial Fulfilment of the Requirement for the Degree of Masters of Science in Chemical Engineering (Process Engineering)

Addis Ababa, Ethiopia

October, 2020

Addis Ababa University

Addis Ababa Institute of Technology

School of Chemical and Bio Engineering

This is to certify that the thesis prepared by Getahun Esubalew entitled: **Extraction, characterization, and optimization of cellulose nanocrystals from corncob** and submitted in partial fulfillment of the requirements for the degree of masters of sciences (chemical and bioengineering) complies with the regulations of the university and meet the accepted standards with respect to originality and quality.

Approved by the Examining Committee:

Dr. Hundessa Dessalegn		
Advisor	Signature	Date
Dr. Shegaw Ahmed		
Internal Examiner	Signature	Date
Dr Ing. Nurelegne Tefera		
External Examiner	Signature	Date
Chairperson	Signature	Date

DECLARATION

I declare this thesis work entitled **"Extraction, Characterization, and Optimization of Cellulose Nanocrystals from Corncob"** submitted for the requirement for a master's degree at Addis Ababa University is my own work. To the best of my knowledge, no work of this type has been reported on the above subject and has not been presented for the award of a degree in any university. All the work presented in this research work is original and in which references have been made, it has been distinctly indicated.

Getahun Esubalew Demewoz

Signature_____

Date of submission_____

ABSTRACT

In this study cellulose nanocrystals were extracted from corncob by the method of sulfuric acid hydrolysis, followed by separation using centrifugation, dialysis, and ultrasonication with the objective of achieving maximum yield. The maximum yield (41.8%) of cellulose nanocrystal was found at the parameter interaction of 65wt.% sulfuric acid concentration,45℃ reaction temperature, and 60 minutes of hydrolysis time. The effect of process parameters (acid concentration, temperature, and hydrolysis time) on the yield of cellulose nanocrystals was optimized using response surface methodology(RSM) and gave 41.74% of cellulose nanocrystals yield with the sulfuric acid concentration 61.66wt.%, the reaction temperature 45℃, and the hydrolysis time 59. 92minutes.The experimental yield was 40.94±0.25% after doing triple experiments using the optimal conditions are acid concentration (61.66wt.%), reaction time (59.93 min), and temperature (45℃). The size and surface morphology of cellulose nanocrystals were characterized by particle size analyzer and scanning electron microscopy respectively. Fourier transform infrared showed that the structural change occurs by the chemical treatments (by alkaline treatment and bleaching) due to most of the lignin and hemicellulose were removed from the raw corncob. The result reveals Cellulose nanocrystals prepared from the hydrolysis of the isolated cellulose in the sulfuric acid had needle-shaped morphology, an average length of 170.3nm, and a crystallinity index of 79.3%. The crystallinity index obtained from x-ray diffraction for cellulose nanocrystal was found higher than extracted cellulose with a value of 79.3% and 76.4% respectively.Thermal stability by thermogravimetric analysis showed that the degradation temperature of the cellulose nanocrystals reached around 327℃, which was higher than that of the raw corncob and extracted corncob cellulose. These results showed that corncob cellulose and cellulose nanocrystals (CNCS) were successfully extracted from corncob by sulfuric acid and might be potentially used for different applications.

***Keywords**:* Corncob, Cellulose nanocrystals, Acid hydrolysis, Characterization, Optimization

ACKNOWLEDGMENTS

First of all, and for most, I would like to thank almighty God for He has given me strength, potential, and patience to complete this thesis work successfully. Moreover, I would like to express my sincere gratitude to my advisor **Dr. Hundessa Dessalegn** for his invaluable advice, Fruitful advice, proper supervision of the thesis, and reading the manuscript throughout my thesis work.

I am gratefully acknowledging Addis Ababa Institute of Technology, especially the School of Chemical and BioEngineering, for financial assistance and precious support. I am also thankful to the department of biomedical Engineering of Addis Ababa University for their permission to use laboratories.

I would like to say thanks to my friends and laboratory staff of the School of Chemical and Bioengineering for their constant encouragement. Finally, my thanks go to all the people who have supported me to complete the research work directly or indirectly.

TABLE OF CONTENTS

LIST OF TABLES

LIST OF FIGURES

LIST OF SYMBOLS AND ABBREVIATIONS

SYMBOLS

µm	Micrometer
A	Angstrom
℃	Degree centigrade
cm	Centimeter
GPa	Gigapascal
kHz	Kilohertz
kV	Kilovolt
mA	Milliampere
mg	Milligram
min.	Minute
mL	Milliliter
nm	Nanometer
V11	Volume 11
wt.%	Weight percent
X	Magnification

ABBREVIATIONS

AAiT	Addis Ababa Institute of Technology
AFM	Atomic Force Microscopy
ANOVA	The Analysis of Variance
ASTM	American Standard Test Method
BNC	Bacterial Nanocellulose
CCD	Central Composite Design
CNC	Cellulose Nanocrystals
CNF	Cellulose Nanofibers
DF	Degree of freedom
DLS	Dynamic Light Scattering
DTG	Differential Thermogravimetry
FTIR	Fourier Transform Infrared Spectroscopy
H_2SO_4	Sulfuric Acid
Kcps	Kilo Count Per Second

NaClO	Sodium Hypochlorite
$NaClO_2$	Sodium Chlorite
NaOH	Sodium Hydroxide
Rpm	Revolutions Per Minute
RSM	Response Surface Methodology
SEM	Scanning Electronic Microscopy
Std.Dev	Standard Deviation
TAPPI	Technical Association of The Pulp and Paper Industry
TEM	Transmission Electron Microscopy
TEMPO	(2,2,6,6- Tetramethyl Piperidine-1-Oxyl)-Mediated Oxidation
TGA	Thermogravimetric Analysis
XRD	X-Ray Diffraction Analysis

CHAPTER 1 INTRODUCTION

1.1. Background

The depletion of petroleum-based resources and the attendant environmental problems, such as global warming, ocean acidification, and sea-level rise have stimulated considerable interest in the development of environmentally sustainable materials, which are composed of cellulose, hemicellulose,and lignin as a means of overcoming environmental problems(Dufresne, 2017a). Lignocellulose materials are the most abundant biomass found in almost all plant-derived materials, from wood and grass to agricultural residues and municipal solid wastes that can be used as a substitute for petroleum-based resources and sustainability production(Yang et al, 2017).

Human beings become aware of environmental conservation and applications of renewable resources become more and more important for their daily life since they are friendly to nature and will replenish to replace the portion depleted by usage and consumption, either through natural reproduction or other recurring processes in a finite amount of time in a human time scale. The production of innovative materials from renewable and abundant bioresources, such as nano cellulose obtained from cellulosic sources, is becoming an important area of research since it offers a unique combination of high physical properties producing a variety of high-value products with low impact on the environment(Faria & Pothan, 2015).

Nanocellulose is a natural nanomaterial that can be extracted from the plant cell wall, with its nanometer size in diameter, and consists of attractive properties such as high strength, excellent stiffness, and high surface area. Also, with its structure, nanocellulose contains a plentiful of hydroxyl groups which are accessible for surface modification(Phanthong & Xu, 2018).

Maize is one of the important cereal crops grown in Ethiopia. It is accompanied by an enormous amount of agro-waste generation, is a potential feedstock for the production of biogas, biodiesel, and bioethanol to fulfill the increasing demand for biofuels, and about 30 % of maize agro waste is corncob, and it is underexplored(Pointner & Kahr, 2014).

Due to its chemical composition(45% cellulose,35% hemicellulose, and 15% lignin), corncob residues has such amount of natural biopolymer that is abundantly available in the plant cell show great potential as a molecules renewable raw material for producing a variety of added-value chemicals, such as cellulose nanocrystals, lactic acid, citric acid, sugars, and ethanol(Upadhyaya, et al., 2010).

Many researchers (Silvério,&Pasquini, 2013; Alves et al.,2013) use corncob for the preparation of cellulose nanocrystals using sulfuric acid. The acid hydrolysis promotes the removal of the amorphous regions in the cellulose and the isolation of nanocrystals. In the hydrolysis process, glycosidic bonds of the amorphous regions of cellulose may suffer hydrolytic cleavage, which is promoted by hydronium ions, with the release of the individual crystallites(Phanthong et al., 2018).

Cellulose nanocrystals are needle-shaped cellulose particles with at least one dimension equal to or less than 100 nm and have a highly crystalline nature. The unique combination of amazing physicochemical properties and environmental benefits allows that the cellulose nanocrystals offer a wide range of potential applications(Vijay Kumar Thakur, 2015). At present, the main application of cellulose nanocrystals is as a reinforcing agent, paints, coatings, special papers, cosmetics, pharmaceuticals, biomedical materials, textiles, the automotive industry, aerospace, building materials, the electronic and electrical industry, and many others(Santos et al., 2013).

In this study, cellulose nanocrystal was prepared from corncob using acid hydrolysis (H_2SO_4), with the optimum conditions that consider the temperature correlation, hydrolysis time, and acid concentration was investigated and optimized using response surface method. Therefore, in this work, the preparation and characterization were systematically examined by analysis of surface morphology studies (SEM), particle size (DLS), chemical functional groups (FTIR), crystallinity (XRD), and thermal stability (TGA) of cellulose nanocrystals (CNCs) were described.

1.2. Statement of problem

The high cost of non-renewable(synthetic) products circulating currently in the industry is among the major reasons initiating the search for alternate and viable materials that are sustainable, renewable, environmentally acceptable materials, and that can either partially or fully replace the synthetic products. Lignocellulosic biomass (corncob, water hyacinth, bamboo, etc.) is a source of natural fiber that can substitute petroleum-based polymers due to its outstanding environmentally friendly properties.

Most of the recent industrial products are largely not friendly to the environment upon usage (non-degradable disposal) and most of them are not easily degradable which is causing a serious environmental problem that affects society's health. Even if Ethiopia is said to be maize rich country and the remaining part of the maize like corncob is the naturally degradable product but it has been suffering from the use of the environmentally unfriendly synthetic product. Besides, the wastes from lignocellulose biomass such as agricultural wastes(corncob) and forest remnants have a high potential for reuse feedstock for the production of high enhanced materials without the competitiveness with human and animal food chains.

Corncob is an agro-industrial waste available in large quantities and various renewable biomass resources are accepted as waste material and are mostly burnt, so the raw material is cheap and available in major parts of the country especially in the Oromia and Amhara regions of Ethiopia. The utilization of unused logging residues as a type of woody biomass, have environmental effects related to the improvement of energy efficiency and the slowing of global warming and incorporating it into a polymer matrix for the production of green polymer composite materials that can be fully degraded is an alternate solution proposed to overcome the global environmental problems.

In this regard, the production of maize and disposition of corncob has increased in Ethiopia, and in parallel to that, the import of cellulose nanocrystal products has increased in the last few years. Therefore, the main objective of this research is to extract corncob cellulose from corncob and characterize the produced cellulose nanocrystals. The study also aims at the optimization of the process conditions and yield.

1.3. Objectives

1.3.1. General objective

The main aim of this study was the extraction, characterization, and optimization of cellulose nanocrystals from Corncob.

1.3.2. Specific objectives

The specific objectives were:

- To characterize (proximate analysis) the raw material corncob
- To extract cellulose nanocrystals from corncob using acid hydrolysis
- To investigate the effects of acid concentration, reaction temperature, and hydrolysis time and determine the optimum parameters on the yield of cellulose nanocrystals
- To characterize the physicochemical properties of product cellulose nanocrystal from corncob

1.4. Significance of the study

The significance of extracting cellulose from corncob and synthesis of cellulose nanocrystals can be used in different ways for the whole environment. Because corncob is a renewable resource, its utilization can contribute to the solution of socio-economic problems associated with it. This study contributes to a significant improvement in inefficient resource utilization by converting waste to wealth and for the researcher, it will provide opportunities to increase practical knowledge.

Cellulose nanocrystals obtained from naturally occurring cellulose fibers include cotton, flax rayon, and jute are biodegradable and renewable and hence they serve as a sustainable and environmentally friendly material for most applications. However, there is an alternative option such as the production and application of biodegradable cellulose nanocrystal based on natural resources derived from corncob that provide environmental benefits.

The economical benefit extracting of cellulose nanocrystals from corncob will decrease the cost for the importation of the cellulose nanocrystal from petroleum-based resources and because of the occurrence of hydrogen bonding between its chains, a small concentration of cellulose nanocrystals successfully improved the tensile and modulus properties of materials.

Using a renewable and abundant natural resource such as corncob for the production of cellulose nanocrystals can provide a viable solution to overcome the issues concerning diminishing petroleum resources coupled with the global environmental problem. Apart from these, the investigation of this research was important to provide the opportunity for

nanoengineering that opens new areas of research in Ethiopia for converting unused corncob and its waste into cellulose nanocrystals.

1.5. Scope of the study

This work concentrates on the basic study of corncob utilization for the extraction of cellulose and the production of cellulose nanocrystals. First, cellulose isolation and purification were carried out using the soxhlet extraction (dewaxing process), alkaline treatment, and bleaching as pretreatment steps. Then cellulose nanocrystals were prepared from obtained cellulose by using the acid hydrolysis method. Here, cellulose nanocrystal (CNC) was synthesized with a controlling parameter at the different reaction temperatures, hydrolysis time, and acid concentration.

The obtained cellulose nanocrystals (CNCs) were purified using successive centrifugation and membrane dialysis. Finally, the suspension of cellulose nanocrystals was ultrasonicated to get homogenized dispersion, freeze-dried, and characterized. To study the effects of the acid hydrolysis conditions on the yield of cellulose nanocrystals the central composite design (CCD) method is used to determine the maximum yield of cellulose nanocrystals (CNCs).

The yield of cellulose nanocrystals will be measured as a function of acid concentration, hydrolysis time, and reaction temperature, whereby the sulfuric acid concentration in the range of 45 to 65 wt.%, hydrolysis time from 30 to 60 minute, and reaction temperature between 45 and 60 °C used as hydrolysis conditions. The effects of process parameters (acid concentration, temperature, and hydrolysis time) on the yield of cellulose nanocrystals were investigated and optimized using the response surface method.

Lastly, the optimum yield of cellulose nanocrystals was characterized by X-ray diffraction (XRD), thermogravimetric analysis (TGA), scanning electronic microscopy (SEM), dynamic light scattering (DLS), and Fourier-transform infrared (FTIR) spectroscopy.

CHAPTER 2 LITERATURE REVIEW

2.1. Lignocellulosic Biomass

Lignocellulosic biomass is a complex biopolymer that is derived from agricultural wastes or byproducts and composed of cellulose, hemicellulose, and lignin. It is abundant in nature and is considered to be the largest renewable resource on earth. In addition, it has the advantage of being available worldwide, with large quantities in many regions of the planet. It has a higher amount of oxygen, and lower fractions of hydrogen and carbon with respect to petroleum-based resources. Owing to this compositional variety, more classes of products can be obtained from lignocellulosic biorefineries than petroleum-based ones. Nevertheless, a relatively larger range of processing technologies is needed for the treatment of lignocellulosic biomass(Isikgor & Becer, 2015).

There are different pre-and post-treatment methods for the degradation of lignocellulosic biomass into its components (cellulose, hemicellulose, and lignin).These are physical processes (size reduction, boiling, ultrasonication, etc.), physicochemical processes (liquid hot water, ammonia fiber explosion, etc.), chemical processes(acid, base, salt, solvents, etc.), and biological processes (white-rot fungi, brown rot fungi, and bacteria) have been developed which alter the structure of lignocelluloses and removes the lignin(Bhikhu & Gaurav, 2017).

Among the biomass pretreatment, chemical pretreatment proved to be the most efficient method and cost-effective for biomass deconstruction with low pretreatment severity (Sun et al., 2004). The biomass pretreatment is aimed to break the lignocellulosic complex, solubilize the non-cellulosic contents (lignin and hemicellulose) but preserve the materials for further valorization, reduce cellulose crystallinity, and increase the porosity of the materials for subsequent depolymerization process(Pereira & Arantes, 2018a).

The cell wall structure of lignocellulosic biomass mainly consists of three kinds of polymers. These are lignin, hemicellulose, cellulose, and a small number of extractive substances. However, the composition and the content of these three components are varied due to the difference in species, types, and sources of lignocellulosic biomass(Phanthong et al., 2018). The major advantages of lignocellulosic materials are that they are sustainable, carbon-neutral, abundant in nature, and there is a strong desire to reduce these emissions. The utilization of plant/crop-based feedstock for the production of chemicals could deliver greenhouse gas emission reductions(Sauer, 2016).

2.1.1. Cellulose

Cellulose is one of the most common biopolymers representing about 1.5×10^{12} tons of cellulose produced annually by photosynthesis(Kadimi, et al.,2016). It is regarded as an inexhaustible raw material for the production of eco-friendly and biocompatible products, and organic compound with the formula $(C_6H_{10}O_5)n$, ($n < 20{,}000$)(Tayeb, et al., 2018). Like starch, cellulose is a polymer that consists of glucose monomer units, but the glucose monomer units are linked together by $\beta(1\rightarrow4)$ linkage as opposed to $\alpha(1\rightarrow4)$ linkage in insoluble starch (Ogunbayo, et al., 2016).

Cellulose (carbohydrate polymer) is the most abundant renewable polymer in nature, linear, crystalline (polysaccharide) macromolecule of high molecular weight having a high degree of polymerization(Hamad, 2017). Several mechanical processes like high-pressure homogenizers, cryo-crushing, high-intensity ultrasonic treatments, and micro fluidization techniques were utilized for the extraction of cellulose microfibril. Using either enzymatic or acid hydrolysis conversion of cellulose microfibrils into nanocrystalline components, which rod-like cellulose nanomaterials(Vijay Kumar Thakur, 2015). With the use of appropriate chemical, mechanical, and/or enzymatic methods, cellulose can reduce its size in diameter or both diameter and length, up to the nanoscale(Blanco et al., 2018).

Cellulose, the ubiquitous renewable natural biopolymer on earth, is considered to be one of the most important organic compounds produced in the biosphere and biosynthesized by several living organisms ranging from lower to higher plants, sea animals, bacteria, and fungi(Trache et al., 2016). It is obtained from these sources needs to be isolated through pulping to remove unwanted lignin, hemicellulose, and other extractives such as pectins, waxes, mineral matters, and proteins(Jasmani & Thielemans, 2018). Dilute alkaline solutions of NaOH, KOH and mechanical defibrillation treatments can also be used to break up the entangled cellulose networks to obtain pure microfibrils (Vijay Kumar Thakur, 2015).

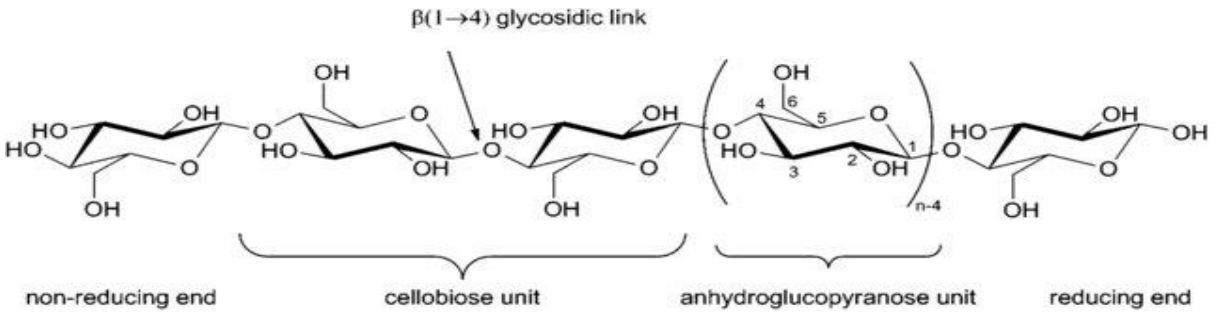

Figure 2-1: Molecular structure of the cellulose chain *(Trache et al., 2016)*

2.1.2. Hemicellulose

The second most polysaccharide component of lignocellulose and carbohydrate polymers is hemicellulose, which accounts for 15-35% of the plant cell wall. It is embedded in the plant cell walls, and one of its main functions is to bind cellulose microfibrils to strengthen the cell wall. It is defined as the alkali-soluble material after removal of the pectic substances, and have a much lower degree of polymerization as compared to that of cellulose(Tomkinson, 2014).

Unlike cellulose, hemicellulose has a random and amorphous structure, which is composed of several heteropolymers including xylan, glucuronoxylan, arabinoxylan, glucomannan, and xyloglucan(Abdel-Hamid& Cann, 2013). It is insoluble in water at low temperatures. However, its hydrolysis starts at a temperature lower than that of cellulose, which renders it soluble at elevated temperatures (Matsutani, & Takaoka, 1993).

The effective utilization of hemicellulose in lignocellulosic biomass is a promising alternative for the replacement of limited fossil resources to produce furfural, it is a typical product that could be obtained from hemicellulose in raw biomass and is also a key platform chemical produced in lignocellulosic biorefineries that could further be transformed to fuels and useful chemicals, which is widely used in oil refining, plastics, pharmaceutical and agrochemical industries(Luo et al., 2019).

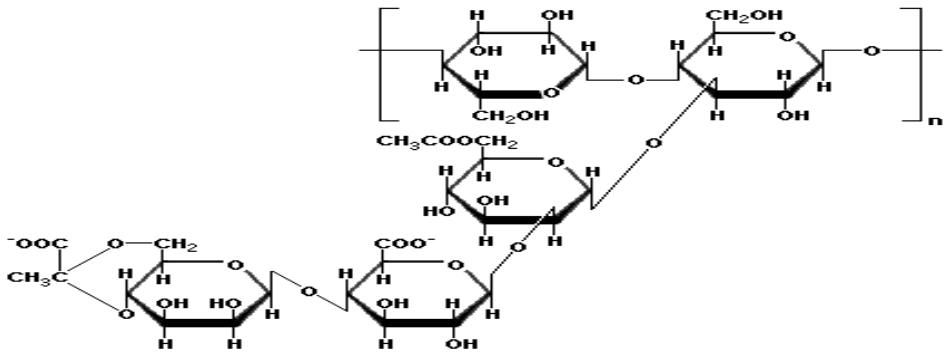

Figure 2-2:Molecular structure of hemicellulose (Maniruzzaman, & Morshed, 2014)

2.1.3. Lignin

Unlike cellulose and hemicellulose, lignin is a non-carbohydrate polymer but it is an aromatic heteropolymer that is derived from the oxidative coupling of three different phenylpropane building blocks and represents about 10–25% by weight of dry lignocellulosic biomass (Abdel-Hamid et al., 2013). It is a three-dimensional polymer of phenylpropanoid units and it is amorphous and hydrophobic. It functions as the cellular glue which provides compressive strength to the plant tissue and the individual fibers, stiffness to the cell wall, and resistance

against insects and pathogens(Isikgor & Becer, 2015).In the plant cell walls, lignin serves as the binder which holds between and around cellulose and hemicellulose complexion. With its binding function, lignin provides stiffness, compressive strength, resistance to decay, and water impermeability to plant cell walls (Phanthong et al., 2018).

The presence of lignin in lignocellulosic biomass is the main obstacle to biomass recalcitrance during the separation process. Lignin act as a protective barrier for plant cell permeability and resistance against microbial attacks and thus prevents plant cell destruction(Ballesteros,& Ballesteros, 2016). Removal of lignin is necessary to enhance biomass digestibility up to the point where both hemicellulose and cellulose are exposed for the solubilization process. It is generally difficult to treat or convert and it may make the pretreatment of lignocellulosic biomass more difficult. Lower lignin content is therefore preferred(Ruan et al., 2019).

Table 2-1: Organic components of some lignocellulosic biomass

Lignocellulosic biomass	Cellulose (%)	Hemicellulose (%)	Lignin (%)	Extractives %	References
Cotton	80-95	5-20	-	-	(Song & Li, 2019a)
Sugar Bagasse	43.6	33.5	18.1	3.1	(J. Sun et al., 2004)
Onion Skin	41.1	38.91	16.2	3.8	(Rhim & Luo, 2015)
Corncob	45	35	15	5	(Zhen, 2007)
Corn Stover	40	25	17	18	(Yang, 2017)
Wheat Straw	38.2	21.2	23.4	17.2	(Silva, & Rocha, 2014)
Water Hyacinth	43	33	18	6	(Bährle-Rapp, 2007)
Eucalyptus	50	13	28	9	(Ruan et al., 2019)
Hard Wood	40-50	23-39	20-30		(Rosa et al., 2010)
Soft Wood	40-45	30	36-34		(Yang, & Si, 2018)
Pineapple Leaf	34-40	21-25	25-29		(Pandey et al., 2015)
Sisal Leaf	71.4	16.6	12	-	(Zhu,& Hao,2019)
Rice Straw	38.3	31.6	18.8	11.3	(Battegazzore et al.,2014)
Barley Straw	35-40	20-35	15-25	-	(Fowler et al., 2011)
Spent Grain	44.5	33.8	22.7	-	(Wimmer et al.,2017)
Waste Paper	76	13	11	-	(Rodriguez,&Arbelaiz,2017)

2.2. Corncob

Maize (Zea mays L.) is one of the main foods and feed crops in Ethiopia and worldwide, and is the lowest cost caloric source among all major cereals, which is significant given that cereals dominate household diets in Ethiopia. Its production in Ethiopia has shown a considerable increase over the last 15 years with a drastic increment in recent years. The production increased from as low as 3.1 million tons in 2000 to over 7.2 million tons in 2014, which represents an increase of 130 percent(Negatu et al.,2018).

From this maize corn stover, cornstalk and corncob are the major wastes that are removed in most of the countries, but in Ethiopia, the corn stover can be used as a feed for animals and both stalk and corncob can be used for cooking. Corncob (central part of maize) is either treated as waste or burnt as fuel causing environmental concern. To achieve its value addition in new research areas, corncob can be processed chemically to find ways to generate new end products with added values at a very low price(S. Kumar& Upadhyaya, 2010).

To minimize the waste of bioconversion and maximize the environmental benefits, the concept of the comprehensive utilization of lignocellulosic biomass has been developed to produce bioethanol, biochemicals, and biobased products through reorganizing the commercial supply chain. Corncob is lignocellulose biomass having a Chemical composition of cellulose (45%), hemicellulose (35%), lignin (15%), and others (5%)(Lee et al., 2014, Zhen, 2007).

It is used for the production of furfural (Zhang, 2014),Briquette(Mitchual&Akowuah,2013), Activated carbon(Armonio et al.,2019),Natural Xylan(Arifan, 2019), Ethanol (Luque et al., 2016),and Particleboard(Scatolino & Mendes, 2013).Corncob is a cheap and widely available agricultural waste material and has the potential of being a renewable source for energy as well as packaging industries. It is primarily comprised of cellulose, hemicellulose, and lignin; however, it also contains a small quantity of starch, protein, fat, pectin, and inorganic substances(M. Li et al., 2014). Due to this, nowadays many researchers focus on the extraction of cellulose from corncob for the production of many products.

Some of them are effect of Incorporating Cellulose nanocrystals from corncob on the tensile, thermal, and barrier properties of Poly(Vinyl Alcohol) nanocomposites(Pasquini, 2013), physicochemical, spectroscopic, and thermal properties of microcrystalline cellulose derived from corncob(Azubuike & Okhamafe, 2012), and also extraction of cellulose nanocrystals from corncob as a reinforcing agent in nanocomposites (Alves&Pasquini,2013).

Figure 2-3:Corncob

2.3. Nano cellulose

The word “Nanocellulose” generally refers to cellulosic materials with one dimension in the nanometer range. There is a wide range of cellulose particle types that are being studied for various commercial applications. The diversity of cellulose particle types depend on cellulose source and extraction processes(Cotana & Kenny,2013). It is the natural fiber that can be extracted from cellulose, and special attention is the size of nanocellulose fiber which generally contains less than 100 nm in diameter and several micrometers in length(Phanthong et al., 2018).

Nanocellulose is attracting more and more attention from scientists due to its high mechanical strength and environmental sustainability. Some beneficial attributes of nanocellulose are its sustainability, abundance, mechanical properties such as large surface to volume ratio, high tensile strength and stiffness, high flexibility, and good electrical and thermal properties(Liu & Bhattacharyya, 2015). It is based on conducting composite films that show promise in the application of nano paper-based sensors, flexible electrodes, and conducting adhesives (Börjesson & Westman, 2015).

Nanocellulose can be classified into three main categories, namely: cellulose nanofibers (CNFs), cellulose nanocrystals (CNCs), and bacterial nanocellulose (BNC), based on their shape, dimension, function, and preparation method, which in turn primarily depend on the cellulosic source and processing conditions(Thomas & Grohens, 2016). Although all types are similar in chemical composition, they are different in morphology, particle size, crystallinity, and some properties due to the difference of sources and extraction methods(Phanthong et al., 2018).

2.3.1. Cellulose nanocrystals (CNC)

Cellulose nanocrystal is a kind of nanomaterial derived from cellulose mainly by strong acid hydrolysis at elevated temperature, possessed lots of desirable property, like extremely outstanding mechanical strength, biocompatible and biodegradable, high specific surface area, and so on (Song et al., 2019a). It has a short-rod-like or whisker shape with 2–20 nm in diameter and 100–500 nm in length. Also, it contains 100% cellulose chemical composition mainly in crystalline regions (high crystallinity around 54–88%)(Phanthong et al., 2018).

CNCs are isolated from native cellulose mostly using acid hydrolysis, enzymatic hydrolysis using cellulases(Jasmani&Thielemans,2018), ionic liquids(Man et al., 2011), TEMPO(2,2,6,6-tetramethyl piperidine-1-oxyl)-mediated oxidation(Jasmania,2018), and recently a new method using gas-phase hydrochloric acid hydrolysis at room temperature for 30 min was patented (Kontturi, 2018). Cellulose nanocrystal that is formed through the acidic treatment is of colloidal dimensions and forms an aqueous suspension when stabilized.

The critical concentration of the colloidal suspension, which is the lowest concentration where the whiskers self-organize, depends on particle size, acidic treatment, preparation conditions, aspect ratio, and ionic strength(Börjesson & Westman, 2015). The most important method used for the extraction of CNCs is acid hydrolysis. In this process, a strong acid such as H_2SO_4 dissolves the amorphous portions of cellulose, resulting in the formation of a nanocrystal structure(Kargarzadeh et al., 2018).

When sulfuric acid is used it grafts negatively charged sulfate half-ester groups (a dicarboxylic acid where only one of the acid groups have been esterified) onto the surface, which makes the particles repel each other through electrostatic repulsion; therefore, it prevents aggregation in aqueous suspensions. The amorphous regions of cellulose are more accessible to acid attack compared to crystalline regions and therefore, under controlled conditions, the amorphous regions are assumed to be removed whereas the crystalline regions remain, this assumption has been proven by x-ray diffraction, which has shown that the acid-treated rod-like particles have the same crystal structure as original cellulose(Faria et al., 2015).

2.3.2. Cellulose nanofibrils (CNF)

The preparation of cellulose nanofibrils is rather straightforward since it involves the use of a refining machine to produce fibrils with nanosized dimensions. It can be manufactured by mild acid hydrolysis coupled with a steam explosion, whereas cellulose nanocrystals are made by a strong acid like sulfuric acid (H_2SO_4), which destroys all the amorphous portion (disordered

region) and leads to the nanocrystal structure(Gopakumar et al.,2016). The main important issue that needs to be addressed when preparing cellulose nanofibrils is how to minimize the use of energy(Jasmania, 2018). It is the long, flexible, and entangled nanocellulose which can be extracted from cellulose fibrils by mechanical methods, such as high-pressure homogenization, grinding, and refining. The equipment commonly used to produce cellulose nanofibril(CNF)includes high-pressure homogenizers, refiners, grinders, crushers, and microfluidizers (Zhang et al.,2013).

These cellulose nanofibrils materials have unique properties such as low density, high aspect ratio, and high specific strength with the ability for chemical modification. Preparations of cellulose nanofibrils can also be chemical treatment or enzymatic treatment, a combination of both chemical/enzymatic treatments with mechanical destructuring can occur. Moreover, they have high barrier properties and are biodegradable and sustainable, and not hazardous. These properties generate intensive research by different research groups to find applications in the production of nano paper and films, composites, and laminates, as well as foams and aerogels (Mohammad,& Bous,2018).

Comparing with nanocrystalline cellulose, nanofibrillated cellulose has a longer length with a high aspect ratio (length to diameter), high surface area, and high extensive of hydroxyl groups which are easily accessible for surface modification. It is an aggregation of fibrils made up of crystalline and amorphous parts with micrometer length and 10–100 nm in diameter(Phanthong et al., 2018).

2.3.3. Bacterial nanocellulose (BNC)

Bacterial cellulose is mainly produced by the bacteria of Acetobacter Gluconacetobacter xylinus species by cultivation in aqueous culture media containing carbon and nitrogen sources within days(Reiniati,2017). The resulting cellulosic network structure is in the form of a pellicle of randomly assembled ribbon-shaped fibrils less than 100nm wide, which are in turn composed of a bundle of much finer nanofibrils (2–4nm in diameter). These bundles are relatively straight, continuous, and dimensionally uniform(G. Zhu & Lin, 2019).

Bacterial nanocellulose is another kind of nanocellulose which is different from cellulose nanocrystals and nanofibrillated cellulose because cellulose nanocrystals and nanofibrillated celluloses can be extracted from lignocellulosic biomass (top-down process)(G. Zhu & Lin, 2019), but bacterial nanocellulose is produced from building up of low molecular weight of

sugars by bacteria mainly by Gluconacetobacter xylinus for a few days up to two weeks (bottom-up process)(Jeremic et al., 2019).

As such, the bacterial nanocellulose is always in the pure form without other components from lignocellulosic biomass such as lignin, hemicellulose, pectin,and so on(Phanthong et al., 2018). Bacterial nanocellulose emerged as an attractive advanced biomaterial that provides desirable properties such as high strength, lightweight, tailorable surface chemistry, hydrophilicity, and biodegradability. These polymers can be biosynthesized by bacteria of some genera, but the most efficient producers of cellulose belong to the genus Gluconacetobacter, which secrets an abundant 3-D network of cellulose fibrils(Gorgaslidze et al., 2017).

Table 2-2:summary of different types of nanocellulose, formation, and sizes

Processes	Abbreviations	Synonyms	Average sizes
Chemical	CNC, CNW, NCC	Cellulose nanocrystals, Crystalline nanocellulose, Whiskers, and Crystal of cellulose	Diameter =50-70 nm Length =100-250 nm
Mechanical	CNF, MFC, NFC	Cellulose nanofibrils, nanofibrillated cellulose, cellulose microfibers, and fibrillated cellulose	Diameter =50-60 nm Length =several micrometers
Enzymatic	BNC, BC, MBC	Bacterial nanocellulose, microbial cellulose, Bio cellulose	Diameter=20-100 nm Length=different types of nanofiber networks

From the three types of nanocellulose, cellulose nanocrystals are enjoying worldwide interest as a sustainable bio-based nanomaterial due to their unique structural and physicochemical properties such as renewability, low density, biocompatibility, adaptable surface chemistry, optical transparency, non-toxic, biodegradability, and improved mechanical and also with unique morphology, high surface-to-volume ratio, and high modulus and strength, the rigid rod-like CNCs are frequently applied as nanofillers to reinforce polymeric materials which are similar to other inorganic nanofillers, including layered silicates(Ramos & Garrigós, 2016).

2.4. Extraction of Cellulose Nanocrystals

The extraction of cellulose nanocrystals from renewable sources has gained more attention in recent years due to their exceptional physicochemical and mechanical properties, large specific surface area, low cost, and environmental benefits(Malladi & Robert, 2018). The isolation of

cellulose nanocrystals from plant sources is generally conducted as purification of the raw material to remove nanocellulose components from the plant material, isolate purified cellulose, and remove local interfibril crystalline contacts, and release cellulose nanocrystals, and subsequent mechanical or ultrasound treatment(Phanthong et al., 2018).

Some new methods to prepare cellulose nanocrystals(CNCs) appeared gradually, such as enzymatic hydrolysis,oxidative degradation, mechanical methods, ionic liquid, acid hydrolysis, and subcritical hydrolysis (Xie et al.,2018). Some of these preparation methods were described in the following section.

2.4.1. Mechanical treatment methods

The mechanical treatment process is the isolation of cellulose fibrils by applying a high shear force to cleavage the cellulose fibers in the longitudinal axis, resulting in the nanofibrillated cellulose. Mechanical methods have also been widely investigated for the production of nanoscale cellulose particles, either as of the fabricating process employing combinations of acid hydrolytic, oxidative, and enzymatic treatment, or directly(Hussin, & Thakur, 2017). The mostly used mechanical approaches include high-pressure homogenization, ultrasonication, and ball milling methods. However, the main drawback of the mechanical process is high energy consumption. Therefore, the mechanical process is generally combined with other pretreatment methods for decreasing energy(Phanthong et al.,2018).

2.4.2. Enzymatic hydrolysis methods

Enzymatic hydrolysis is the biological treatment process in which enzymes are used for digesting or modifying cellulose fibers and conducted using mild conditions. The cellulases cut the cellulose molecules into shorter polysaccharides by the hydrolysis of β-1, 4-D-glycosidic bonds of the glucose units(Sharma& Meena, 2019).

Enzymes from cellulases, Viscozyme, and endoglucanases have been used for the synthesis of different types of cellulosic nanoparticles. This method is similar to that of acid hydrolysis treatment, but enzymes break the glycosidic bonds of the amorphous domain thereby producing individual highly crystalline particles(Mokhena & Mochane,2018). Micro-organisms such as brown, white, and soft rot fungi and bacteria are also used in biological treatment to degrade lignin and hemicelluloses from lignocellulosic material(Trache et al.,2017).However, a long time of operation and high cost is needed for biological treatment because of enzymes and other microorganisms used. Generally, biological treatment with an enzyme can be performed in mild conditions; however, a long time of operation is needed (Kumari et al.,2019).

Compared with the acid hydrolysis, the enzymatic hydrolysis process for the preparation of cellulose nanocrystal is environment-friendly, while the experimental conditions are harsh, the yield of cellulose nanocrystal is low, and the reaction time is long. But the major drawback of enzyme hydrolysis is that it produces less and requires long-time cellulose nanocrystals when compared to that of acid hydrolysis(Phanthong et al., 2018). Enzymatic hydrolysis of raw cellulose materials is promising for the industrial production of cellulose nanocrystal, so further research of efficient enzymatic hydrolysis is imperative and urgent(Xie et al., 2018).

2.4.3. Chemical treatment methods

Chemical treatment is the most promising method of preparing nanocellulose especially cellulose nanocrystalline(CNC), which was mainly carried out by acid hydrolysis.The chemical method produces rod-like short nanocrystals with improved crystallinity by reducing energy consumption and is better than other methods (Zheng, & Liu, 2013).

The chemical method includes; alkali pretreatment, oxidizing agent, acid hydrolysis, and ionic liquids pretreatment. Among them, acid hydrolysis is the most commonly used method to prepare cellulose nanocrystalline due to its moderate operating conditions and good stability of the resulting suspension. The acid hydrolysis processes need to go through very harsh reaction conditions which usually require concentrated acid, so it is often done using dilute acids to reduce the problems associated with the use of concentrated acids like the corrosion of the reactors, other equipment, and energy requirement for acid recovery(Xie et al., 2018).

From the above extraction of cellulose nanocrystal methods, the chemical treatment methods are preferable, due to the chemical methods have high crystallinity, length with good yield. But the chemical type, acid concentration, hydrolysis time, and hydrolysis temperature are factors that have been shown to govern the products of the hydrolysis process, the crystallinity, and yield(Oke, 2010). The chemical treatment methods have the following process.

2.4.3.1.Pretreatment process

The main pretreatment process for chemical methods is size reduction and washing, drying, milling, dewaxing, alkaline treatments, and bleaching. Dewaxing, alkaline treatment, and bleaching are usually involved in purification procedures. An efficient pretreatment helps to reduce energy consumption by 20 to 30-fold. It is worth noting that appropriate pretreatment of cellulose fibers promotes accessibility, increases the inner surface, alters crystallinity, breaks hydrogen bonds, and boosts the reactivity of the cellulose. Thus, it decreases the energy demand and facilitates the process of CNC production(Qiao, Chen, Zhang, & Yao, 2016)

Dewaxing is the process to remove wax, pigments, and oils from the lignocellulosic biomass, and the alkaline treatment is the application of alkaline for removing the amorphous polymer of hemicellulose and the remaining lignin. The generally used alkaline is sodium hydroxide (1.5-20 wt.%), which is always stirred with holocellulose for 1-5h. Then, the obtained solid products are washed by distilled water until reaching the neutral pH and finally dried in an oven at 50°C. The obtained fiber products from this treatment are mainly in the form of cellulose, and other non-cellulosic materials have been removed (Phanthong et al., 2018).

Bleaching is an important factor that must be considered because it does not only act as an unwanted color remover, but also increases the degree of whiteness, low chemical & energy consumption, and capable of degrading non-cellulose compounds(Brooks & Moore,2000). The bleaching process is influenced by various factors such as temperature, pH, stirring, and processing time. Chlorite, hypochlorite, and hydrogen peroxide are bleach agents that have been widely used, however, hypochlorite is known to produce chloride dioxide compounds which cause environmental pollution(Richana, & Candra Sunarti, 2019).

2.4.3.2.Acid hydrolysis process

Acid hydrolysis is the most common method for the extraction of nanocellulose from cellulosic materials by dissolving amorphous domains of cellulose fiber and results in nanocrystalline cellulose. It is one of the main processes for the extraction of nanocellulose from cellulosic materials(Mascheroni et al., 2016).

Due to the combination of ordered and disordered regions in cellulose chains, the disordered regions can be easily hydrolyzed by acid, and the ordered parts are left as the remaining. The main controlling factors which affect the properties of obtained nanocellulose are reaction time, temperature, and acid concentration(Phanthong et al.,2018). The typical acids used for hydrolysis of cellulose are sulfuric acid (Xie et al.,2018),(Qiao et al.,2016), hydrochloric acid(Qiao et al., 2016), hydrobromic acid (Qiao et al., 2016), Phosphoric acid (Xie et al., 2018), Maleic acid(Xie et al., 2018) and others. Conventionally, sulfuric acid is one of the most popular acids that are used to fabricate cellulose nanocrystals.

For a typical procedure, the CNCs were obtained using 45–65wt.%(Dufresne, 2017b) sulfuric acid aqueous solution with the ratio of 1: 8 to 1: 20 (g/mL) of raw material containing cellulose (weight) vs. acid (volume) (Qiao et al., 2016) at a temperature range from 45 to 60°C (Sultan & Alothman, 2017), and the treatment time can be from 30- 60 min under vigorous and constant stirring(Alves et al., 2013).If the temperature of acid treatment is less than 30°C, then the

hydrolysis process needs a long time too. On the other hand, if the hydrolysis temperature is higher than 60°C darkening of cellulose particles takes place due to hydration and carbonization(Saba et al., 2017).

If the hydrolysis time employed is inadequate, then incomplete removal of amorphous fractions can occur, which results in a reduction in crystallinity and change in particle morphology. Similarly, increasing the reaction time beyond a point can lead to depolymerization of crystalline cellulose, which decreases the aspect ratio of the nanocrystals and sometimes even leads to the formation of a much smaller spherical particle(Vijay Kumar Thakur, 2015).

Typically, the concentration of sulfuric acid in hydrolysis reactions to obtain cellulose nanocrystals is around 65wt.% (Dufresne, 2017b). The method that is most widely used for the preparation of cellulose nanocrystals is acid hydrolysis. This method is easy and fast to produce nanocellulose that has better properties. Some researchers have reported that the crystallinity index of cellulose nanocrystals produced by acid hydrolysis was higher than other methods. The cellulose nanocrystals obtained from the acid hydrolysis also has a smaller size. These are the reasons that the acid hydrolysis method is selected to obtained cellulose nanocrystals (Ostiguy & Emond, 2016).

The crystallinity of cellulose nanocrystals affected by the preparation technique, pretreatment, and the type of acid. Although acid hydrolysis is widely used for the production of CNCs, certain problems must be overcome, such as high consumption of energy and chemicals, acidic corrosion of equipment, and health and environmental hazards. Recently, several studies have focused on hydrolysis parameter optimization, corrosion prevention, and waste reduction of cellulose nanocrystals extraction using sulfuric acid (Qiao et al., 2016).

2.4.3.3.Post hydrolysis stage

After the acid hydrolysis stage, the resulting suspension is subjected post-hydrolysis treatment stage which consists of a series of steps. These are dilution of the suspension with distilled water, successive washing by centrifugations, dialysis, sonication, and drying(P. Huang,& Wu, 2019).

The suspension was diluted with plenty of deionized water to end the hydrolysis reaction and was followed by centrifuging for several minutes to remove the excess acid solution. The precipitates obtained were washed with deionized water and the suspension was centrifuged again. This process was repeated several times and then the suspension was dialyzed with

deionized water until the pH value reached neutral (alternatively, ammonia or NaOH aqueous solution can be used for neutralization before dialysis)(Qiao et al., 2016).

The supernatant was separated and the deposit was mixed with distilled water and centrifuged to remove the acid in a better way. In the end, the material obtained by centrifuge was kept in the dialysis bag (12,000–14,000 Da) for 4 days to reach a neutral pH value while the water content was refreshed every day. The sample was then homogenized by the ultrasound device (350 W) for 3 min to obtain the final nanocrystalline particles. Finally, it was placed in a freeze dryer for 72 h and stored in plastic containers for further analysis(Qiao et al., 2016). The pretreatment methods, acid hydrolysis, and the process conditions used by different studies to produce crystalline nanocellulose are summarized in Table 2.3.

Table 2-3**:**Summary of the common literature on process conditions of cellulose nanocrystals

Lignocellulosic materials	Chemicals and process condition used			Crystallinity (CrI) and Yield (Y%)	References
	Alkaline treatment	Bleaching	Acid hydrolysis		
Corncob	3wt.% NaOH solution for 3 h/100 ℃	NaClO (0.02wt.%) at 80℃ / 2 h	H_2SO_4 (64 wt.%) at 45 ℃,60 min	CrI=83.7 Y=41.5	(Alves et al., 2013)
Office Waste Paper	7.5 wt.%NaOH solution for 90 min at 100℃ using a paper/ NaOH solution ratio of 1:20 (w/v).	2% (v/v) of reagent grade, NaClO	64 wt.% H_2SO_4 at 45℃ for 30 min under continuous stirring, and the ratio of 1:14 (w/v)	CrI=75.9 Y=41	(Hazman et al., 2015)
Onion skin	17.5wt.%NaOH solution at 20 ℃ for 45 min.	0.7 % (w/v) $NaClO_2$ solution (fiber to liquor ratio of 1:50)	65 % H_2SO_4) (fiber to liquor ratio of 1:20) at 60 ℃ / 3 h	CrI=63 Y= 39.5	(Reddy, 2015)
Sugar bagasse	5%(w/v) NaOH at 80 ℃ for 1 h	3.3% (w/v) $NaClO_2$ 90 ℃/1 h	64% (w/w) H_2SO_4 at 45℃/60 min	CrI=56.7 Y=30	(Miranda et al.,2017)
Cassava Bagasse	250 mL of NaOH solution for 5 h with a fiber/solution ratio of 1:50 (w/v)	hydrogen peroxide (H_2O_2) (4% v/v) at 75℃ for 30 min	64 wt.% H_2SO_4 at 45℃ /120 min, fiber to acid ratio was 1:10 (w/w)	CrI=56.3 Y=10.5	(Prestes & Demiate, 2017)
Potato peel Waste	0.5 N aqueous NaOH solution at 80℃ for 2.5h	2.3 wt.% $NaClO_2$ solution in 70℃ for 2 h	64 wt.% H_2SO_4 to 45℃/60 min agitation by mechanical stirrer	CrI= 72.53 Y=44	(Thompson, & Liu, 2012)

Banana peels	5% w/v KOH at 25 ℃/ 4h under mechanical stirring	1% (w/v) $NaClO_2$ at pH 5.0 at 70°C for 1 h	1% (v/v) H_2SO_4 solution at 80°C for 1 h under mechanical Stirring	CrI=61.5 Y=35.9	(Maria, Andrade-mahecha, José, & Cecilia, 2017)
Palm Oil Empty Fruit	17.5% (w/v) (NaOH) solution for 2 hours at 45℃	1.7wt% $NaClO_2$ in water, mixtures of 27 g of NaOH & 75 mL glacial acetic acid in 1 L of distilled water at 80℃/4h.	64 wt.% H_2SO_4 solution under strong agitation at 45℃ for 45 min.	CrI=61.5 Y=54.6	(Lani, Ngadi, Johari, & Jusoh, 2014)
Pineapple leaf	2% (wt/wt) NaOH for 4h at 100℃ under mechanical stirring	1.7 wt.% $NaClO_2$ in water, mixtures of 27 g of NaOH and 75 mL glacial acetic acid in 1 L of distilled water at 80℃ for 4 h	H_2SO_4 64%(wt/wt) at 45 ℃ for 60 min under constant stirring	CrI=73.63 Y=50	(Marcos et al., 2013)
Rice straw	600 mL 5% KOH at room temperature for 90 min	1.4% acidified $NaClO_2$(1000 mL), at 70℃ for 5h	64-65 wt.% sulfuric acid at an 8.75 mL/g acid to cellulose ratio at a temperature of 45℃ for 45 min	CrI= 61.8 Y= 45	(P. Lu & Hsieh, 2012)
Corn stover	2.0 % NaOH solution at 80 °C / 4 h	1.7%NaClO and buffer solution (CH3COOH / NaOH) 1:1 (w / v) at 60 °C / 24h	H_2SO_4 at 60 % (v / v) for 50 °C for 20 min	CrI=55.04 Y=64	(Costa et al., 2015)
Tunicate	3% NaOH for 2h at 180℃	3%NaClO for 1h at 75℃, under mechanical stirring	1% H_2SO_4 for 2h at 180℃ Under mechanical stirring	CrI= 73± 6 Y= 44 ± 8	(Acharya, & Bissessur, 2018)

The shape and size of nanocrystals are more or less fixed by the source of cellulose. This means that different dimensions of nanocrystals can be obtained from different sources of cellulose even under similar experimental conditions. However, the properties of cellulose nanocrystals for a given raw material are affected by the degree of acid hydrolysis, and the exact hydrolysis conditions(Dufresne, 2017b).

2.5. Structures and Properties of Cellulose Nanocrystals

It is well known that the structural parameters of the rod-like cellulose nanocrystals, the length, and width, vary widely mainly depending on the source and the hydrolysis conditions of cellulose. The geometrical dimensions of cellulose nanocrystals(CNCs) can vary widely, with a diameter in the range of 4–25nm and length in the range of 100–1000nm and the degree of crystallinity of cellulose nanocrystals is greater than 70%(Chang& Huang, 2019).

X-ray diffraction determined the longitudinal modulus of cellulose nanocrystals to be in the range of 90–138GPa(Spagnol et al.,2018), and the thermal decomposition temperature of cellulose is about 300℃(Chang et al.,2019), and meets the requirements of the thermal processing of composite materials. However, the normal extraction method uses sulfuric acid for hydrolysis, which makes it easy to introduce the sulfate ester groups on the surface of the cellulose nanocrystals obtained, leading to the diminishment of the thermal stability and the thermal decomposition onset temperature of cellulose nanocrystals(Qiao et al., 2016).

Because the surface of cellulose nanocrystals presents abundant hydroxyl groups, cellulose nanocrystals with high hydrophilicity can be stably dispersed in water to form a relatively homogeneous suspension. The hydrophilicity of cellulose nanocrystals could be mainly characterized by water contact angles. Generally, the lower the water contact angle of cellulose nanocrystals, the higher the hydrophilicity of CNCs(Chang et al., 2019). With the increased concentration of cellulose nanocrystals, more birefringence in cellulose nanocrystals colloid suspension was observed. Moreover, cellulose nanocrystals could spontaneously arrange or self-assemble into a highly ordered structure and subsequently form an anisotropy region when a critical concentration of cellulose nanocrystals in the colloid suspension was reached(Hall& Chen, 2007).

The rheological properties of cellulose nanocrystals show that as the viscosity of cellulose nanocrystals suspension increased with an increase in cellulose nanocrystals concentration, and at lower shear rates, the viscosity of cellulose nanocrystals s suspension linearly decreased when the shear rates further increased(Huang et al., 2019). The mechanical properties of CNCs

are extremely challenging due to the small particle size and the non-availability of metrology techniques to characterize such small particles. The dimensions in the nanometer scale and extremely high mechanical properties make CNCs ideal candidates to improve the mechanical properties of polymeric materials(Vijay Kumar Thakur, 2015).

The main features that drive the development of CNC as polymer reinforcement agents are their large specific surface area (estimated to be several hundred of m^2g^{-1}), their very high modulus of elasticity (approximately 150GPa), their large aspect ratio(l/d), and their ability to act as a significant reinforcement at low filler loading levels. Other attractive advantages of CNCs are their low density (about 1.566 gm^{-3}), nonabrasive nature, non-toxic character, biocompatibility, and biodegradability (C. Dubois et al., 2018).

Additionally, cellulose nanocrystals come from renewable natural sources that are very abundant and therefore low in cost, so it is not necessary to synthesize them, and they allow the production of composite films with excellent visible light transmittance that can be easily modified chemically (their structure has a reactive surface of $-OH$ side groups that facilitate grafting chemical species to achieve different surface properties)(Flauzino Neto, et al., 2013).

2.6. Application of Cellulose Nanocrystals (CNCs)

Cellulose nanocrystal as nanofiller has been a focus of attention as it exhibits attractive characteristics such as low cost, low density, high aspect ratio biodegradability, better uniformity, and durability. The high strength and stiffness, as well as the small dimensions of cellulose nanocrystal, may well impart useful properties to composite materials reinforced with these fibers, which could subsequently be used in a wide range of applications.

Optical applications: Cellulose nanocrystal have been shown to display iridescent properties. By evaporating droplets containing Cellulose nanocrystal, an iridescent film was produced. The concentration of CNC had an impact on the Colour of the region produced (Thompson et al., 2019).

Paper and packaging industry: Applications of nanocellulose is mostly adopted by the paper and packaging industries to replace the use of synthetic polymers derived from petrochemical resources(Taheri & Mohammadi, 2015).

Electronics industry: Nanocellulose composites films can be a potential candidate for use in another major field like the electronics industry owing to their enhanced conductivity and flexibility. For example, polyaniline nanocellulose composite films are mostly studied in the

literature for various end uses in electronic fields such as paper-based sensors, flexible electrodes, electronic devices, and conducting adhesives(Taheri & Mohammadi, 2015).

Biomedical applications: Nanocellulose having some unique properties like a high surface area to volume ratio, high strength, and modifiable surface chemistry, have found applications in biomedical fields. The most potent application is to develop nanocellulose reinforced hydrogel composites which can enhance the mechanical properties in polymeric gel formulations and having the desirable properties of both the reinforcement phase and the host matrix phase (Pandey et al., 2015).

Food and Beverages: Consumers are demanding ever-increasing quality in food and beverage products. CNC can be a component in developing healthy, sustainable, and safe food and beverages that appeal to ever more exacting customer needs. It forms very emulsions which can improve the texture and suspension quality of products in this sector(Mascheroni & Piergiovanni 2015).

Reinforcement for Polymeric Matrix: The usage of natural fibers as reinforcement in bioplastic polymer composite has garnered attention during the last few decades. This is due to the limitations of biodegradable polymer-based materials that have an intractable nature, poor water-sensitivity, poor mechanical strength, and are brittle. Natural fibers are preferred as they can be obtained naturally, be safely collected, and can save costs compared to glass fibers. Moreover, natural fibers can be used to make various products including filters, brushes, mats, cushions, rope, and shelter for fish breeding. However, many waste products are generated from fibers and fruits(Ilyas, Sapuan, & Zainudin, 2017).

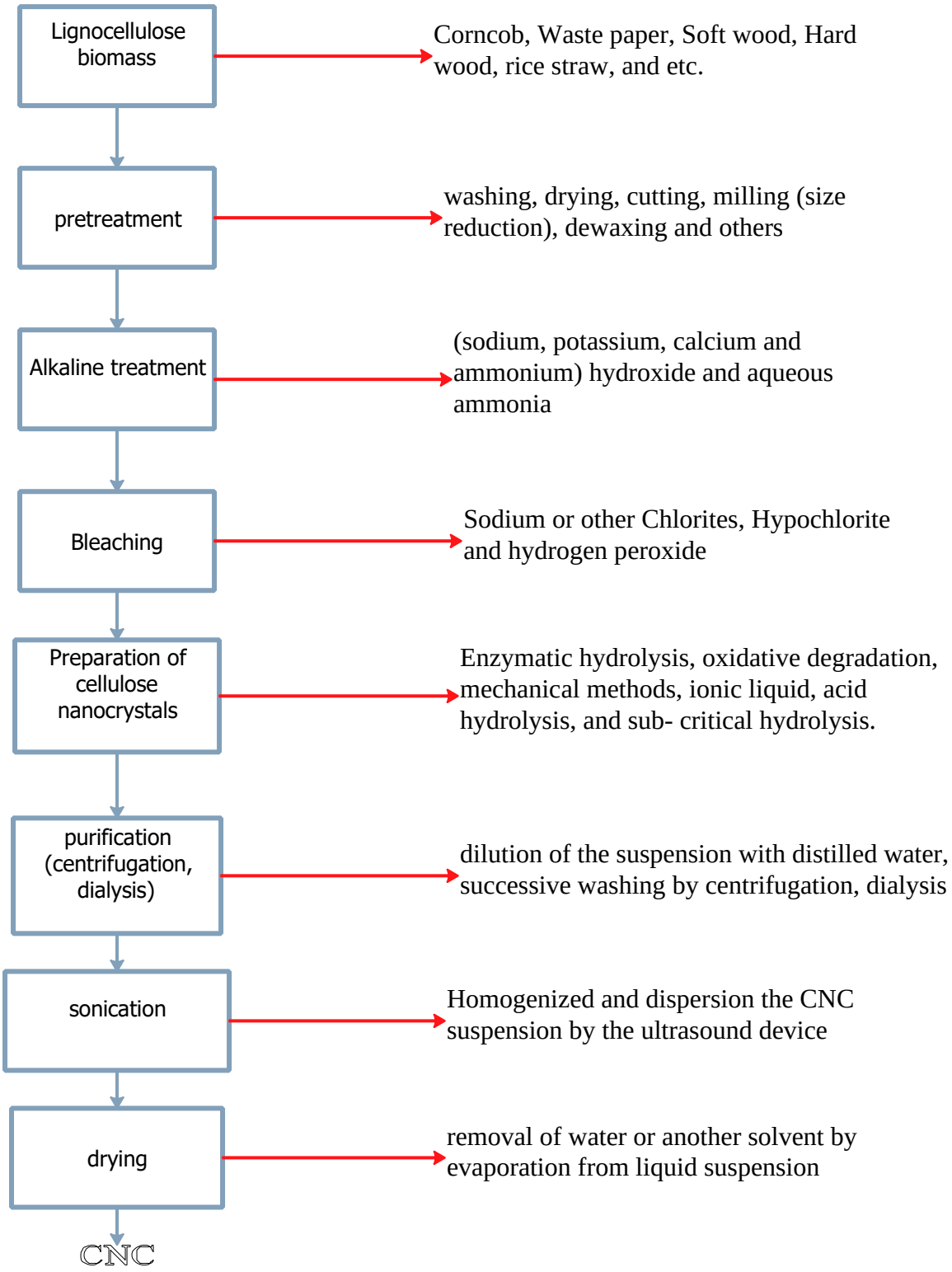

Figure 2-4:General procedures for processing CNCs from lignocellulosic biomass

CHAPTER 3 MATERIALS AND METHODS

3.1. Experimental framework

The experimental framework consists of a structure of an experiment that shows how cellulose nanocrystals were extracted from corncob using sulfuric acid hydrolysis.

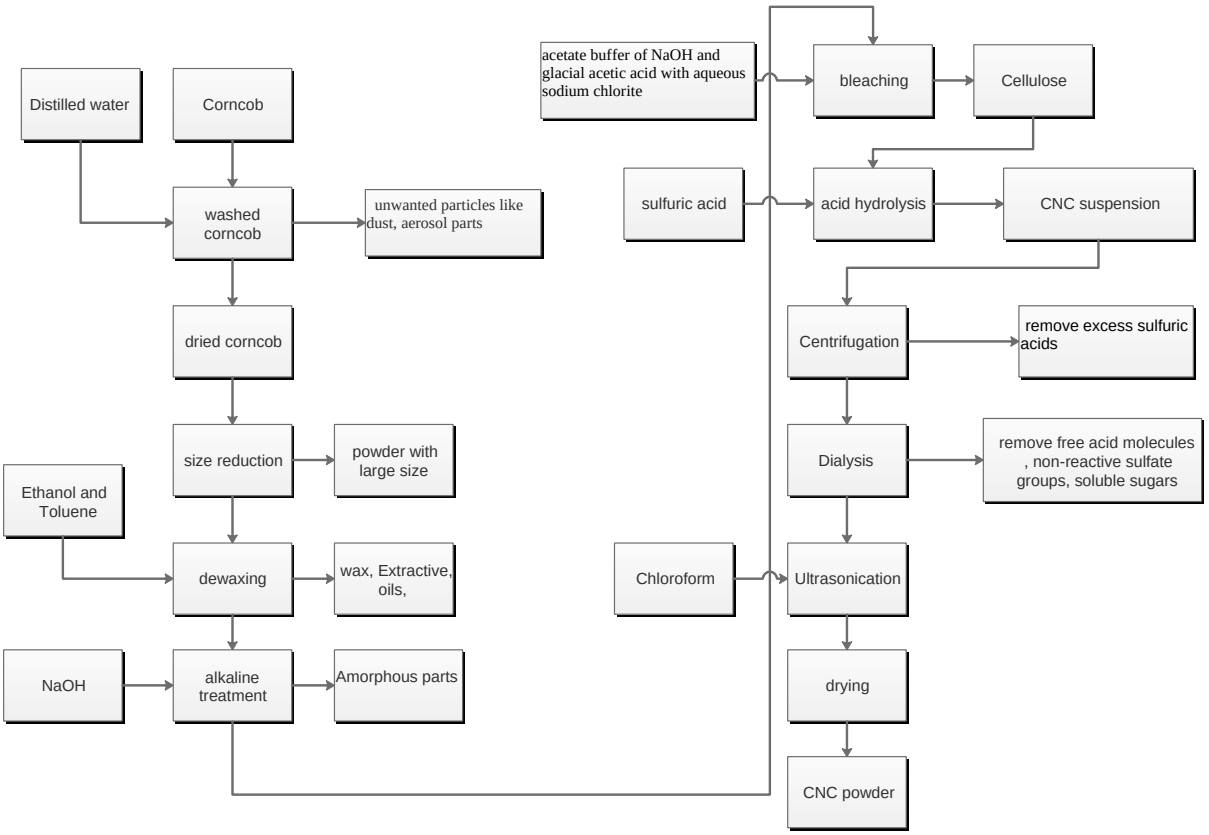

Figure 3-1:Over all framework of the experiments

3.2. Materials

The experimental works were conducted at Addis Ababa Institute of Technology (AAiT) in the Chemical and Bio Engineering school laboratory and in Biomedical Engineering laboratory.

3.2.1. Equipment

The equipment and instruments such as miller, weight balance, soxhlet apparatus, pH meter, oven dryer, filter paper, vacuum pump, desiccator, centrifuge, refrigerator, dialysis membrane, ultrasonicater, and dryer were used in this study. In addition to the above equipment's Particle Size Analyzer (ZEN3600), Scanning Electron Microscopy (FEI-INSPECT-F50), Attenuated Total Reflection Fourier Transform Infrared Spectroscopy (Thermo SCIENTIFIC iS50 ABX), and X-ray diffraction (BTX-528) were used for characterization of the raw material and the product.

3.2.2. Chemicals

The chemicals used for the study were sulfuric acid (98%), sodium hydroxide, sodium chlorite, distilled water, toluene (99%) and ethanol (97%), glacial acetic acid (99.5%), chloroform (99%), and hydrogen peroxide(H_2O_2). All the chemicals used in experiments were of analytical grade and used without further purification.

3.3. Methods

3.3.1. Sample Collection and Preparation

The Corncob collected from a local field in Ethiopia from west Gojjam primarily were washed with deionized water to remove unwanted particles, like dust, and aerosol parts. Then the washed corncob dried in an oven dryer at the temperature of 50℃ for 24 hours was milled with a blender to pass through a 35-mesh screen(Jiang & Hsieh, 2015). After that, the obtained powder which is less than 150μm was sealed in a plastic (polyethylene) bag and stored in a desiccator until use(Sakinah& Ahmad, 2019).

Then sample was dewaxed in a soxhlet apparatus using a mixture of toluene(400mL) and ethanol(200mL) solvents with the ratio of 2:1 (v/v) for 6 h at a temperature of 70℃ in a water bath to remove wax, phenolic pigments, and oils, and after that, the powder was washed by distilled water. Lastly, the dewaxed powder was dried in an oven at 50℃ for 24 h to determine the number of extractives and to prepare for the next steps. Here no color change occurs between the waxed powder and the corncob powder (G. Zhang et al., 2019).

3.3.2. Extraction of Cellulose

The process of extracting cellulose from corncob which consists of breaking up the cobs and the non-cellulosic components in corncobs were removed to isolate cellulose by incorporating and streamlining procedures (P. Lu & Hsieh, 2012). Due to these extractives and impurities, it required several pretreatments to isolate its cellulosic component before acid hydrolysis.

These are dewaxing and both Alkali and bleaching treatments that are usually implemented to remove hemicellulose and lignin. Then, during acid hydrolysis, amorphous domains of cellulose are preferentially hydrolyzed, because crystalline regions have a higher resistance to acid attacking(P. P. Zhang et al., 2014).

3.3.2.1.Alkaline Pretreatment

The dewaxed corncob (40g) was treated with a sodium hydroxide aqueous solution of 4% (w/w) the liquid to solid mass ratio of 20:1 for 2 h at 80℃ temperature and 500 rpm under mechanical stirring (Siwei Huang et al., 2017). It was done to remove lignin and hemicellulose from corncob and to purify the cellulose(Thakur et al., 2020).

Then the suspension that is alkaline treated was vacuum filtered and washed several times with distilled water until the alkali was completely removed. The alkali treatment was repeated four times(Larissa & Druzian, 2015), and finally dried at 50℃ for 24h in an air-circulating oven, and submitted to the bleaching process for whitening the color.

3.3.2.2.Bleaching

After alkaline treatment, the dried sample was bleached with a solution made up of equal parts (v:v) of acetate buffer (27 g NaOH and 75 mL glacial acetic acid(CH_3COOH), diluted to 1 L of distilled water) and aqueous sodium chlorite (1.7 wt.% $NaClO_2$ in water) and the ratio powder to liquid was 1:20 (g/mL)(P. P. Zhang et al., 2014).

Here for bleaching 40 g of alkaline treated powder with a ratio powder to liquid 1:20 (g/mL) was used for bleaching purposes. Then the solution was treated at a temperature of 70°C for 4 hours in a water bath under continuous mechanical stirring at speed of 600rpm for the removal of lignin and any organic residues. The suspension was vacuum filtered and the solid was repeatedly washed with distilled water until the yellow color disappeared (P. P. Zhang et al., 2014), and until the pH of the fibers became neutral and subsequently dried at 50 ℃ for 12 h in an air-circulating oven(Flauzino & Pasquini, 2013).

This procedure was repeated three times using the same conditions and the material which resulted after the purification was corncob cellulose. Lastly, some of the corncob cellulose was sealed in a plastic (polyethylene) bag for characterization purposes and the others are used for acid hydrolysis to prepare cellulose nanocrystals.

3.2.3. Preparation of cellulose nanocrystals

The corncob cellulose was milled and sieved before hydrolysis, and used for the extraction of nanocrystals by acid hydrolysis. In the acid hydrolysis, the diffusion of acid into the amorphous regions and subsequent cleavage of glycosidic bonds takes place(Dan Chen et al., 2011).

By considering corncob cellulose to acid solution constant(1:15 g/mL)(Xie et al., 2018), and the three most important factors were selected. These are reaction temperature (℃), reaction

time(min), and acid concentration(wt.%). Therefore, the parameter was designed to study if the concentration will affect the hydrolysis time. The treated corncob was mixed with sulphuric acid and the experiment was performed by using different hydrolysis times, temperatures, and acid concentrations. The mixture was stirred mechanically continuously until the hydrolysis time was completed(Manaf et al., 2019).

In this research, it was used 10 g of purified and bleached cellulose were hydrolyzed with a different sulfuric acid concentration of (45,55, and 65 wt.%)), temperature (45, 52.5, and 60℃), and reaction time (30, 45, and 60 min) with constant cellulose to acid (1:15 g/mL) solution under vigorous and constant stirring in the water bath was used based on literature (Lin et al., 2019).

After the hydrolysis of amorphous cellulose was completed, the suspension was diluted with ten times of distilled water (1500 mL) was added to the reaction mixture just after termination time to quench the hydrolysis reaction and then the diluted suspensions were cooled to room temperature. The suspension was transferred to a 15 mL centrifuge tube and then centrifuged at 6000 rpm (Addis Ababa Institute of Technology, Biomedical Engineering laboratory) for 15 min to remove excess sulfuric acids.

The cellulose nanocrystal was rewashed with distilled water and re-centrifuged 3 times until the pH of the suspension becomes above five(Lin et al., 2019). Then the suspension was collected and diluted with distilled water. This raw product was dialyzed (regenerated dialysis tube) against distilled water using a cellulose membrane for 4 days to neutralize, to remove the remaining acid, and fully remove free acid molecules such as non-reactive sulfate group, salts as well as soluble sugars.

Finally, the suspension of CNCs was sonicated using probe ultrasonication at 25 kHz for 15 min to get aqueous homogenized dispersion and labeled as the CNCs suspension. Here a few drops of chloroform were added to the freshly prepared suspension to prevent degradation of the cellulose nanocrystals and then stored in a refrigerator at 4℃ for characterization. The dimension, surface morphology, crystallinity index, and thermal stability were measured to determine the relationship between the manufacturing process conditions and the resulting properties(Lin et al., 2019).

3.4. Experimental design

Experimental data analysis was done using Design-Expert v11 software. The experimental design selected for this study was response surface methodology, three factors, quadratic model, central composite design (CCD) and the response variable measured was the yield (Y%) of cellulose nanocrystals(Mefteh et al., 2019).

Response surface methodology was used to analyze the optimum condition of the acid hydrolysis process in CNC production. It was also used to describe the significance of the independent variables toward the response, where the significance was determined when the p-value < 0.05(Aparamarta& Gunawan, 2019).

The CCD is a five-level fractional factorial design, which comprises a two-level factorial design, central designs, and two axial designs. But the BBD is a spherical, rotatable, or nearly rotatable second-order design. It is based on a three-level incomplete factorial design, which consists of the center point and middle points like the edge of a cube. It can be considered as three interlocking factorial designs along with center points(Norhaffis et al., 2019).The cellulose nanocrystals production was fitted using a second-order polynomial equation and multiple regression of the data was carried out for obtaining an empirical model related to the most significant factors. The general form of the second-order polynomial equation (Wijaya et al., 2019) is:

$$Y = \beta_0 + \sum \beta_i x_i + \sum \beta_{ii} x^2 + \sum \beta_{ij} x_i x_j \quad (3.1)$$

Where: Y is the predicted response, xi and xj are independent factors, $\beta 0$ is the model intercept, βi is the linear coefficient, βii is the quadratic coefficient and βij is the interaction coefficient.

In this research, the yield of cellulose nanocrystals was conducted using response surface methodology using CCD design where the reaction variables (temperature = A, time = B, and acid concentration = C) were varied to observe its impact on preselected responses of yield (Y%) of finally extracted cellulose nanocrystals. The process optimization was carried out to get maximum yield (Y%) of cellulose nanocrystals. The analysis of variance (ANOVA) such as the regression (R^2), adjusted R^2, predicted R^2 and lack of fit was performed to justify the adequacy and significance of the developed regression model. The three independent variables studied for the hydrolysis process of cellulose were reaction temperature, time, and acid concentration as summarized in the following Table 3.1.

Table 3-1: Independent variables and levels for central composite design (CCD)

Independent variables	Unit	Levels		
		-1	0	1
Temperature	℃	45	52.5	60
Reaction time	Min.	30	45	60
Acid concentration	Wt.%	45	55	65

The response was the yield of cellulose nanocrystals and the selection range of each variable as shown in Table 3.2.

Table 3-2**:**Central composite design (CCD) for CNCs using RSM and experimental data.

		Factor 1	Factor 2	Factor 3	
Std.	Run	A:Temperature, deg c	B:Time, min	C:Acid concentration, wt.%	Yield
6	1	60	30	65	
1	2	45	30	45	
17	3	52.5	45	55	
19	4	52.5	45	55	
4	5	60	60	45	
20	6	52.5	45	55	
2	7	60	30	45	
8	8	60	60	65	
7	9	45	60	65	
9	10	39.89	45	55	
10	11	65.11	45	55	
13	12	52.5	45	38.18	
5	13	45	30	65	
15	14	52.5	45	55	
3	15	45	60	45	
18	16	52.5	45	55	
12	17	52.5	70.23	55	
16	18	52.5	45	55	
14	19	52.5	45	71.81	
11	20	52.5	19.77	55	

3.5. Characterization of corncob

3.5.1. Chemical composition of corncob

The chemical composition of corncob that is cellulose, hemicellulose, lignin, and extractives was analyzed using the gravimetric method under the conditions defined by (Oresegun, & Oladimeji, 2015).

3.5.1.1.Hemicellulose determination

1 g of extracted dried biomass was transferred into a 250 mL flask and then 150 mL of 500molm^{-3} NaOH was added. The mixture was boiled for 3.5 h with distilled water. It was filtered after cooling through vacuum filtration and washed until neutral pH. The residue was dried to a constant weight at 105℃ in a convection oven. The difference between the sample weight before and after this treatment is the hemicellulose content (%w/w) of dry biomass of corncob (Ayeni et al., 2015).

3.5.1.2.Lignin content determination

The lignin content was determined according to the TAPPI norm T222 om-88. Briefly, 1 g of corncob powder was added into the 15 mL H_2SO_4 solution and maintained at room temperature for 2 h. Then, the distilled water, 560 mL, was added and boiled the mixture for 4 h before the centrifuge to get the insoluble lignin. The obtained lignin was oven-dried and weighed. The lignin quantity was determined using Equation(3.3) (Song, & Li, 2019b).

$$\text{Lignin}(\%) = \frac{M_1}{M} \tag{3.2}$$

Where: $M1$ was the obtained lignin mass, M was the initial sample mass.

3.5.1.3.Extractive determination

The extractive was determined by taking 2.5 g of dried raw biomass was loaded into the cellulose thimble. With the soxhlet extractor set up, 150 mL of ethanol and toluene mixtures were used as a solvent for extraction. Residence times for the boiling and rising stages were carefully adjusted to 70 ℃ and 25 min respectively on the heating mantle for a 4 h run period. After extraction, the sample was air-dried at room temperature for a few minute and the constant weight of the extracted material was achieved in a convection oven at 105℃(Ayeni et al., 2015).

3.5.1.4.Determination of Ash Content

The ash content will be determined by using ASTM D2017 (1998). A measured amount of corncob was placed in a pre-weighed crucible is incinerated in a muffle furnace at (750-760)℃ until complete ash will achieve (8-10) min then it transferred to a desiccator for cooling. Then, calculated by

$$\text{Ash content}(\%)=\frac{w_2-w_0}{w_1-w_0}\times 100 \quad (3.3)$$

Where: w_0 = Weight of the crucible, w_1 = Weight of the crucible and sample before incineration and w_2 = Weight of the crucible and sample after incineration.

3.5.1.5.Cellulose content determination

The cellulose content (%w/w) was calculated by difference, assuming that extractives, hemicellulose, lignin, ash, and cellulose are the only components of the entire biomass(Ayeni et al., 2015).

3.5.1.6.Determination of Moisture content

The moisture content of the corncob will be determined by the oven-drying method. The corncob was weighed and then dried at a temperature of $105 \pm 3℃$ until a constant weight was obtained, in accordance with ASTM D1037 (1991). Then it is calculated by the formula.

$$\text{Moisture content}(\%)=\frac{w_0-w_f}{w_0} \quad (3.4)$$

Where: Wo is the initial weight of corncob and Wf is the final weight of corncob

3.6. Characterization of cellulose nanocrystal

3.6.1. Yield

The yield of cellulose nanocrystals after drying with respect to the initial amount of dried corncob cellulose was calculated using the equation (3.5). The yield of cellulose nanocrystals will different as it depends on the temperature, hydrolysis time, and acid concentration parameters. The acid hydrolysis was able to hydrolyze the cellulose chains to separate the crystalline part from the amorphous part and it was used to remove the amorphous regions of the cellulose and release cellulose nanocrystals from the cellulose substrate(Hazman et al., 2015).

$$\text{Yield}(\%) = \frac{W_1}{W_2} \times 100 \quad (3.5)$$

Where: W_1 = represents the dried weight of CNCs obtained after hydrolysis, and W_2 = represents the dried weight of cellulose obtained before hydrolysis.

3.6.2. Scanning Electron Microscopy (SEM)

Scanning electron microscopy (FEI-INSPECT-F50) was performed to observe the morphology and surface structure by scanning the ruptured surface of corncob, alkali-treated corncob, corncob cellulose, and cellulose nanocrystals. It was used to study the effects of various treatments like alkali treatment of sodium hydroxide (NaOH), bleaching ($NaClO_2$) on the morphology of the samples(Chieng & Yoon Yee, 2017). The effectiveness of the alkali treatment of sodium hydroxide (NaOH), bleaching ($NaClO_2$) was evaluated through surface morphology and structure of the cellulose nanocrystal.

According to ASTM E986-04(2017), standard practice for scanning electron microscope beam size characterization, the range of SEM magnification at which this practice is of utility is from 1000 to 50 000 X. Higher magnifications may be attempted, but the difficulty in making precise measurements can be expected(Friel, 2003).

The operation principle for scanning electron microscopy to cross-sectional morphology of the sample was done under vacuum at an accelerating voltage of 2kV and x8984 magnification. All the samples were firstly mounted on the surface of carbon tapes, loading on the top of aluminum stubs. The dirt was cleaned by the air jet and the samples were coated by a fine layer of gold with 20mA for 2 minutes to avoid charge(Manaf et al., 2019).

3.6.3. Particle Size Determination

The dynamic light scattering (DLS) technique (Malvern, Zetasizer Nano ZS) was employed to measure the size of corncob cellulose, and cellulose nanocrystal (Kashaninejad & Barani, 2018). Malvern Zeta sizer nano (ZE3600) is used to measure particle size, zeta potential, and molecular weight of cellulose nanocrystals. According to ASTM E2834-12(2018) standard guide for measurement of the particle size distribution of nanomaterials in suspension by nanoparticle tracking analysis (NTA)(Zheng, & Zhan, 2012). Here the cellulose nanocrystal suspension was diluted with distilled water and the measurement was conducted at 25℃ with a calibration time of 80 seconds. Three measurements were used and the averaging was done.

3.6.4. Thermogravimetric analysis (TGA)

Thermal stability of raw corncob, alkali-treated corncob, corncob cellulose, and cellulose nanocrystals was determined by thermogravimetric analysis(TGA Q500, Thermal Analysis Instruments), which is a technique wherein the loss of mass of a substance is monitored as a function of temperature or time while the sample specimen is subjected to a controlled temperature program in a controlled atmosphere(P. Lu & Hsieh, 2012).

The Thermogravimetric (TGA) curve shows that the loss or gain in weight with a change in temperature and DTG (derivative thermogravimetric) is a type of thermal analysis in which the rate of material weight changes upon heating is plotted against temperature. The range of temperature for DTG and TGA 25 and 100℃ respectively. The analysis conditions for TGA Q500 is a nitrogen atmosphere with a flow of 30 mL min^{-1}, Sampling Cycle 1500, a heating rate of 20℃ min^{-1}, temperature range from 25 to 600℃, sample mass between 5 and 7 mg, and aluminum pans(Henrique& Pasquini, 2013).

3.6.5. Fourier Transform Infrared Spectroscopy (FTIR)

Fourier Transform Infrared Spectroscopy (Thermo SCIENTIFIC iS50 ABX) was used to investigate changes that occur in the chemical structure of raw corncob after chemical treatments (alkaline, bleaching) and acid hydrolysis. The change of the functional groups of raw corncob, alkali-treated corncob, corncob cellulose, and cellulose nanocrystals (CNCs) was investigated using Fourier transform infrared spectroscopy(FTIR) equipped with KBr beam splitter(Evans et al, 2019).

This technique was used to manipulate structural changes in samples and to examine the changes in functional groups induced by various treatments as a result of chemical modification by the identification of the functional group(Chieng &, Yoon Yee, 2017), where the spectra are performed at room temperature in the range of 500 to 4000cm^{-1} with the resolution of 4cm^{-1} and a total of 3736 points for each sample(Kandhola et al., 2020).

3.6.6. X-ray diffraction (XRD)

X-ray diffraction (BTX-528) was used to study the crystalline structure of Corncob, alkali-treated corncob, Corncob cellulose, and cellulose nanocrystals (CNCs).

Here the operating system (measurement Condition) was set at the voltage of 30 kV and current of 40 mA by applying the irradiation of Cu Kalfa (1.54) (Hemmati et al.,2018), at room temperature using a sampling pitch of 0.0200 (deg) and preset time 0.40 (sec)within a 2θ

ranging from 10 to 60^{o} and a scan rate of $3^{o}\,min^{-1}$ in continuous scan mode(Henrique,& Pasquini, 2013).

The reduction of amorphous cellulose and increase of crystalline cellulose was evidenced by the crystallinity index (CrI) analysis(P. Lu & Hsieh, 2012). The crystallinity index (CrI) denotes the ratio of the crystalline constituents to the amorphous regions of material and calculated using the equation (3.6)(Manaf et al., 2019)

$$CrI=\frac{I_{200}-I_{am}}{I_{200}}\times 100 \qquad (3.6)$$

Where: I_{200} is the peak intensity at the plane (200) and I_{am} is the minimum intensity at the valley between the plane (200) and (110)

Crystallite size generally corresponds to the coherent volume in the material for the respective diffraction peak. Sometimes, it also corresponds to the size of the grains of a powder sample, or the thickness of the polycrystalline thin film or bulk material(Kumar, & Joshi, 2017). The Scherrer's equation is used for the determination of the size of particles of crystals in the form of powder, which can be represented as follows:

$$d=\frac{\kappa\lambda}{\beta\cos\theta} \qquad (3.7)$$

in which, d is the mean size of the ordered (crystalline) domains, k is a shape factor constant value of 0.9, β represents full-width half maximum of maximum (FWHM) intensity in radians and λ is constant radiation with the value of 0.1574 nm and θ is the Braggs' angle (deg.).

CHAPTER 4 RESULTS AND DISCUSSION

4.1. Yield

Cellulose was successfully isolated from cleaned and dried raw corncob powder through a straight forward process of dewaxing, alkaline treatment, and bleaching. The color of the raw corncob powder was reduced with each step of the delignification process as lignin and hemicellulose removal. After that cellulose nanocrystals were produced by sulfuric acid hydrolysis and the yields of the cellulose nanocrystals with respect to the initial amount of dried corncob cellulose were calculated by using the equation (3.5).

The maximum yield of cellulose nanocrystal(41.8%) was obtained at the interaction parameters of t temperature of 45℃, hydrolysis time of 60 min, and acid concentration of 65wt.%. Under this condition of parameter interaction, the predicted yield of cellulose nanocrystal (CNC) by using experimental design was obtained 41.50%. These values are consistent with the literature data(Oliveira,&Pasquini,2013).

The decrease in the level of cellulose nanocrystal yield by employing higher acid concentration may be related to the hydrolysis process in which cellulose is degraded into its building blocks namely glucose. The acid hydrolysis was able to hydrolyze the cellulose chains to separate the crystalline part from the amorphous part(Park, & Lee, 2017).

Higher levels of acid may also degrade the crystalline parts of the corncob cellulose in addition to the amorphous part that lowers the production yield of cellulose nanocrystals. On the other hand, the treatments with low acid concentrations result in low dispersity values or aggregation of the structures. The increase in the time and temperature of the hydrolysis process higher than the maximum point may generate glucose employing the degradation of cellulose which in turn lowers the production yield of the cellulose nanocrystals.

These differences in yield of the cellulose nanocrystals in Table 4.9 may be related to the different cellulose nanocrystal yield calculation methods, nature of the utilized raw materials, acid concentration, hydrolysis time, and the temperature plus the formulation conditions during the production of CNCs(Kashaninejad, & Barani, 2018). The yield of cellulose nanocrystals and the selection range of each variable was shown in Table 4.9.

4.2. Chemical composition of corncob

The chemical composition of corncob was determined according to TAPPI standards and the present result found for the cellulose, hemicellulose, and lignin content of the corncob under analysis Table 4.1 are consistent with the work described by (Kim, & Nanoparticles, 2015).

High hemicellulose content should absorb more moisture so pretreatment basically removes the recalcitrance nature of biomass by disrupting and removing these components. Hence, after pretreatment the composition of hemicellulose and lignin component decrease while cellulose increase. Besides, higher quantities of extractives may promote fiber degradation at low temperatures(Matheus Poletto, 2014)

Table 4-1:The proximate analysis of corncob

Component	Composition(wt.%)
Cellulose	45
Hemicellulose	35
Lignin	13.3
Extractives	5
Ash content	1.7
Moisture content	30

4.3. Morphological analysis

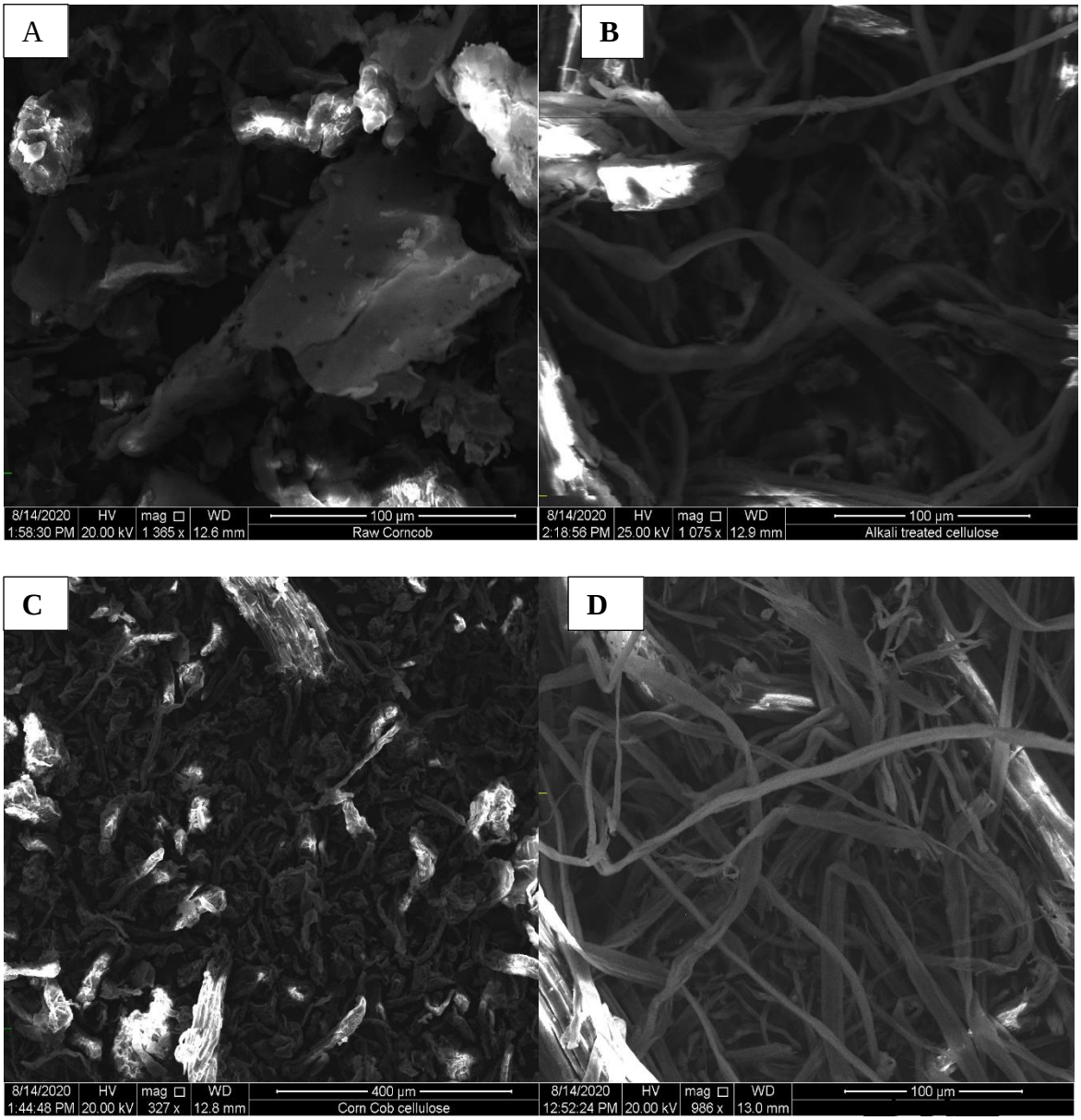

Figure 4-1:SEM images of (a)raw corncob, (b) alkali-treated corncob, (c)corncob cellulose, (d) and CNC.

From these four images, it is clear that the morphology of the raw corncob changed with each chemical treatment concerning surface smoothness and size(Espino et al.,2014).In Figure 4.1a, the raw corncob fibers have become narrow fibrils and reticular structure which is an indication of composed of hemicellulose and lignin. But Figure 4.1b shows the morphology of the alkali-treated corncob and the fiber appeared smoother than the raw corncob, due to hemicellulose has an amorphous structure that was hydrolyzed and got to be water-soluble.

The SEM image of the corncob cellulose in Figure 4.1c shows that the fiber appeared even smoother than the alkali-treated corncob and it is a micro-sized fiber that exhibits an irregular

shape. Compared to raw and alkali-treated corncob, the surface of corncob cellulose (Figure 4.1c) became rougher and cleaner, indicating the effective removal of the hemicellulose and the lignin by the chemical treatments. This is also an indication of the process of purifying and bleaching did not break the cellulose structure, and there were no impurities in it(Zheng, & Liu, 2013).

Figure 4.1d shows the scanning electron microscopy images of cellulose nanocrystals after the corncob cellulose was hydrolyzed by sulfuric acid treatment. The rod shape of cellulose nanocrystal as shown is so small, this is due to the concentration of sulfuric acid and hydrolysis time is so high, that affects the crystalline part of cellulose after destroying the amorphous region(Bhattacharya,&Goswami, 2020).

The features of the CNC showed that there was a reduction in the fibrillar structure size and intermittent breakdown in fibrillar structure into individualizing fibrils. These findings agreed with the findings of(Zanon, & Menegalli, 2017). The results of the morphological investigation by SEM are consistent with other reports in the literature, where CNC was extracted from different sources (P. Lu & Hsieh, 2012, Alves et al., 2013, Peña-Rodriguez, & Arbelaiz, 2017).

4.4. Particle size analysis

The measurement was conducted at room temperature and the particle size distribution of cellulose nanocrystals was obtained from diffusion light scattering (DLS) techniques. Figure 4.2 shows the particle size distribution for corncob cellulose indicating an average particle size (diameter) of 1963nm at a measurement position of 0.85mm and a count rate of 9.1(kcps). But Based on the results obtained from dynamic light scattering illustrated in Figure 4.3 indicates that the intensity of particle size distribution of CNC produced under the condition of the optimized yield at a desirable parameter interaction of acid concentration, reaction time, and the temperature is an average particle size (diameter) of 170.3nm at measurement position of 0.85mm and count rate of 9.4(kcps).

This average particle size (170.3nm) is a good result that shows the extraction of cellulose nanocrystals from corncob is possible since cellulose nanocrystals have a length in the range of 100-1000 nm (Pereira & Arantes, 2018b) and a width between 2 and 15 nm(Patients et al., 2012) depending on the cellulose source and the chemical treatment applied. Compared to corncob cellulose particle size (1963nm), the particle size of CNC (170.3nm) was much smaller, this is because the average particle size (diameter) of CNC depends on hydrolysis parameters that affect the yield.

Polydispersity Index (PDI) is dimensionless and scaled such that values smaller than 0.05 are rarely seen other than with highly monodisperse standards. Values greater than 0.7 indicate that the sample has a very broad size distribution and is probably not suitable for the DLS technique(Fan & Li, 2012).

Table 4-2:Particle size of corncob cellulose

			Size (d. nm):	% Intensity:	Standard Dev (d. nm)
Z-Average(d.nm)	1963	Peak 1:	909.3	100.0	150.4
PdI	0.763	Peak 2:	0.000	0.0	0.000
Intercept	0.840	Peak 3:	0.000	0.0	0.000
Result quality	GOOD				

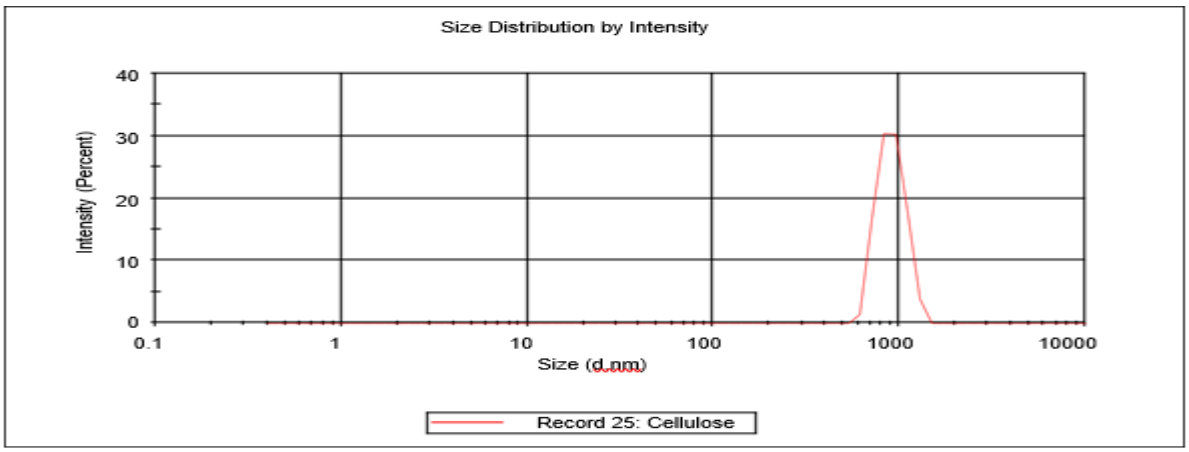

Figure 4-2:Size distribution report for corncob cellulose by the intensity

The analysis of the sample of corncob cellulose powder dispersed in water by particle size analyzer showed in Figure 4.2. The percentage shown for the peak represented the amount of each peak concerning the overall number of particles counted. The peak, the recorded particle size was 909.3 nm and it accounts for 100 percent of the overall intensity distribution.

Table 4-3:Particle size of cellulose nanocrystals by the intensity

			Size (d. nm):	% Intensity:	Standard Dev (d. nm)
Z-Average(d.nm)	170.3	Peak 1:	119.5	100.0	24.63
PdI	0.552	Peak 2:	0.000	0.0	0.000
Intercept	0.823	Peak 3:	0.000	0.0	0.000
Result quality	GOOD				

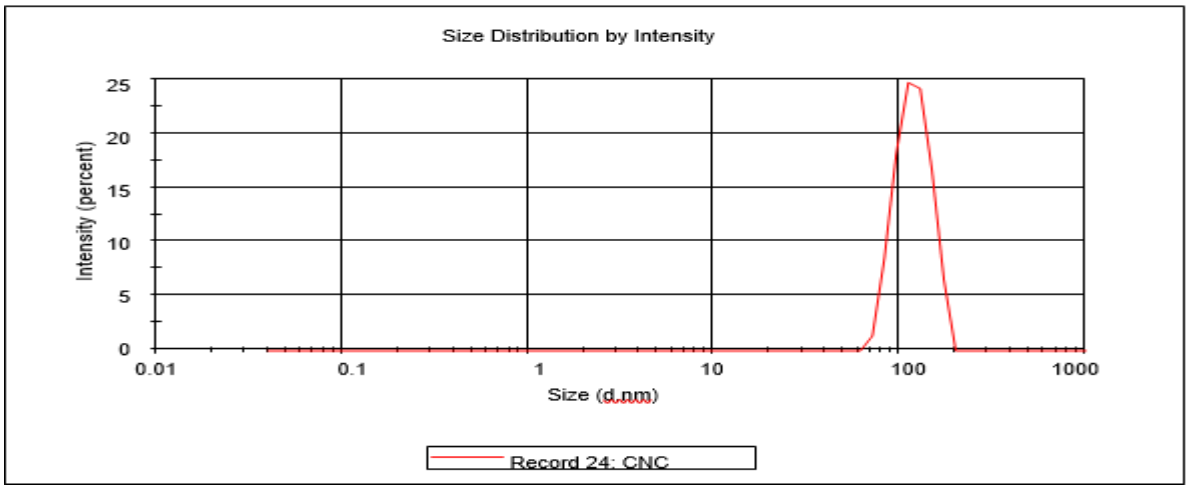

Figure 4-3:Size Distribution Report of CNC by Intensity

Size distribution by intensity data shows that CNC particles with a smaller size of 170.3 nm account for 100% intensity with 24.63 standard deviations.

Table 4-4: Particle size of cellulose nanocrystals by volume

			Size (d.nm):	% volume:	Standard Dev (d.nm)
Z-Average(d.nm)	170.3	Peak 1:	125.4	100.0	249.9
PdI	0.552	Peak 2:	0.000	0.0	0.000
Intercept	0.823	Peak 3:	0.000	0.0	0.000
Result quality	GOOD				

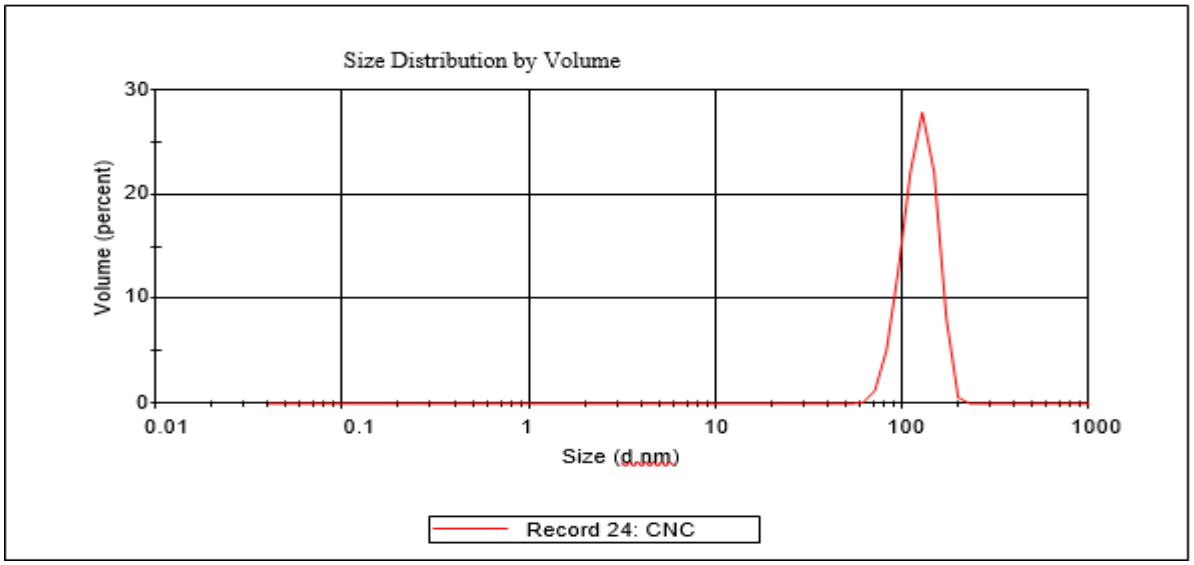

Figure 4-4:Size Distribution Report for CNC by Volume

As shown in Table 4.5 and Figure 4.4. Size distribution by volume for cellulose nanocrystals has one peak 125.4 nm(diameter) size that accountable for 100% of volume and the CNCs particles have an average diameter of 170.3 nm with Standard Deviation (249.9nm) diameter.

4.5. Thermogravimetric (TGA) analysis

The thermal stability of the raw corncob, alkaline treated corncob, corncob cellulose, and the CNC can be determined by using thermogravimetric analysis (TGA).

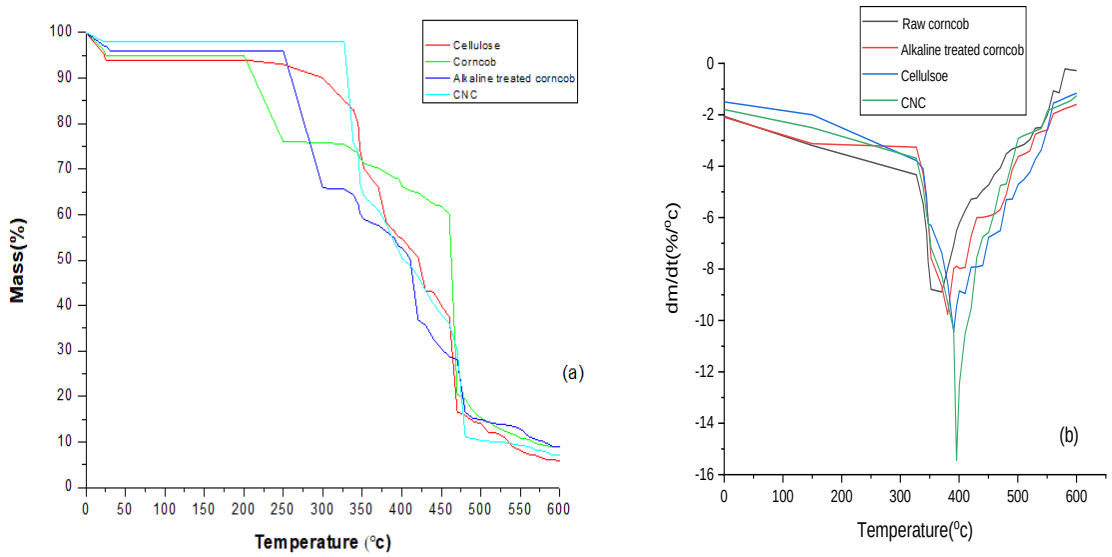

Figure 4-5:shows(a) TGA and (b) DTG curves of raw corncob, alkali-treated corncob, corncob cellulose, and CNC.

From the TGA curves in Figure 4.5a, there are three stages of thermal degradation in the form of weight loss were observed. The first stage of the elimination of some volatile compounds mass loss and occurring between room temperature and 160℃, which is attributed to the presence of water absorbed or bound to the fibers.But the second stage is between 160 and 450℃ occurs the loss of mass is attributed to the thermal degradation of organic compounds, such as cellulose, hemicellulose, and lignin. This first degradation step corresponds basically to cellulose degradation processes(Dantas,& Pasquini,2013). The final stage of rapid depolymerization of carbon residues occurred after 450 °C and values in the three stages of thermal degradation are consistent with the values of isolation and characterization of cellulose nanocrystals from jackfruit peel by(Trilokesh & Uppuluri, 2019).

For raw corncob, there is a slight weight loss at 25℃, which corresponds to the initial thermal decomposition. After the initial mass loss, the degradation of raw corncob was followed by a drastic weight loss at 200–250℃, and then there was a weight loss up to 450℃. But for alkaline

treated corncob the first degradation temperature is 250℃, and for corncob cellulose, the first degradation is 270℃. Here the chemical treatments (alkaline treatment, bleaching, and acid hydrolysis) can affect the degradation temperature of a raw corncob.

As we saw in Figure 4.5a the degradation temperature of corncob is lower than alkaline treated corncob, corncob cellulose, and cellulose nanocrystals (CNC). The lower degradation onset temperature of raw corncob compared to that of alkaline treated corncob, corncob cellulose, and CNC, is due to the presence of lignin, hemicellulose, and other extractives which decompose at low temperature(Peña-Rodriguez, & Arbelaiz, 2017).

From the TGA curve of Figure 4.5a for cellulose nanocrystals, the initial onset of degradation around 327℃, and there is a significant weight loss in the range of 482℃. But in general, the thermal decomposition temperature of cellulose is about 300℃ and meets the requirements of the thermal processing of composite materials. However, the normal extraction method uses sulfuric acid for hydrolysis, which makes it easy to introduce the sulfate ester groups ($O-SO3$) as a substitute for hydroxyl groups during acid hydrolysis the CNCs obtained, leading to the diminishment of the thermal stability and the thermal decomposition onset temperature of CNCs(Chang et al., 2019).

Moreover, based on the DTG (derivative thermogravimetric) curve which measures give as the mass difference with temperature change.As shown in Figure 4.5(b) the thermal decomposition peaks of the maximum weight loss for raw corncob, alkaline treated corncob, corncob cellulose, and cellulose nanocrystals appear at 350,380,390 and 400℃, respectively. Decomposition of raw corncob, alkali-treated corncob, corncob cellulose, and cellulose nanocrystals are different, indicating the presence of different components that decompose at different temperatures(P. Lu & Hsieh, 2012).

All of the above results from the TGA and DTG graphs indicate that the thermal stability of CNC is higher than that of corncob cellulose and alkaline treated corncob. However, some publications reported that the thermal stability of cellulose nanocrystal prepared by sulfuric acid hydrolysis was lower than that of native cellulose(Q. Lu et al.,2014). This phenomenon occurred because the presence of sulfate groups decreased the thermal stability by the dehydration reaction(Neto, & Pasquini, 2013). Usually, the higher sulfate group content in cellulose leads to a lower temperature of thermal degradation of cellulose.

Table 4-5:Onset and peak degradation temperatures

Samples	Onset temperature (℃)	Peak temperature (℃)
Corncob	200	472
Alkali treated corncob	250	470
Corncob cellulose	270	487
CNC	327	482

4.6. Fourier transform infrared (FTIR) spectroscopy analysis

The Fourier transform infrared (FTIR) spectroscopy technique was carried out to study the functional groups present in raw corncob, alkaline treated corncob, corncob cellulose, and cellulose nanocrystals (CNCs).

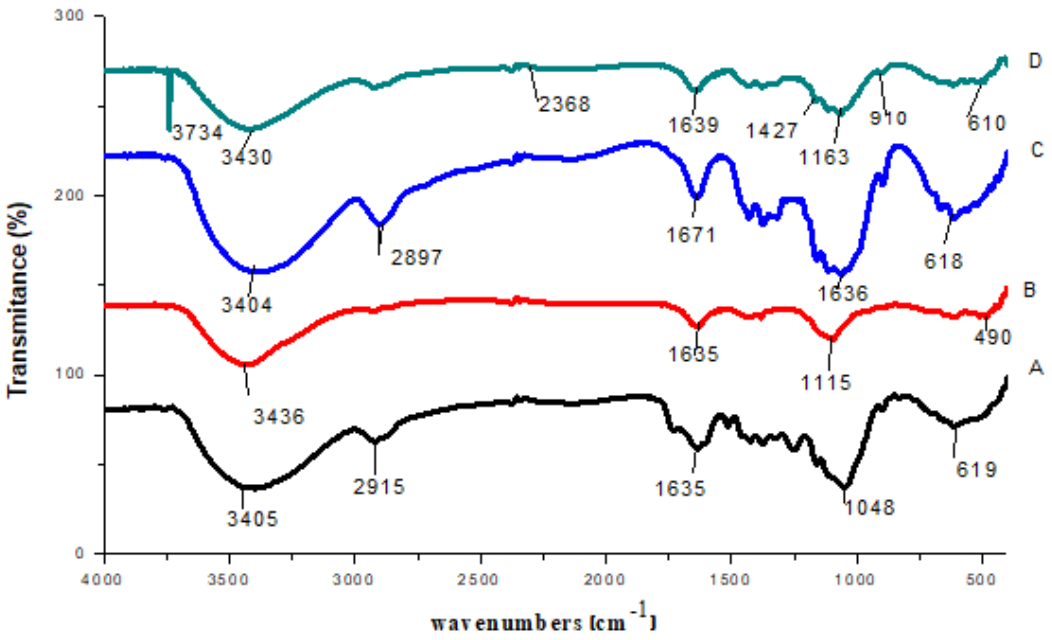

Figure 4-6:FTIR spectra of (a) raw corncob, (b) alkali-treated corncob, (c) corncob cellulose, and (d) CNC.

In Figure 4.6a and b broad peaks at 3405 and 3436cm^{-1} was observed in both raw corncob and alkaline treated corncob samples respectively, associated with the hydrogen bond O – H stretching vibration, which is indicative of the hydrophilic tendency of the fibers(Singh et al., 2017). Another peak that is present only in the spectrum of raw corncob is 2915cm^{-1} which is in the range of 3000 to 2850 cm^{-1} due to C – H stretching for alkanes and aromatics(Yoon

Yee et al., 2017).The peak at 1635 cm^{-1} represented the $C = C$ stretching vibration of the lignin which means indicative of the presence of lignin.

In Figure 4.6b for alkaline treated corncob, the C=O stretching vibration of the carbonyl and acetyl groups disappears due to the removal of carboxylic groups, which may be traces of fatty acids present on the fiber surface. The peaks 1635,1115 and 490 cm^{-1} in alkaline treated corncob indicates medium C=C stretching alkene, medium O−H bending carboxylic acid, and strong C−O stretching secondary alcohol group respectively(Orue et al., 2017).

In Figure 4.6c, the peaks found at 2897 and 1671 cm^{-1} in the case of corncob, cellulose indicates the presence of medium C-H stretching of alkane and weak $C \equiv C$ stretching of alkyne group respectively. The peaks at 2368 and 1639cm^{-1} in Figure 4.6d were attributed to the stretching vibrations of $O - H$ bending and $C - O$ stretching respectively(Singh et al.,2017).

The intensity of these peaks is sharply weakened after acid hydrolysis treatment, because of the removal of the main hemicellulose material. The small peak at 1163 cm^{-1}in the spectrum of CNC is related to $S = O$ vibration, due to the esterification reaction which occurred in the hydrolysis process.The FTIR spectra showed that the acid hydrolysis treatment did not affect the chemical structure of the CNCs isolated from the corncob (Alves et al., 2013).

4.7. X-ray diffraction (XRD) analysis

The X-ray diffraction patterns were obtained to determine the crystalline index of the raw corncob, alkali-treated corncob, corncob cellulose, and cellulose nanocrystals. The crystallinity index (CrI) refers to the ratio of the crystalline to the amorphous regions of cellulose(Yoon Yee et al., 2017).

Cellulose has a crystalline structure, unlike hemicellulose and lignin. The cellulose crystallinity is due to the interactions between hydrogen and Van der Waals forces between adjacent molecules. X-ray diffraction (Figure 4.7) was used to determine if there were changes in material crystallinity after different chemical treatments.

The diffraction peak for raw corncob as shown in Figure 4.7 was relatively broader and became sharper and narrower after chemical treatments (alkaline and bleaching). But the peak of cellulose nanocrystals was sharper and narrower. This indicates that the content of cellulose and the degree of crystallinity was increased and the crystallinity of cellulose is affected by chemical treatments(Thakur et al., 2020).

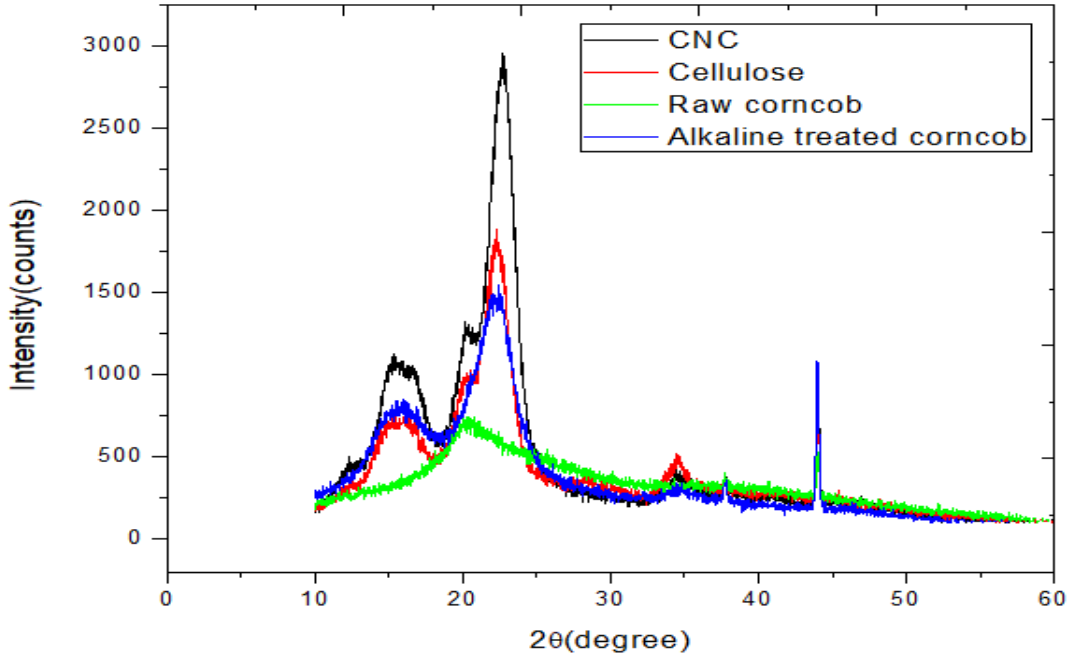

Figure 4-7:X-ray diffractogram of raw corncob, alkaline treated corncob, corncob cellulose, and cellulose nanocrystals.

As shown in the above Figure, cellulose nanocrystal has a sharp and large peak, this is due to the amorphous parts of the raw corncob were removed by alkaline, bleaching, and acid hydrolysis treatments. All have the particularity that they show a peak of around 2θ= 22 degrees.

The crystallinity index(CrI) calculated by the equation (3.6) for raw corncob, alkaline treated corncob, corncob cellulose, and cellulose nanocrystals were 57.88,60.74,76.43 and 79.31 respectively. The higher CrI value of corncob cellulose compared to raw corncob and alkaline treated corncob can be well understood by the reduction and removal of amorphous non-cellulosic compounds induced by the alkali and bleaching treatments performed in the purification process.

The increase in the CrI (%) value of cellulose nanocrystals in regard to corncob cellulose was also observed, due to the partial removal of the paracrystalline domains during the acid hydrolysis. It can be observed that the acid treatment results in narrow, sharper peaks for the cellulose nanocrystals, because of the higher crystallinity of such nanostructures, compared to the raw fibers (Teixeira et al., 2010).

Table 4-6:Crystallinity index of corncob,alkaline treated corncob,corncob cellulose, and CNCs.

Samples	2θ (amorphous)(°)		2θ (002) (°)		CrI (%)
	Degree	Intensity (I_{am})	Degree	Intensity(I_{002})	
Raw Corncob	34.12	310	20.15	736.41	57.88
Alkaline treated corncob	19.12	603.08	22.31	1536.27	60.74
Corncob cellulose	17.86	445.04	22.42	1887.87	76.43
CNC	17.86	598.72	22.75	2893.5	79.31

After alkali treatments and elimination of hemicellulose and lignin present in raw corncob and following acidic hydrolysis by sulfuric acid, amorphous regions in cellulose structure are removed and the crystallinity index is enhanced. Here, after acidic hydrolysis, the crystallinity index was raised from 57.88 to 79.31%. The increase in the crystallinity index for the raw corncob was due to the removal of hemicellulose and lignin, which exist in amorphous regions. This value is consistent in studies using acidic hydrolysis, the crystallinity index was between 64 and 91%; however, in most cases it was around 70%(Hernandez, & Rosa, 2018).

The crystallinity degree is dependent on the source of the raw materials, purification time of the sample, and hydrolysis conditions(Hemmati et al.,2018). From Figure 4.8d there are 11 peaks and the crystallite size calculated by using the equation(3.7) for cellulose nanocrystals were shown in the following Table 4.7.

Table 4-7: Peak data list and average crystallite size for cellulose nanocrystals

Peak no.	2θ (deg)	d(A)	I/I1	FWHM (deg)	Intensity (Counts)	Integrated Intensity (Counts)
1	12.484	7.08448	6	1.68000	95	9614
2	15.393	5.75140	27	2.23200	449	37127
3	16.531	5.35822	24	2.14280	399	35354
4	20.321	4.36644	33	1.60000	546	52367
5	22.666	3.91980	100	2.00700	1662	161652
6	25.190	3.53245	4	1.00000	73	8736
7	34.708	2.58251	6	2.06000	94	10890
8	37.802	2.37795	4	0.70670	67	3898
9	44.008	2.05593	16	0.56400	262	7620
10	64.368	1.44617	12	0.56140	199	5818
11	77.473	1.23102	13	0.55070	210	5761

4.8. Experimental Design Analysis

In this study, Response surface modeling based on the central composite design (CCD) was used to determine the effect of each parameter on the yield of cellulose nanocrystals (CNCs). The relationship between the factors and the performance measures are expressed by multiple regression equations, which can be used to estimate the expected values of the performance level for any factor levels.

The experimental result was analyzed using Design-Expert v11 software to develop a single model equation that can describe the hydrolysis parameters significance. The dependent variable used as a response parameter was the yield of cellulose nanocrystal. All experiments were carried out in a randomized order to minimize the effect of unexpected variability in the observed response due to extraneous factors. As shown in Table 4.8 the suggested choice of model was a quadratic model that fits the data.

Table 4-8:Model Summary Statistics

Source	Std.Dev.	R^2	Adjusted R^2	Predicted R^2	PRESS	
Linear	4.13	0.2811	0.1463	-0.2289	467.46	
2FI	2.69	0.7532	0.6392	0.4198	220.71	
Quadratic	**0.3680**	**0.9964**	**0.9932**	**0.9882**	**4.49**	**Suggested**
Cubic	0.4249	0.9972	0.9910	0.9452	20.84	Aliased

The regression model was found to be highly significant with the correlation coefficients of determination of R^2, adjusted R^2, and predicted R^2 having a value of 0.9964,0.9932 and 0.9882 respectively.It implies that 99.64% of the total variation in data was explained by the regression model and indicating a good fit between the model and experimental data.

R-squared is a goodness-of-fit measure for linear regression models. This statistic indicates the percentage of the variance in the dependent variable that the independent variables explain collectively. R-squared measures the strength of the relationship between your model and the dependent variable on a convenient 0 – 100% scale. In general, the coefficient of determination R^2 is defined to be the ratio of the explained variation to the total variation, which reflects the degree of fitness of the model. A big value of R^2 indicates the good relevance of the dependent variables in the model. Acceptable values of adjusted R^2 were indicative of the good accuracy of the model in predicting CNCs yields within the experimental ranges tested in this study.

4.9. Model equation

A model equation is a mathematical correlation that expresses the relation between the factors and the response. The model equation was developed to show the correlation between the hydrolysis parameters and yield of cellulose nanocrystals (CNCs). Design expert v11 software, a quadratic model was found to be adequate for the prediction of the given yield as shown by the following equation.

Final Equation in Terms of Coded Factors

$$\begin{aligned}\text{Yield}=&39.64-1.90A+0.3455B-2.03C-1.24AB\\&-4.56AC+0.3125BC-1.43A^2-0.9019B^2-2.14C^2\end{aligned} \tag{3.8}$$

where: A is the Temperature (℃), B is the time(min)and C is the acid concentration (wt.%), of the reaction.

The equation in terms of coded factors can be used to make predictions about the response for given levels of each factor. By default, the high levels of the factors are coded as +1 and the low levels are coded as -1. The coded equation is useful for identifying the relative impact of the factors by comparing the factor coefficients.

Final Equation in Terms of Actual Factors

$$\begin{aligned}\text{Yield}=&-276.455+6.26\times\text{Temperature}+0.8467\times\text{Time}+5.25\times\text{Acid concentration}\\&-0.011\times\text{Temperature}\times\text{Time}-0.0608\times\text{Temperature}\times\text{Acid concentration}\\&+0.02083\times\text{Time}\times\text{Acid concentration}-0.025462\times\text{Temperature}^2-0.00401\times\text{Time}^2\\&-0.021393\times\text{Acid concentration}^2\end{aligned} \tag{3.9}$$

The equation in terms of actual factors can be used to make predictions about the response for given levels of each factor. Here, the levels should be specified in the original units for each factor. This equation should not be used to determine the relative impact of each factor because the coefficients are scaled to accommodate the units of each factor and the intercept is not at the center of the design space.

Table 4-9: CCD matrix of independent variables with an experimental and predicted value

		Factors			Yield(Y%)	
Std	Run	A:Temperature , deg c	B:Time , min	C:Acid concentration ,wt.%	Experimental	Predicted
6	1	60	30	65	27.50	27.26
1	2	45	30	45	33.50	33.26
17	3	52.5	45	55	39.60	39.64
19	4	52.5	45	55	40.00	39.64
4	5	60	60	45	38.80	38.66
20	6	52.5	45	55	39.80	39.64
2	7	60	30	45	40.90	41.07
8	8	60	60	65	26.00	26.10
7	9	45	60	65	41.80	41.50
9	10	39.89	45	55	38.60	38.79
10	11	65.1	45	55	32.40	32.40
13	12	52.5	45	38.18	37.00	37.00
5	13	45	30	65	37.70	37.71
15	14	52.5	45	55	39.00	39.61
3	15	45	60	45	35.70	35.80
18	16	52.5	45	55	39.30	39.64
12	17	52.5	70.23	55	37.60	37.67
16	18	52.5	45	55	40.20	39.64
14	19	52.5	45	71.82	30.00	30.19
11	20	52.5	19.77	55	36.40	36.51

4.9.1. Model Adequacy Checking

The model was tested for adequacy by analysis of variance. The sequential model sum of squares, model summary statistics, and the analysis of variance for the Quadratic model are shown in Tables 4.10,4.11,4.12 respectively. With the sum of squares analysis, only the p-value of the quadratic model is **<0.0001** (Table 4.10), which means that the quadratic model is significant. With variance analysis, the F value of the quadratic model is **311.04** (Table 4.12) and the lack of fit value is **0.3608** (Table 4.11), which indicates that the quadratic model is fit for the experimental design.

Table 4-10:Sequential Model Sum of Squares

Source	Sum of Squares	Df	Mean Square	F-value	p-value	
Mean vs Total	26776.56	1	26776.56			
Linear vs Mean	106.92	3	35.64	2.09	0.1425	
2FI vs Linear	179.56	3	59.85	8.29	0.0024	
Quadratic vs 2FI	**92.54**	**3**	**30.85**	**227.82**	**< 0.0001**	**Suggested**
Cubic vs Quadratic	0.2709	4	0.0677	0.3753	0.8190	Aliased
Residual	1.08	6	0.1805			
Total	27156.94	20	1357.85			

Select the highest order polynomial where the additional terms are significant and the model is not aliased.

Table 4-11:Lack of Fit Tests

Source	Sum of Squares	Df	Mean Square	F-value	p-value	
Linear	272.46	11	24.77	124.47	< 0.0001	
2FI	92.90	8	11.61	58.35	0.0002	
Quadratic	**0.3590**	**5**	**0.0718**	**0.3608**	**0.8562**	**Suggested**
Cubic	0.0880	1	0.0880	0.4423	0.5354	Aliased
Pure Error	0.9950	5	0.1990			

Table 4-12: ANOVA for response surface quadratic model

Source	Sum of squares	DF	Mean square	F value	Prob > F	
Model	379.02	9	42.11	311.04	< 0.0001	Significant
A	49.22	1	49.22	363.54	< 0.0001	
B	1.63	1	1.63	12.04	0.0060	
C	56.07	1	56.07	414.13	< 0.0001	
A^2	29.56	1	29.56	218.33	< 0.0001	
B^2	11.72	1	11.72	86.58	< 0.0001	
C^2	65.96	1	65.96	487.13	< 0.0001	
AB	12.25	1	12.25	90.48	< 0.0001	
AC	166.53	1	166.53	1229.95	< 0.0001	
BC	0.78	1	0.78	5.77	0.0372	

Residual	1.35	10	0.14			
Lack of Fit	0.36	5	0.072	0.36	0.8562	Not signficatnt
Pure Error	1.00	5	0.20			
Cor Total	380.38	19				

The Model F-value of **311.04** implies the model is significant. There is only a 0.01% chance that a Model F-value this large could occur due to noise. Values of Prob > F less than 0.0500 indicate model terms are significant.

In this case, A, B, C, A^2, B^2, C^2, AB, AC, BC are significant model terms. Values greater than 0.1000 indicate the model terms are not significant.

The Lack of Fit F-value of 0.36 implies the lack of fit is not significant relative to the pure error. There is an 85.62% chance that a lack of fit F-value this large could occur due to noise. A non-significant lack of fit is good .we want the model to fit. The ANOVA results prove that the response surface models for predicting the yield of cellulose nanocrystals are considerably coherent. Furthermore, the ANOVA results showed a desirable and coherent agreement with the adjusted R^2.

Therefore, the use of the quadratic models could be used to optimize the system under the same given condition instead of the conventional method. The temperature of the reaction, concentration of sulphuric acid, and time are taken for the reaction have a significant effect on the response as indicated by the value of P which is less than 0.05 (Table 4.12).

The adequate precision ratio and the low values of the coefficient of variation (CV) validated the reliability and good precision of the models as shown in Table 4.13. A precision greater than 4 indicated that the model was significant while the CV should be ≥ 0.1.

Table 4-13: Fit Statistics

Std. Dev.	0.368	R-Squared	0.9964
Mean	36.59	Adj R-Squared	0.9932
C.V.	1.01	Pred R-Squared	0.9982
PRESS	4.49	Adeq Precision	59.176

The Predicted R^2 of 0.9882 is in reasonable agreement with the Adjusted R^2 of 0.9932; i.e. the difference is less than 0.2. Adeq Precision measures the signal to noise ratio. A ratio greater than 4 is desirable. The ratio of 59.176 indicates an adequate signal. This model can be used to navigate the design space. Multiple regression coefficients R^2 is calculated from the second-degree polynomial equation is 0. 998.

The adequacy of the model was further checked with analysis of variance (ANOVA) as shown in Table 4.12, based on a 95% confidence level. F - value is a test for comparing model variance with residual (error) variance.

As shown in Figure 4.8 below the result demonstrates that the regression model equation provides a very accurate description of the experimental data, in which all the points are very close to the line of a perfect fit. All valves for 20 numbers of the experiment were shown in the Table of diagnostics case statistics with its residual and leverage values (Appendix C).

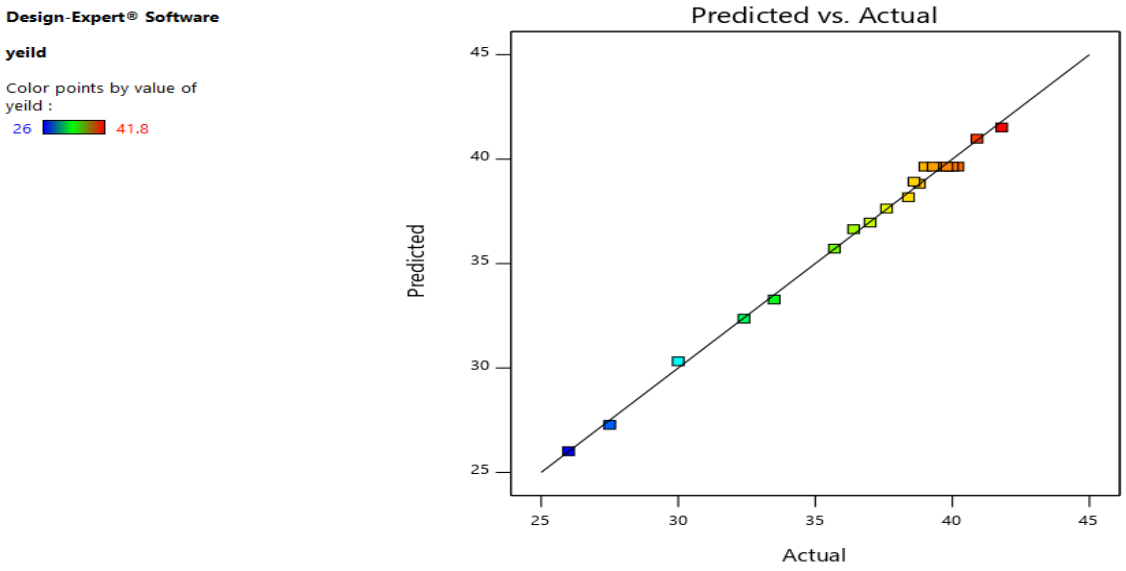

Figure 4-8: Actual versus predicted data plot of response values in the regression model.

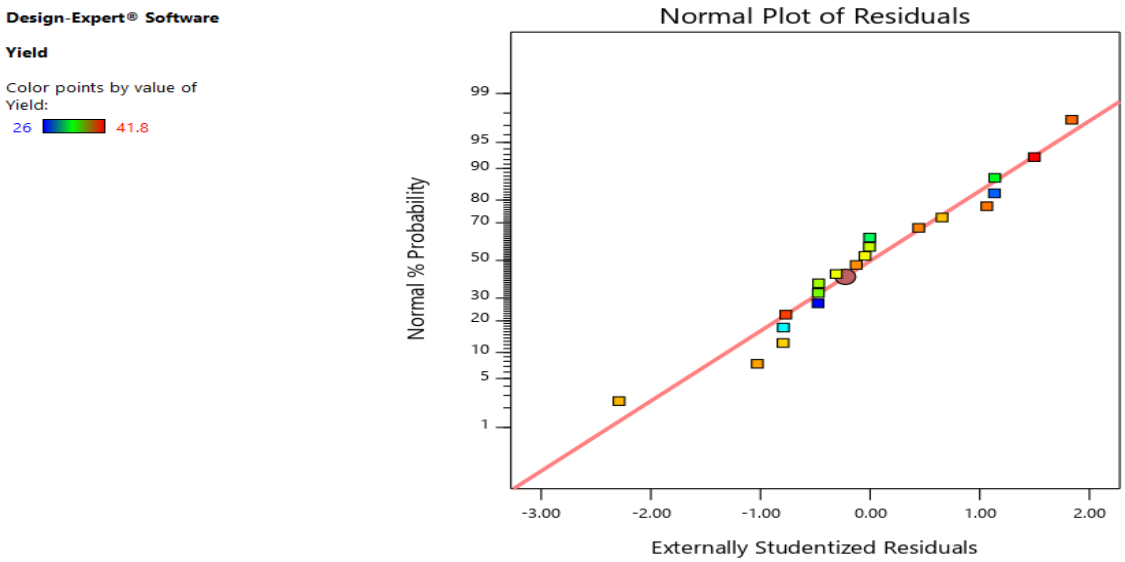

Figure 4-9:Normal probability plot for the residuals from the CNCs yield model.

4.10. Effects of experimental variables on the yield Cellulose nanocrystals

4.10.1. Individual Effect of Factor on the yield of cellulose nanocrystals

The yield of cellulose nanocrystals was affected by sulfuric acid concentration, hydrolysis temperature, and reaction time. Individual effects using a design expert software graph were used to investigate the cause-effect interaction of three process variables: temperature (45- 60 °C), hydrolysis time (30-60 min), and concentration (45-65 wt.%).

4.10.1.1. Effect of acid concentration on the yield of cellulose nanocrystals

The effect of acid concentration on the yield of cellulose nanocrystals when the temperature was 52.5℃ and hydrolysis time was 45 minutes, the results were shown in Figure 4.10. In this part, therefore, we intended to investigate the effect of sulfuric acid concentration condition on the yield of the prepared cellulose nanocrystals

As shown in the Figure, the yield of CNCs is increased at the starting of hydrolysis with increasing acid concentration. This is due to the high penetration of acid to the amorphous part of cellulose which enhances the conversion of cellulose to CNCs. The yield reaches its optimum at an acid concentration of 51.04 wt.% and then decreased with further increasing of acid concentration up to 65wt.% due to the over degradation of cellulose to undesired products.

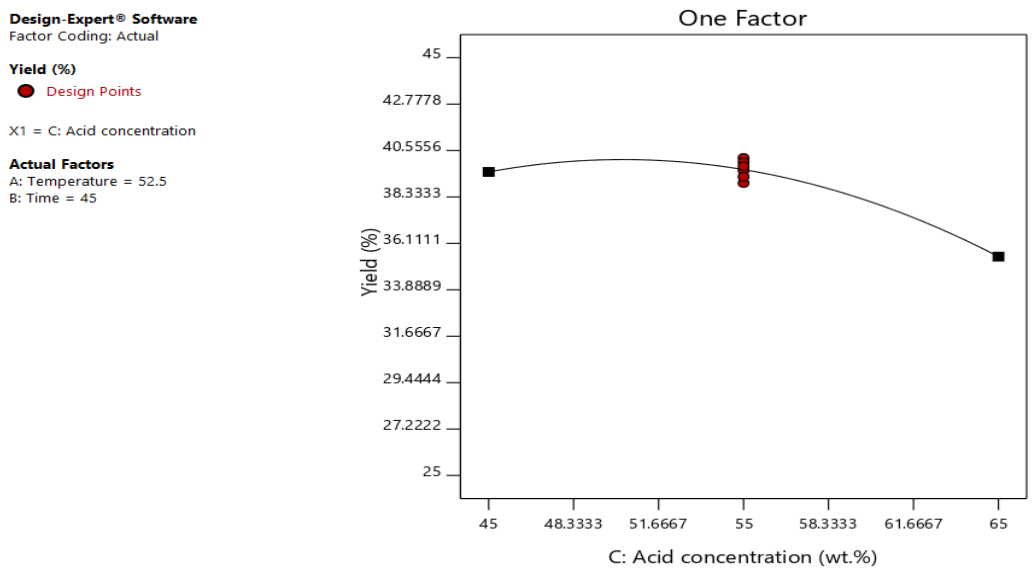

Figure 4-10:Effect of acid concentration on the yield of CNCs

4.10.1.2. Effects of temperature on yield of cellulose nanocrystals

The effect temperature on the yield of cellulose nanocrystals when the acid concentration was 55 % and the hydrolysis time was 45 minutes, the results were shown in Figure 4.11. As shown in the Figure, at the lower level of temperature, the yield is lower and increased with increasing the temperature since the increment of the temperature enhances the hydrolysis reaction at the starting of the reaction. After it reaches the optimum value at around 47.5℃, increasing the temperature lowers the values of the yield due to another to the over the degradation of cellulose as temperature further increased.

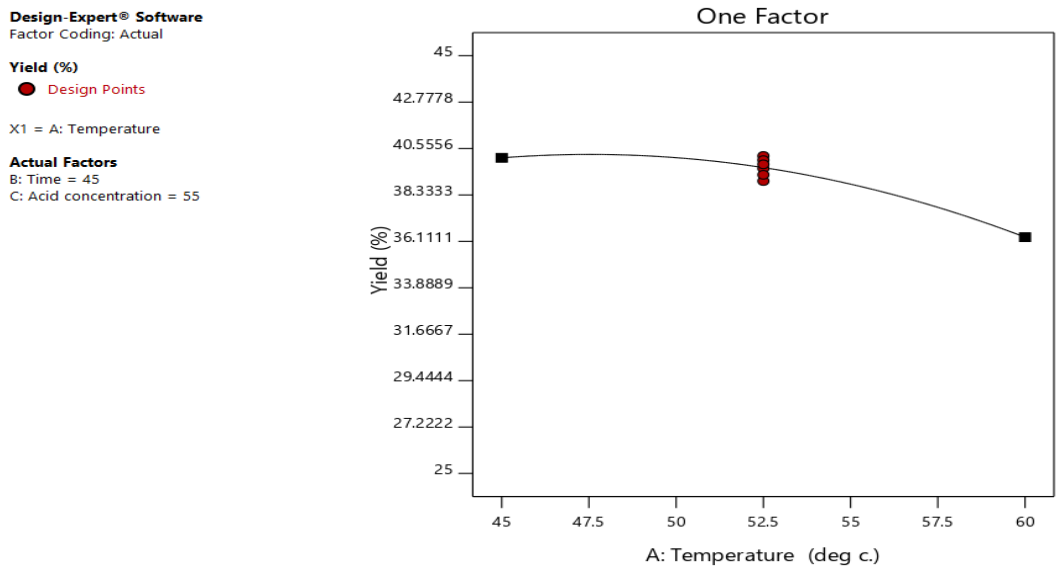

Figure 4-11:Effect of temperature on yield of CNCs

4.10.1.3. Effect of hydrolysis time on the yield of cellulose nanocrystals

Reaction time is one of the most important parameters to consider in the sulfuric acid hydrolysis to extract cellulose nanocrystals from corncob cellulose. Figure 4.12, shows the effect of hydrolysis time on the yield of cellulose nanocrystals when the acid concentration 55wt.% and temperature 50.85℃.

It was observed that at the lower level of time minimum value of yield was obtained and increased with increased values of time, while other parameters were kept at their fixed values. The maximum value of yield was obtained when the hydrolysis time reaches 51.95 minutes. As the operating time increased, the cellulose can degrade further and results in the decrease of the CNCs yield. Hydrolysis time has the highest effect on the acid hydrolysis yield of cellulose nanocrystals compared to acid concentration and temperature, as indicated in the equation (3.8).

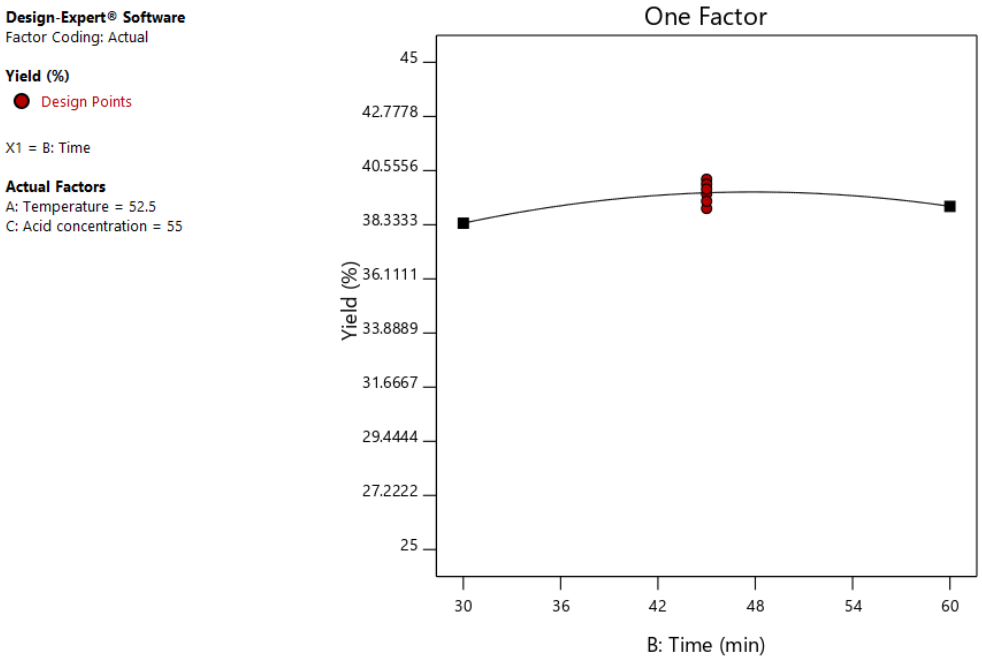

Figure 4-12:Effect of hydrolysis time on the yield of CNCs

4.10.2. Interaction Effect of Factors on the yield of cellulose nanocrystals

The interaction effects and optimal levels of acid concentration, temperature, and hydrolysis time were determined by plotting the response surface curves. To study the interactive effects on the yield of cellulose nanocrystal production, the response surface methodology of the quadratic model was used and both three-dimensional response surface plots and corresponding contour plots were constructed.

The contour plot forms show the nature and magnitude of the interaction between distinct variables. These plots depicted the combined effects of two factors on cellulose nanocrystals yield, while other factors were kept constant at their medium levels. Elliptical contour plots imply that the interaction between the variables is significant and circular contour plots mean that the interaction between the variables is not important(Kandhola et al., 2020).

4.10.2.1. Effects of temperature and acid concentration on the yield of CNCs

The effect of temperature and acid concentration on the yield of cellulose nanocrystals at a constant hydrolysis time of 45 minutes was shown in Figure 4.13. The Figure depicted that a maximum cellulose nanocrystals yield was obtained at a medium concentration of both temperature (48.75-52.5℃) and concentration of acid(55-65wt.%). The relationship of their interaction effect on the yield was also shown from the regression coefficient of their interaction in equation (3.8).

From the equation (3.8) the interaction of temperature and acid concentration negatively affects the yield of CNCs after its optimum point as shown in Figure 4.15. It was observed that at a lower level of temperature, a lower value of acid concentration gives high yield and decreased with increasing temperature.

However, at a higher level of temperature, the variation of acid concentration has no significant effect. It was also observed that the effect of acid concentration variation on the yield at the lower level of temperature was high than that observed at the higher level of temperature. Even if both variables of the process affect the yield of cellulose nanocrystals, acid concentration affects less than the temperature.

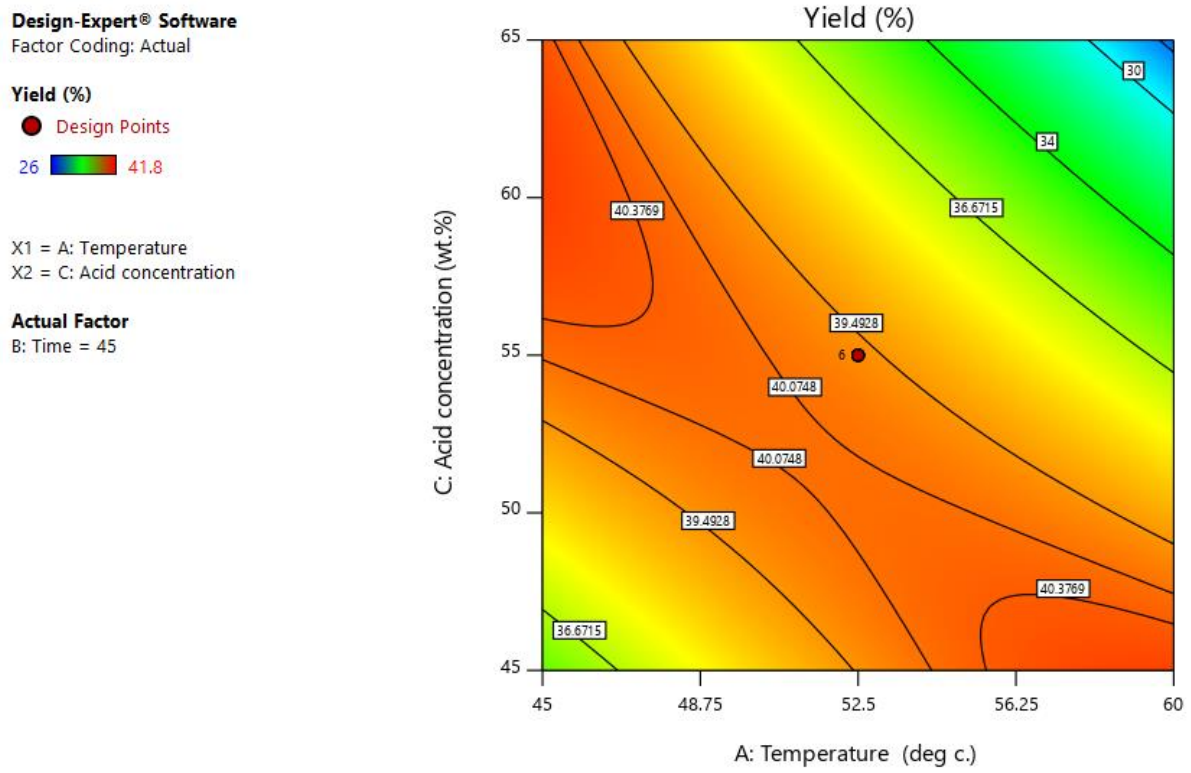

Figure 4-13: Contour plot showing the effect of reaction temperature and acid concentration on the yield of CNCs

4.10.2.2. Effect of temperature and time on the yield of CNC

The effect of temperature and time on the yield of cellulose nanocrystals, when the acid concentration was fixed at 55wt.%, the response surface curves and contour plot graphs were represented in Figure 4.14. From the graph high yield of cellulose nanocrystal was obtained at lower temperature and higher hydrolysis time. It was observed that yield was decreased with increasing temperature and increasing time at the starting of the hydrolysis reaction. At a higher

temperature level, the variation of hydrolysis time had less effect on the variation of the yield. However, at a lower level of temperature, the yield was highly affected by the variation of the time. At a reaction time of 45-60 min and a temperature of 45-52.5°C, the highest yield can be obtained.

With the reaction time rising to a certain level, at a lower level of temperature the yield of CNC increases. The decrease in the yield of CNC for longer reaction times and a higher temperature is due to the overreaction. When the over-reaction occurred with excess reaction time, cellulose was broken into its component of sugar molecules by hydrolysis(Thakur et al., 2020).

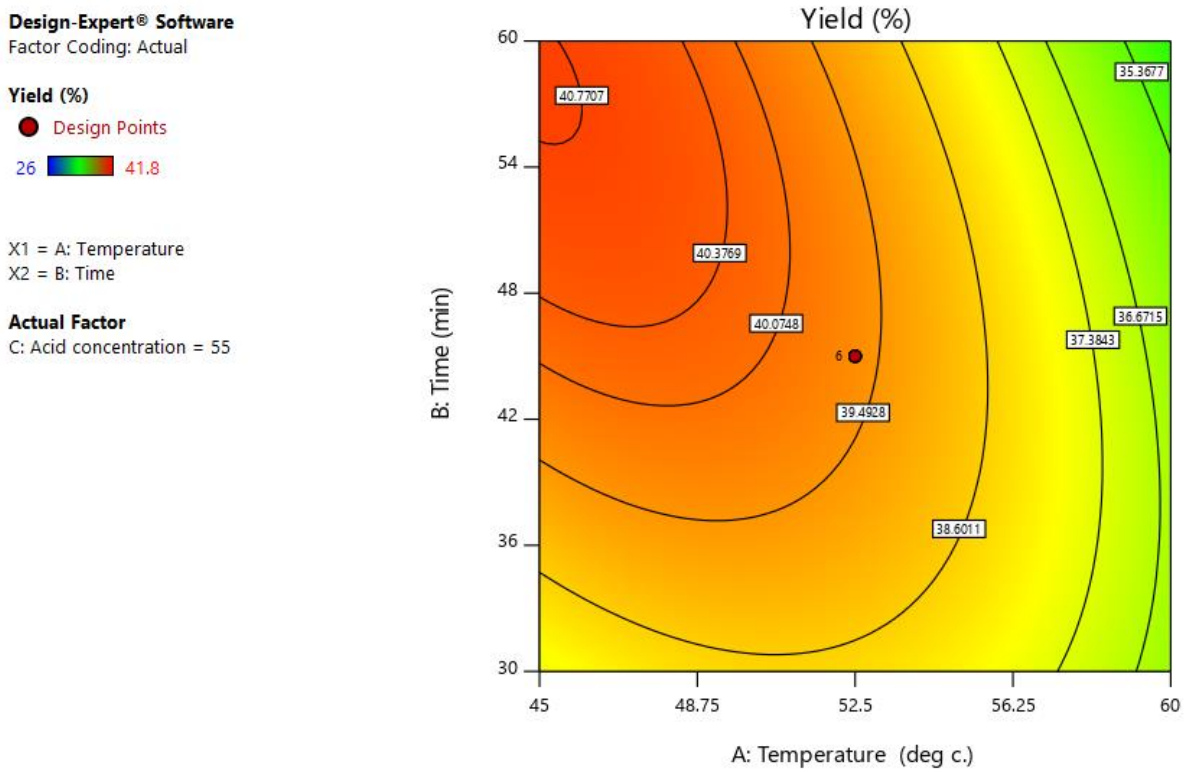

Figure 4-14: Contour plot showing the effect of reaction temperature and reaction time on the yield of CNCs

4.10.2.3. Interaction effect of time and acid concentration on yield of CNC

When the temperature was fixed at 50.85°C,the interaction effect of time and acid concentration was shown in Figure 4.15. The curves of time and acid concentration are nearly parallel to each other showing their interaction effect on the yield at the constant reaction temperature. It is shown that in equation 3.8, the interaction effects of time and acid concentration on the yield of CNCs are highly significant as compared to other interactions. It is observed that the highest yield was obtained at a reaction time of 42-50 min and an acid concentration of 50-55 wt.%

can be obtained. But at a lower level of time and acid concentration, at a lower level of time and higher value of acid concentration, at a higher level of time and acid concentration the yield of cellulose nanocrystals was low.

From graph 4.15, with increasing both the acid concentration and time, the yield of cellulose nanocrystals was decreased. This is due to the degradation of cellulose to undesired products as both time and acid concentration increased. Reaction time plays an important role in the degradation of cellulose. In a short period of time, the hydrolysis of cellulose could not happen effectively.

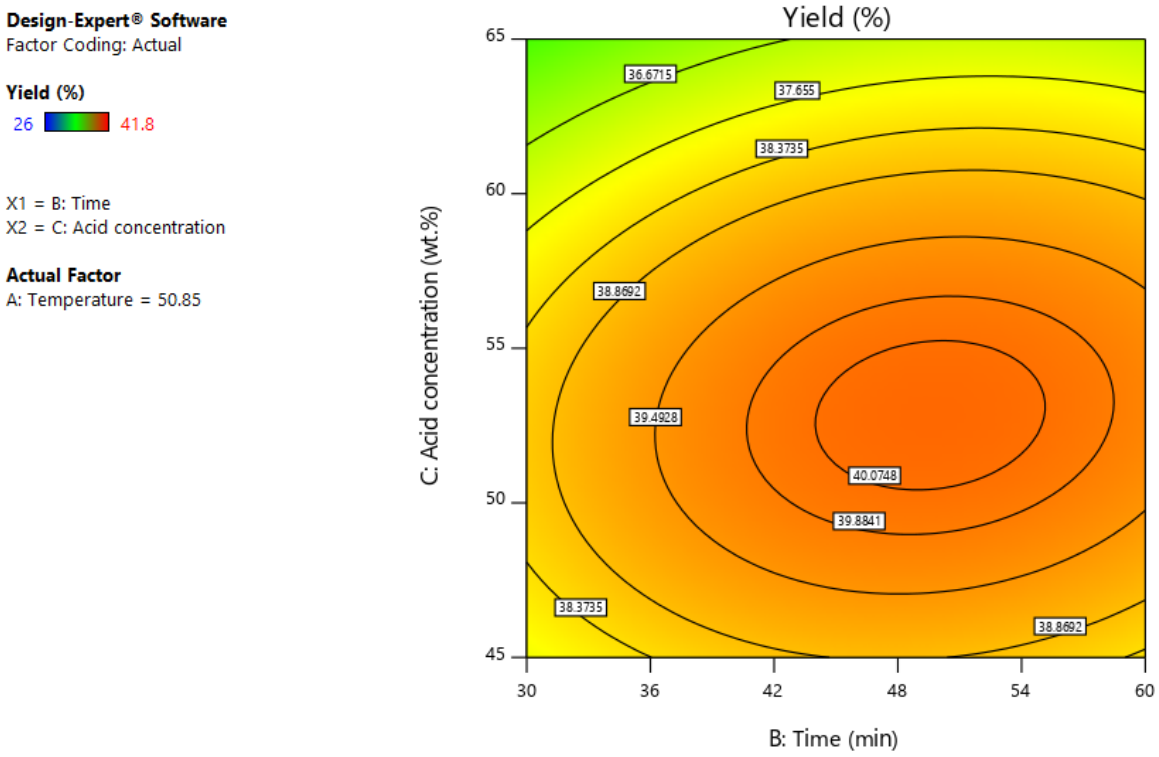

Figure 4-15: Contour plot showing the effect of acid concentration and reaction time on the yield of CNCs

Elliptical plots imply that the interaction between the variables is significant and circular contour plots mean that the interaction between the variables is not important(Thakur et al., 2020). Generally, response surface plots show the combined effects of two variables on the response as other variables are kept constant.From interaction effect acid concentration and time interaction effect on the yield of cellulose nanocrystals have a significant effect. The response surface plot for the interaction effect of acid concentration, reaction time, and temperature on the yield of cellulose nanocrystals were shown in appendix C (Figure C-2).

4.11. Optimization of the acid hydrolysis process

Optimization is a method of analysis to identify the combination of variable settings that jointly optimize a single response or a set of responses. The aim of this work is to hydrolysis cellulose with a maximum yield of cellulose nanocrystals. The central composite design, using the design space (defined limits of parameters) and maximum yield of cellulose nanocrystals optimization of the process was carried out(P. Lu & Hsieh, 2012). The principle of optimization tells us to maximize the economic benefit by minimizing process cost, the process variables need to set as much as possible at their minimum value and the response variable cellulose nanocrystal yield was set to maximum(Kandhola et al., 2020).

Optimization of hydrolysis process factors (sulfuric acid concentration, temperature, and hydrolysis time) and response (yield of CNC) was carried out by a multiple response method called desirability (D) function to optimize the different combinations of process parameters. Numerical optimization was used to identify the optimum level of hydrolysis process factors.

Table 4-14:Constraints for the factors and responses in numerical optimization

Parameters	Goal	Lower limit	Upper limit
Temperature	In the range	45	60
Time	In the range	30	60
Acid concentration	In the range	45	65
CNC Yield	Maximize	26	41.8

According to the experimental work done in Table 4.9,the maximum yield cellulose nanocrystal of 41.8% was obtained at the interaction parameter of temperature(45℃), time(60min), and acid concentration (65 wt.%). Under this condition of parameter interaction, the predicted yield of CNC obtained was 41.50%. This shows that the predicted values of the CNC yield agreed with that obtained from experimental work. From the response optimization technique used in this study, the yield of cellulose nanocrystal was optimized to 41.74 %, at a desirable parameter interaction of acid concentration (61.66 wt.%), reaction time (59.93 min), and temperature (45℃) as shown in Table C-2.

The values of desirability are varied from zero to one and show the location of maximized responses. The value equals to 1 indicates a very satisfying solution, while 0 indicates that the response is out of the acceptable limits. For both optimizations, the deciding goal was the maximum solution with the lower response value of 0 and the target or upper response value of 100(Aparamarta, & Gunawan, 2019). The unit value of desirability implies that some of the solutions are located beyond the specified upper limit.

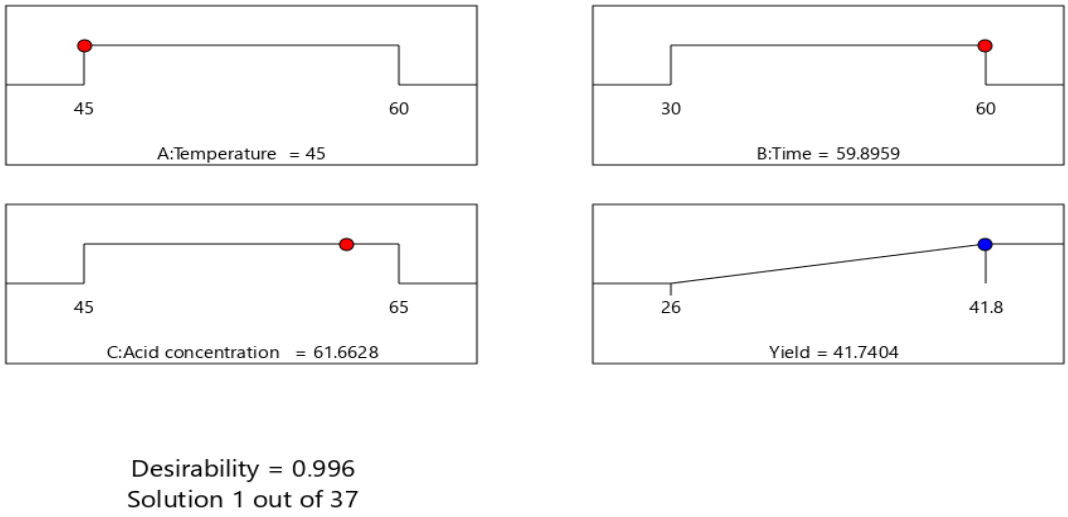

Figure 4-16:Ramps numerical optimization of parameters and response

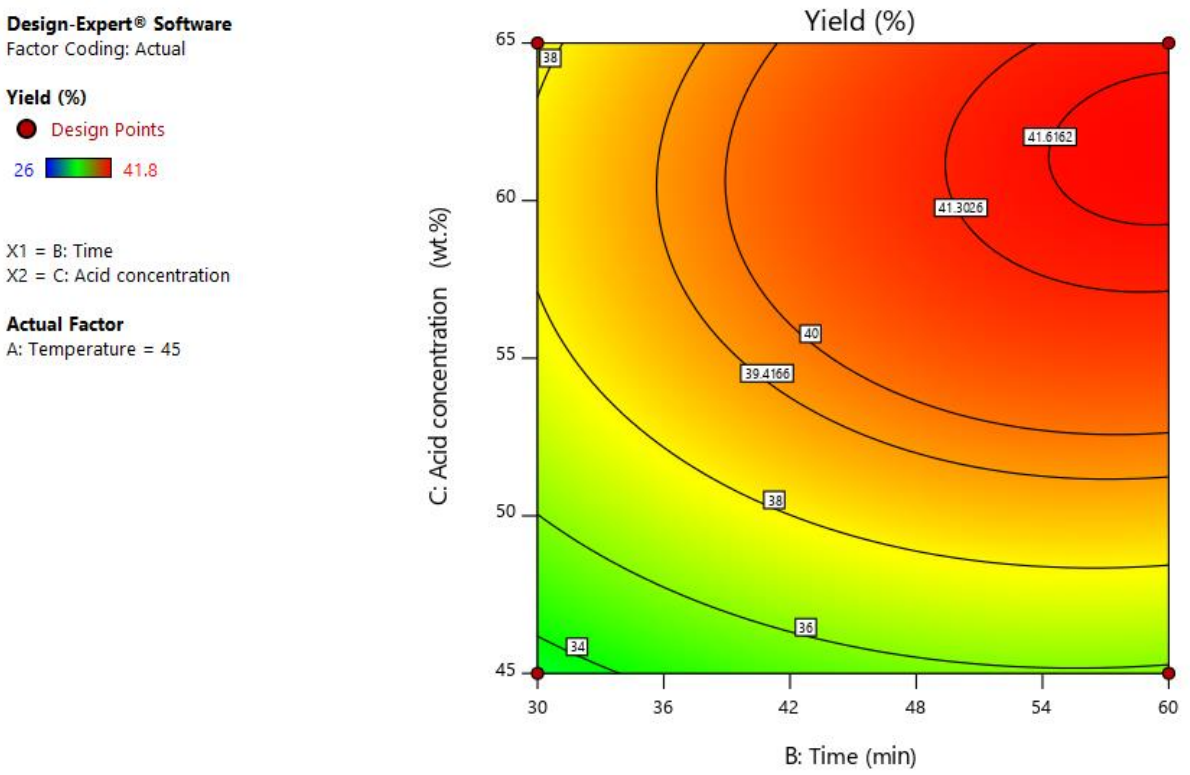

Figure 4-17:The contour of numerical optimization process parameters and the yield of CNCs

As shown in the above Figure, as hydrolysis time increases from 30 to 60 minutes and acid concentration from 45 to 65 wt.%, the desirable yield increases.

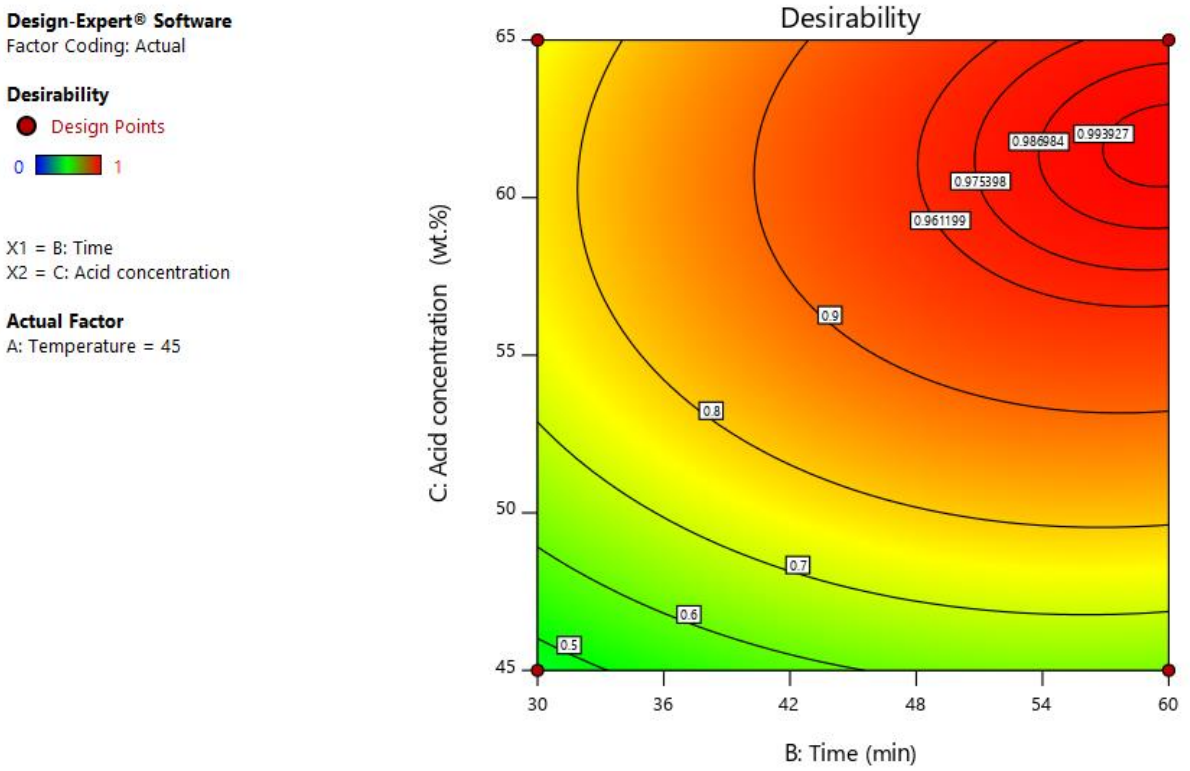

Figure 4-18:The contour of numerical optimization process parameters and the desirability

4.12. Validation of an optimization model

To confirm the optimized model, the actual validation experiment was carried out at optimum conditions that were obtained in a design expert. These optimum points were acid concentration (61.66wt.%), reaction time (59.93 min), and temperature (45℃). To validate the optimum conditions predicted by the response surface methodology model results, triplicate experiments were conducted at the above specified optimum process conditions predicted by the model.

After optimization, triplicate experiments were performed using these optimized process conditions. At this condition, the mean percentage of yield obtained was 40.94% as shown in Table 4.15 and which was then related to the data obtained from optimization analysis using the desirability function.

Table 4-15:Result of optimization and model validation

Number	Acid concentration (wt.%)	Temperature (℃)	Time (min)	Yield (%)
Predicated	61.66	45.00	59.93	41.74
Experimental	61.66	45.00	59.93	40.94±0.25

The mean percentage of yield obtained by triplicate experiments 40.94±0.25% which is not significantly different from the predicted value of 41.74 % yield of the optimal conditions are acid concentration (61.66wt.%), reaction time (59.93 min), and temperature (45℃).

Therefore, the model was valid and capable of predicting the maximum cellulose nanocrystal yield i.e. numerical optimization can be taken as an optimal value because the predicted value was close enough to the experimental value. In summary, this study shows that sulfuric acid, temperature, and time could be used for the optimization of cellulose nanocrystals extracted from corncob and the yield could be optimized by tuning sulfuric acid concentration, temperature, and time parameters.

CHAPTER 5 CONCLUSIONS AND RECOMMENDATIONS

5.1. Conclusions

This experimental work was performed to valorize corncob for the production of cellulose nanocrystal. The cellulose nanocrystals obtained was prepared by alkali treatment using sodium hydroxide (NaOH) with a concentration of 4 wt.% and bleached with a solution made up of equal parts (v:v) of acetate buffer (27 g NaOH and 75 mL glacial acetic acid(CH_3COOH), diluted to 1 L of distilled water) and aqueous sodium chlorite (1.7 wt.% $NaClO_2$ in water).

After such alkali extraction and bleaching treatment, cellulose nanocrystals were successfully prepared by the acid hydrolysis of the extracted corncob cellulose in sulfuric acid solution. Isolation of cellulose nanocrystal from corncob was successfully carried out by acid hydrolysis based on the selected parameters with optimum acid concentration, temperature, and hydrolysis time. It was found that the optimum parameters to isolate the CNCs from corncob was at 61.66wt.% acid concentration with the hydrolysis time of 59.92 min and a temperature of 45°C with an optimum predicated and experimental yield of 41.74 and 40.94±0.25 % respectively.

The cellulose nanocrystal solution was a milky white stable suspension of needle-shaped nanocrystalline cellulose. The effects of chemical treatments on raw corncob to extract cellulose nanocrystals were shown by scanning electron microscopy images to know surface morphological and from these studies, there was the removal of the amorphous materials and producing white and clean surfaces of cellulose. Particle size analyzer revealed that cellulose nanocrystals from corncob produced have an average length of around 170. 3nm. The structure of the cellulose nanocrystals could be confirmed by the structural analyses, Fourier transform infrared(FTIR) spectroscopy. Meanwhile, the crystallinity of the raw corncob increased after chemical treatment from 57.88% to 76.43% for corncob cellulose and the value of the cellulose nanocrystal was 79.31%.

This finding proved that corncob can be utilized to produce cellulose and cellulose nanocrystal which could be potentially used in many applications including in the field of food, paper, paints, optics, pharmaceutics, environment remediation, composite synthesis, and so forth have been reported. Hence, this studied revealed that the preparation of cellulose nanocrystal from corncob by acid hydrolysis method may be a very effective process to be carried out on a large scale.

5.2. Recommendations

Based on the outcomes of this research work and overall understanding of the extraction, characterization, and optimization of cellulose nanocrystal (CNC) using sulfuric acid the following recommendations are stated.

- Producing cellulose nanocrystals from lignocellulosic biomass pretreatments are the most important and recommended steps to get purified cellulose.
- In bleaching employ, a chlorine-free technique (TCF) to extract and bleach cellulose from biomass due to the overall process does not produce any toxic effluents.
- In alkali treatment use simultaneous steam explosion and alkaline depolymerization to develop an economic and green process for alkaline pretreatment of lignocellulose.
- There are different factors that can affect the yield of cellulose nanocrystals during acid hydrolysis. In this study, only the effects of temperature, hydrolysis time, and acid concentration at constant solid cellulose to the acid ratio on yield were tested. Therefore, other parameters such as solid cellulose to the acid ratio that can affect the yield and properties of cellulose nanocrystals should also be tested and optimized.
- Extensive dialysis is found to be effective in the removal of free acid that remains after centrifugation but uses conductometric titration is commonly used to quantify the sulfur content of cellulose nanocrystal.

REFERENCES

Abdel-Hamid, A. M., Solbiati, J. O., & Cann, I. K. O. (2013). Insights into Lignin Degradation and its Potential Industrial Applications. In *Advances in Applied Microbiology* (Vol. 82).

Alves, H., Pires, W., Neto, F., Oliveira, N., & Pasquini, D. (2013). Extraction and characterization of cellulose nanocrystals from corncob for application as a reinforcing agent in nanocomposites. *Industrial Crops & Products*, *44*, 427–436.

Arifan, F. (2019). Natural Xilan Production From Corncobs (Zea Mays L.) With the Extraction Method. *KnE Social Sciences*, *2019*, 177–185.

Arnata, I. W., Suprihatin, S., Fahma, F., Richana, N., & Candra Sunarti, T. (2019). Cellulose Production from Sago Frond with Alkaline Delignification and Bleaching on Various Types of Bleach Agents. *Oriental Journal of Chemistry*, *35*(Special Issue 1), 8–19.

Ayeni, A. O., Adeeyo, O. A., Oresegun, O. M., & Oladimeji, E. (2015). *Compositional analysis of lignocellulosic materials : Evaluation of an economically viable method suiTable for woody and non-woody biomass American Journal of Engineering Research*. (4), 14–19.

Bhikhu, M., & Gaurav, S. (2017). Lignocellulosic Material "An Alternative Future Fuel Source." *International Journal of Novel Research in Life Sciences*, *2*(February), 69–79.

Blanco, A., Monte, M. C., Campano, C., Balea, A., Merayo, N., & Negro, C. (2018). Nanocellulose for Industrial Use.In *Handbook of Nanomaterials for Industrial Applications*.

Brinchi, L., Cotana, F., Fortunati, E., & Kenny, J. M. (2013). Production of nanocrystalline cellulose from lignocellulosic biomass: Technology and applications. *Carbohydrate Polymers*, *94*(1), 154–169.

Brooks, & Moore, S. B. (2000). *Alkaline hydrogen peroxide bleaching of cellulose*. 263–286.

Chang, C., Hou, J., Chang, P. R., & Huang, J. (2019). *Structure and Properties of Cellulose Nanocrystals*. 21–52.

Chen, D., Lawton, D., Thompson, M. R., & Liu, Q. (2012). Biocomposites reinforced with cellulose nanocrystals derived from potato peel waste. *Carbohydrate Polymers*, *90*(1), 709–716.

D. Bagheriasl, P. J. Carreau, C. Dubois, and B. R. (2018). *Effect of cellulose nanocrystals (CNCs) on crystallinity, mechanical and rheological properties of polypropylene / CNCs nanocomposites Effect of cellulose nanocrystals (CNCs) on crystallinity, mechanical and rheological properties of polypropylene* (2015).

Dufresne, A. (2017a). Handbook of Nanocellulose and Cellulose Nanocomposites. In *Handbook of Nanocellulose and Cellulose Nanocomposites*.

Duque, A., Manzanares, P., Ballesteros, I., & Ballesteros, M. (2016). Biomass Pretreatment. In *Biomass Fractionation Technologies for a Lignocellulosic Feedstock Based Biorefinery*.

Faria, M., Thomas, S., & Pothan, L. A. (2015). *Utilization of various lignocellulosic biomass for the production of nanocellulose : a comparative study*. 1075–1090.

Flauzino Neto, W. P., Silvério, H. A., Dantas, N. O., & Pasquini, D. (2013). Extraction and characterization of cellulose nanocrystals from agro-industrial residue - Soy hulls. *Industrial Crops and Products*, *42*(1), 480–488.

Gopakumar, D. A., Thomas, S., & Grohens, Y. (2016). Nanocelluloses as Innovative Polymers for Membrane Applications. In *Multifunctional Polymeric Nanocomposites Based on Cellulosic Reinforcements*.

Gorgaslidze, N., Nizharadze, N., Nadirashvili, L., Erkomaishvili, G., Antelidze, Z., & Getia, M. (2017). The study of some properties of papain and bromelain containing gels. *Journal of Chemical Engineering & Process Technology*, *08*(04), 7048.

Hazman, W., Abdul, Z., Nazlan, M., Muhid, M., Triwahyono, S., Bakri, M., & RamLi, Z. (2015). The reuse of wastepaper for the extraction of cellulose nanocrystals. *Carbohydrate Polymers*, *118*, 165–169.

Hemmati, F., Mahdi, S., Kashaninejad, M., & Barani, M. (2018). International Journal of Biological Macromolecules Synthesis and characterization of cellulose nanocrystals derived from walnut shell agricultural residues. *International Journal of Biological Macromolecules*, *120*, 1216–1224.

Henrique, M. A., Silvério, H. A., Pires, W., Neto, F., & Pasquini, D. (2013). Valorization of agro-industrial waste, mango seed, by the extraction and characterization of its cellulose nanocrystals. *Journal of Environmental Management*, *121*, 202–209.

Ilyas, R. A., Sapuan, S. M., & Zainudin, E. S. (2017). *Nanocrystalline Cellulose As Reinforcement For Polymeric Matrix Nanocomposites And Its Potential Applications : A Review Nanocrystalline Cellulose as Reinforcement for Polymeric Matrix Nanocomposites and its Potential Applications :*

Isikgor, F. H., & Becer, C. R. (2015). Lignocellulosic biomass: a sustainable platform for the production of bio-based chemicals and polymers. *Polymer Chemistry*, *6*(25), 4497–4559.

Jasmania, L. (2018). Preparation of nanocellulose and its potential application. *International Journal of Nanomaterials, Nanotechnology and Nanomedicine*, *4*(2), 014–021.

Jeremic, S., Djokic, L., Ajdačić, V., Božinović, N., Pavlovic, V., Manojlović, D. D. Nikodinovic-Runic, J. (2019). Production of bacterial nanocellulose (BNC) and its application as a solid support in transition metal-catalyzed cross-coupling reactions. *International Journal of Biological Macromolecules*, *129*, 351–360.

Jiang, F., & Hsieh, Y. Lo. (2015). Cellulose nanocrystal isolation from tomato peels and assembled nanofibers. *Carbohydrate Polymers*, *122*, 60–68.

Kadimi, A., Benhamou, K., Habibi, Y., Ounaies, Z., & Kaddami, H. (2016). Nanocellulose Alignment and Electrical Properties Improvement. In *Multifunctional Polymeric Nanocomposites Based on Cellulosic Reinforcements*.

Kandhola, G., Djioleu, A., Rajan, K., Labbé, N., Sakon, J., Carrier, D. J., & Kim, J. W. (2020). Maximizing production of cellulose nanocrystals and nanofibers from pre-extracted loblolly pine kraft pulp : a response surface approach. *Bioresources and Bioprocessing*.

Kumar, S., Negi, Y. S., & Upadhyaya, J. S. (2010). Studies on characterization of corn cob based nanoparticles. *Advanced Materials Letters*, *1*(3), 246–253.

Kumar, S., Upadhyaya, J. S., & Negi, Y. S. (2010). Preparation of nanoparticles from corn cobs by chemical treatment methods. *BioResources*, *5*(2), 1292–1300.

Kumari, P., Pathak, G., Gupta, R., Sharma, D., & Meena, A. (2019). *Cellulose nanofibers from lignocellulosic biomass of lemongrass using enzymatic hydrolysis : characterization and cytotoxicity*.

Lani, N. S., Ngadi, N., Johari, A., & Jusoh, M. (2014). *Isolation, Characterization, and Application of Nanocellulose from Oil Palm Empty Fruit Bunch Fiber as Nanocomposites*. *2014*.

Larissa, L. A., Fonsêca, A. F., Pereira, F. V., & Druzian, J. I. (2015). Extraction and characterization of cellulose nanocrystals from corn stover. *Cellulose Chemistry and Technology*, *49*(2), 127–133.

Lee, H. V., Hamid, S. B. A., & Zain, S. K. (2014). Conversion of lignocellulosic biomass to nanocellulose: Structure and chemical process. *Scientific World Journal*, *2014*.

Leite, A. L. M. P., Zanon, C. D., & Menegalli, F. C. (2017). Isolation and characterization of cellulose nanofibers from cassava root bagasse and peelings. *Carbohydrate Polymers*, *157*, 962–970.

Li, M., Cheng, Y. L., Fu, N., Li, D., Adhikari, B., & Chen, X. D. (2014). Isolation and characterization of corncob cellulose fibers using microwave-assisted chemical treatments. *International Journal of Food Engineering*, *10*(3), 427–436.

Liu, D. Y., Sui, G. X., & Bhattacharyya, D. (2015). Properties and characterization of electrically conductive nanocellulose-based composite films. *Fillers and Reinforcements for Advanced Nanocomposites*, 3–25.

Lu, H., Gui, Y., Zheng, L., & Liu, X. (2013). Morphological, crystalline, thermal, and physicochemical properties of cellulose nanocrystals obtained from sweet potato residue. *FRIN*, *50*(1), 121–128.

Lu, P., & Hsieh, Y. (2012). Preparation and characterization of cellulose nanocrystals from rice straw. *Carbohydrate Polymers*, *87*(1), 564–573.

Lu, Q., Tang, L., Lin, F., Wang, S., Chen, Y., & Huang, B. (2014). *Preparation and characterization of cellulose nanocrystals via ultrasonication-assisted FeCl3-catalyzed hydrolysis*. (October).

Luo, Y., Li, Z., Li, X., Liu, X., Fan, J., Clark, J. H., & Hu, C. (2019). The production of furfural directly from hemicellulose in lignocellulosic biomass: A review. *Catalysis Today*, *319*(July 2018), 14–24.

Luque, L., Oudenhoven, S., Westerhof, R., Van Rossum, G., Berruti, F., Kersten, S., & Rehmann, L. (2016). Comparison of ethanol production from corn cobs and switchgrass following a pyrolysis-based biorefinery approach. *Biotechnology for Biofuels*, *9*(1), 1–14.

Malladi, R., Nagalakshmaiah, M., & Robert, M. (2018). *Importance of Agricultural and Industrial Waste in the Field of Nanocellulose and Recent Industrial Developments of Wood-Based Nanocellulose*. (February). 25-45

Man, Z., Muhammad, N., Sarwono, A., Bustam, M. A., Kumar, M. V., & Rafiq, S. (2011). Preparation of Cellulose Nanocrystals Using an Ionic Liquid. *Journal of Polymers and the Environment*, *19*(3), 726–731.

Manaf, Mohamad, N., Sakinah, S., & Ahmad, S. (2019). *Extraction and Characterisation of Cellulose Nanocrystals Structures from Waste Office Paper*. *2*(2), 202–211.

Marcos, R., Pires, W., Neto, F., Alves, H., Ferreira, D., Oliveira, N., & Pasquini, D. (2013). Cellulose nanocrystals from pineapple leaf, a new approach for the reuse of this agro-waste. *Industrial Crops & Products*, *50*, 707–714.

Maria, F., Andrade-mahecha, M. M., José, P., & Cecilia, F. (2017). Journal of Colloid and Interface Science Nanocomposites based on banana starch reinforced with cellulose nanofibers isolated from banana peels. *Journal of Colloid And Interface Science*, *505*, 154–167.

Matheus Poletto (2014). *Native Cellulose: Structure, Characterization, and Thermal Properties*. 6105–6119.

Matsutani, A., Harada, T., Ozaki, S., & Takaoka, T. (1993). Inhibitory effects of the combination of CDDP and cepharanthin on the cultured cells from rat ascites hepatoma. In *Journal of Japan Society for Cancer Therapy* (Vol. 28).

Mefteh, F. Ben, Frikha, F., Daoud, A., Bouket, A. C., Luptakova, L., Alenezi, F. N., … Oszako, T. (2019). *Response Surface Methodology Optimization of an Acidic Protease Produced by Penicillium bilaiae Isolate TDPEF30, a Newly Recovered Endophytic Fungus from Healthy Roots of Date Palm Trees.*

Miranda, R., Câmara, P., Maia, J. M. L. L., & Maria, S. (2017). Environmental and technical feasibility of cellulose nanocrystal manufacturing from sugarcane bagasse. *Carbohydrate Polymers*, *175*, 518–529.

Mitchual, Frimpong-Mensah, K., Darkwa, A., & Akowuah, J. O. (2013). Briquettes from maize cobs and Ceiba pentandra at room temperature and low compacting pressure without a binder. *International Journal of Energy and Environmental Engineering*, *4*(1), 1–7.

Mohammad, S., Mousavi, M., Afra, E., Tajvidi, M., & Bous, D. W. (2018). *Progress in Organic Coatings Application of cellulose nanofibril (CNF) as a coating on paperboard at moderate solids content and high coating speed using blade coater*. *122*(May), 207–218.

Mtibe, A., Mokhothu, T. H., John, M. J., Mokhena, T. C., & Mochane, M. J. (2018). Fabrication and Characterization of Various Engineered Nanomaterials. In *Handbook of Nanomaterials for Industrial Applications*.

Norhaffis, M., Shafie, S., Haniff, M., & Sulaiman, Y. (2019). Results in Physics Optimization of power conversion efficiency of polyvinyl-alcohol / titanium dioxide as a light scattering layer in DSSC using response surface methodology / central composite design. *Results in Physics*, *15*(May), 102559.

Ogunbayo, A. O., Olanipekun, O. O., & Babatunde, D. E. (2016). Effect of Pre-treatment method on the Hydrolysis of Corn cob and Sawdust. *Anadolu University Journal of Science and Technology-A Applied Sciences and Engineering*, *17*(3).

Orue, A., Santamaria-Echart, A., Eceiza, A., Peña-Rodriguez, C., & Arbelaiz, A. (2017). Office waste paper as cellulose nanocrystal source. *Journal of Applied Polymer Science*, *134*(35), 1–11.

Pandey, J. K., Takagi, H., Nakagaito, A. N., Kim, H., & Nanoparticles, C. (2015). *Handbook of Polymer Nanocomposites. Processing, Performance, and Application* (1st ed.; J. K. Pandey, ed.). Seoul, Republic of Korea.

Pereira, B., & Arantes, V. (2018). Nanocelluloses From Sugarcane Biomass. *Advances in Sugarcane Biorefinery: Technologies, Commercialization, Policy Issues, and Paradigm Shift for Bioethanol and By-Products*, 179–196.

Phanthong, P., Reubroycharoen, P., Hao, X., & Xu, G. (2018). Nanocellulose : Extraction and application. *Carbon Resources Conversion*, *1*(1), 32–43.

Pointner, M., Kuttner, P., Obrlik, T., Jäger, A., & Kahr, H. (2014). Composition of corncobs as a substrate for fermentation of biofuels. *Agronomy Research*, *12*(2), 391–396.

Pressure, A. (2014). Production of Furfural From Corncobs Agricultural Waste by Acid Hydrolysis at Atmospheric Pressure. *Production of Furfural From Corncobs Agricultural Waste by Acid Hydrolysis at Atmospheric Pressure*, *3*(2), 71–75.

Prestes, A. P. T. E., & Demiate, L. A. P. I. M. (2017). Extraction and Characterization of Nanocrystalline Cellulose from Cassava Bagasse. *Journal of Polymers and the Environment*.

Qiao, C., Chen, G., Zhang, J., & Yao, J. (2016). Structure and rheological properties of cellulose nanocrystals suspension. *Food Hydrocolloids*, *55*, 19–25.

Ramos, M., Valdés, A., & Garrigós, M. C. (2016). Multifunctional Applications of Nanocellulose-Based Nanocomposites. In *Multifunctional Polymeric Nanocomposites Based on Cellulosic Reinforcements*.

Reddy, D. J. P. (2015). *Isolation of cellulose nanocrystals from onion skin and their utilization for the preparation of agar-based bio-nanocomposites films Isolation of cellulose nanocrystals from onion skin and their utilization for the preparation of agar-based bio-nanocomposite*. (January 2014).

Rhim, J. W., Reddy, J. P., & Luo, X. (2015). Isolation of cellulose nanocrystals from onion skin and their utilization for the preparation of agar-based bio-nano composites films. *Cellulose*, *22*(1), 407–420.

Saba, N., Jawaid, M., Sultan, M. T. H., & Alothman, O. Y. (2017). Green biocomposites for structural applications. In *Green Energy and Technology*.

Santos, R. M. dos, Flauzino Neto, W. P., Silvério, H. A., Martins, D. F., Dantas, N. O., & Pasquini, D. (2013). Cellulose nanocrystals from pineapple leaf, a new approach for the reuse of this agro-waste. *Industrial Crops and Products*, *50*, 707–714.

Scatolino, M. V., Silva, D. W., Mendes, R. F., & Mendes, L. M. (2013). Uso do sabugo de milho na produção de painéis aglomerados. *Ciencia e Agrotecnologia*, *37*(4), 330–337.

Shankaran, D. R. (2018). Cellulose Nanocrystals for Health Care Applications. In *Applications of Nanomaterials*.

Silvério, H. A., Flauzino Neto, W. P., & Pasquini, D. (2013). Effect of incorporating cellulose nanocrystals from corncob on the tensile, thermal, and barrier properties of poly(vinyl alcohol) nanocomposites. *Journal of Nanomaterials*, *2013*.

Silvério, H. A., Pires, W., Neto, F., & Pasquini, D. (2013). *Effect of Incorporating Cellulose Nanocrystals from Corncob on the Tensile, Thermal, and Barrier Properties of Poly (Vinyl Alcohol) Nanocomposites*. *2013*.

Singh, S., Gaikwad, K. K., Park, S., & Lee, Y. S. (2017). International Journal of Biological Macromolecules Microwave-assisted step reduced extraction of seaweed (Gelidiella aceroso) cellulose nanocrystals. *International Journal of Biological Macromolecules*, *99*, 506–510.

Siwei Huang, Ling Zhou, Mei-Chun Li, Qinglin Wu, and D. Z. (2017). *Cellulose Nanocrystals (CNCs) from Corn Stalk :* 1–13.

Song, K., Zhu, X., Zhu, W., & Li, X. (2019a). Preparation and characterization of cellulose nanocrystal extracted from Calotropis Procera biomass. *Bioresources and Bioprocessing*, *6*(1).

Song, K., Zhu, X., Zhu, W., & Li, X. (2019b). Preparation and characterization of cellulose nanocrystal extracted from Calotropis Procera biomass. *Bioresources and Bioprocessing*.

Spagnol, C., Fragal, E. H., Witt, M. A., Follmann, H. D. M., Silva, R., & Rubira, A. F. (2018). Mechanically improved polyvinyl alcohol-composite films using modified cellulose nanowhiskers as nano-reinforcement. *Carbohydrate Polymers*, *191*(October 2017), 25–34.

Sun, J. X., Sun, X. F., Zhao, H., & Sun, R. C. (2004). *Isolation and characterization of cellulose from sugarcane bagasse*. *84*, 331–339.

Sun, X. F., Jing, Z., Fowler, P., Wu, Y., & Rajaratnam, M. (2011). Structural characterization and isolation of lignin and hemicelluloses from barley straw. *Industrial Crops and Products*, *33*(3), 588–598.

Tayeb, A. H., Amini, E., Ghasemi, S., & Tajvidi, M. (2018). Cellulose nanomaterials-binding properties and applications: A review. *Molecules*, *23*(10), 1–24.

Thakur, M., Sharma, A., Ahlawat, V., Bhattacharya, M., & Goswami, S. (2020). Process optimization for the production of cellulose nanocrystals from rice straw derived a -cellulose. *Materials Science for Energy Technologies*, *3*, 328–334.

Tomkinson, J. (2014). *Isolation and characterization of hemicelluloses and cellulose from rye straw by alkaline peroxide extraction Isolation and characterization of hemicelluloses and cellulose from rye straw by alkaline peroxide extraction*. (June).

Trache, D., Hussin, M. H., Hui Chuin, C. T., Sabar, S., Fazita, M. R. N., Taiwo, O. F. A., … Haafiz, M. K. M. (2016). Microcrystalline cellulose: Isolation, characterization, and bio-

composites application A review. *International Journal of Biological Macromolecules*, *93*(June 2018), 789–804.

Wijaya, C. J., Ismadji, S., Aparamarta, H. W., & Gunawan, S. (2019). Heliyon Optimization of cellulose nanocrystals from bamboo shoots using Response Surface Methodology. *Heliyon*, *5*(July), 02807.

Wimmer, R., Klímek, P., Wimmer, R., Kumar, P., & Kúdela, J. (2017). Utilizing Brewer's Spent Grain as a Source of Cellulose Nanofibres Following Separation of Protein-based Biomass Utilizing brewer's spent-grain in wood-based particleboard manufacturing. *Journal of Cleaner Production*, *141*(February), 812–817.

Xie, H., Du, H., Yang, X., & Si, C. (2018). *Recent Strategies in Preparation of Cellulose Nanocrystals and Cellulose Nanofibrils Derived from Raw Cellulose Materials*. *2018*.

Yang, S. T. (2017). Bioprocessing-from Biotechnology to Biorefinery. *Bioprocessing for Value-Added Products from Renewable Resources*, (Figure 1), 1–24.

Zhang, G., Wu, F., Ma, T., Zhang, B., Manyande, A., & Du, H. (2019). Preparation and characterization of cellulose nanofibers isolated from lettuce peel. *Cellulose Chemistry and Technology*, *53*(7–8), 677–684.

Zhang, P. P., Tong, D. S., Lin, C. X., Yang, H. M., Zhong, Z. K., Yu, W. H., & Wang, H. (2014). *Effects of acid treatments on bamboo cellulose nanocrystals*. (April), 686–695.

Zhang, Y., Nypelö, T., Salas, C., Arboleda, J., Hoeger, I. C., & Rojas, O. J. (2013). Cellulose nanofibrils: From strong materials to bioactive surfaces. *Journal of Renewable Materials*, *1*(3), 195–211.

Zhu, Z. H., Mo, B. H., & Hao, M. Y. (2019). Study of contents ratio of cellulose, hemicellulose, and lignin on the mechanical properties of sisal fibers reinforced polylactic acid (PLA) composites. *IOP Conference Series: Materials Science and Engineering*, *544*(1).

APPENDICES

Appendix A: Fourier transform Infrared Spectroscopy (FTIR) Correlation Table

Frequency range	Absorption (cm^{-1})	Appearance	Group	Compound Class
4000-3000 cm^{-1}	3700-3584	medium, sharp	O-H stretching	Alcohol
	3550-3200	strong, broad	O-H stretching	Alcohol
	3500	Medium	N-H stretching	primary amine
	3350-3310	Medium	N-H stretching	secondary amine
	3300-2500	strong, broad	O-H stretching	carboxylic acid
	3200-2700	weak, broad	O-H stretching	Alcohol
	3000-2800	strong, broad	N-H stretching	amine salt
3000-2500 cm^{-1}	3333-3267	strong, sharp	C-H stretching	Alkyne
	3100-3000	Medium	C-H stretching	Alkene
	3000-2840	Medium	C-H stretching	Alkane
	2830-2695	Medium	C-H stretching	Aldehyde
	2600-2550	Weak	S-H stretching	Thiol
2400-2000 cm^{-1}	2349	Strong	O=C=O stretching	carbon dioxide
	2275-2250	Strong, broad	N=C=O stretching	Isocyanate
	2260-2222	Weak	C ≡ N stretching	Nitrile
	2260-2190	Weak	$C \equiv C$ Stretching	Alkyne
	2145-2120	Strong	N=C=N stretching	Carbodiimide
	2140-2100	Weak	$C \equiv C$ Stretching	Alkyne
	2140-1990	Strong	N=C=S stretching	Isothiocyanate
	2000-1900	Medium	C=C=C stretching	Allene
2000-1650 cm^{-1}	2000-1650	Weak	C-H bending	aromatic compound
	1818	Strong	C=O stretching	Anhydride
	1815-1785	Strong	C=O stretching	acid halide
	1800-1770	Strong	C=O stretching	conjugated acid halide
	1770-1780	Strong	C=O stretching	vinyl / phenyl ester
	1760	Strong	C=O stretching	carboxylic acid
	1750-1735	Strong	C=O stretching	Esters
	1750-1735	Strong	C=O stretching	δ-lactone
	1745	Strong	C=O stretching	Cyclopentanone
	1740-1720	Strong	C=O stretching	Aldehyde
	1725-1705	Strong	C=O stretching	aliphatic ketone
	1720-1706	Strong	C=O stretching	carboxylic acid
	1710-1680	Strong	C=O stretching	conjugated acid
	1710-1685	Strong	C=O stretching	conjugated aldehyde
	1690	Strong	C=O stretching	primary amide
	1690-1640	Medium	C=N stretching	imine / oxime
	1685-1666	Strong	C=O stretching	conjugated ketone
	1680	Strong	C=O stretching	secondary amide

	1680	Strong	C=O stretching	tertiary amide
1670-1600 $\mathbf{cm^{-1}}$	1678-1668	Weak	C=C stretching	Alkene
	1675-1665	Weak	C=C stretching	Alkene
	1675-1665	Weak	C=C stretching	Alkene
	1662-1626	Medium	C=C stretching	Alkene
	1658-1648	Medium	C=C stretching	Alkene
	1650-1600	Medium	C=C stretching	conjugated alkene
	1650-1580	Medium	N-H bending	Amine
	1650-1566	Medium	C=C stretching	cyclic alkene
	1648-1638	Strong	C=C stretching	Alkene
1600-1300 $\mathbf{cm^{-1}}$	1550-1500	Strong	N-O stretching	nitro compound
	1465-1450	Medium	C-H bending	Alkane
	1390-1380	Medium	C-H bending	Aldehyde
	1385-1380	Medium	C-H bending	Alkane
1400-1000 $\mathbf{cm^{-1}}$	1440-1395	Medium	O-H bending	carboxylic acid
	1420-1330	Medium	O-H bending	Alcohol
	1415-1380	Strong	S=O stretching	Sulfate
	1410-1380	Strong	S=O stretching	sulfonyl chloride
	1390-1310	Medium	O-H bending	Phenol
	1372-1335	Strong	S=O stretching	Sulfonate
	1370-1335	Strong	S=O stretching	Sulfonamide
	1350-1342	Strong	S=O stretching	sulfonic acid
	1350-1300	Strong	S=O stretching	Sulfone
	1342-1266	Strong	C-N stretching	aromatic amine
	1310-1250	Strong	C-O stretching	aromatic ester
	1275-1200	Strong	C-O stretching	alkyl aryl ether
	1250-1020	Medium	C-N stretching	Amine
	1225-1200	Strong	C-O stretching	vinyl ether
	1210-1163	Strong	C-O stretching	Ester
	1205-1124	Strong	C-O stretching	tertiary alcohol
	1150-1085	Strong	C-O stretching	aliphatic ether
	1124-1087	Strong	C-O stretching	secondary alcohol
	1085-1050	Strong	C-O stretching	primary alcohol
	1070-1030	Strong	S=O stretching	Sulfoxide
1000-650 $\mathbf{cm^{-1}}$	995-960	Strong	C=C bending	Alkene
	895-885	Strong	C=C bending	Alkene
	850-550	Strong	C-Cl stretching	halo compound
	840-665	Medium	C=C bending	Alkene
	690-515	Strong	C-Br stretching	halo compound
	600-500	Strong	C-I stretching	halo compound
900-700 $\mathbf{cm^{-1}}$	880 ± 20	Strong	C-H bending	1,2,4-trisubstituted
	880 ± 20	Strong	C-H bending	1,3-disubstituted
	780 ± 20	Strong	C-H bending	1,2,3-trisubstituted
	755 ± 20	Strong	C-H bending	1,2-disubstituted
	750 ± 20	Strong	C-H bending	Monosubstituted

Appendix B: Experimental Result

Table B-1:Moisture content of corncob

Run	Sample weight(g)			Moisture content (%)	Average moisture content (%)
	W_o	W_f	W_o-W_f		
1	42.7	31.2	11.5	36.86	
2	41.7	30.2	11.5	27.58	29.97
3	41.2	30.7	10.5	25.49	

$$\text{Moisture content (\%)} = \frac{wo-wf}{wo} \times 100$$

Table B-2:Ash Content Determination of corncob

	Weight (g)					Ash Content	Average Ash Content
run	w_0	w_1	w_2	$w_1 - w_0$	$w_2 - w_0$	(%)	(%)
1	5	6.28	5.028	1.28	0.028	2.1875	
2	7.5	11.67	7.045	4.17	0.045	1.079	1.6979
3	10	13.34	10.061	3.34	0.061	1.82634	

$$\text{Ash content (\%)} = \frac{w_2 - w_0}{w_1 - w_0} \times 100$$

Where, w_0 = Weight of the crucible, w_1= Weight of the crucible and sample before ashing and w_2 =Weight of the crucible + sample after ashing

Table B-3: Validation of predicated yield

Number of experiments	Acid concentration (wt.%)	Temperature (°C)	Time (min)	Yield (%)	Average Yield (%)
1.	61.66	45.00	59.93	41.54	
2.	61.66	45.00	59.93	42.34	40.94
3.	61.66	45.00	59.93	38.94	

Appendix C: Experimental design and result

Table C-1: Diagnostic report from design expert v11

Std.	Actual value	Predicted Value	Residual	Leverage	Student Residual	Cook's Distance	Outlier t	Run Order
1	33.50	33.26	0.24	0.670	1.121	0.255	1.137	10
2	40.90	41.07	-0.17	0.670	-0.785	0.125	-0.769	5
3	35.70	35.80	-0.10	0.670	-0.492	0.049	-0.472	20
4	38.80	38.66	0.14	0.670	0.676	0.093	0.657	11
5	37.70	37.71	-0.010	0.670	-0.049	0.000	-0.047	15
6	27.50	27.26	0.24	0.670	1.118	0.254	1.134	8
7	41.80	41.50	0.30	0.670	1.412	0.404	1.497	18
8	26.00	26.10	-0.10	0.670	-0.494	0.049	-0.474	6
9	38.60	38.79	-0.19	0.607	-0.809	0.101	-0.794	19
10	32.40	32.40	-0.00089	0.607	-0.004	0.000	-0.004	2
11	36.40	36.51	-0.11	0.607	-0.489	0.037	-0.469	7
12	37.60	37.67	-0.075	0.607	-0.324	0.016	-0.309	12
13	37.00	37.00	-0.00151	0.607	-0.007	0.000	-0.006	13
14	30.00	30.19	-0.19	0.607	-0.806	0.101	-0.791	14
15	39.00	39.64	-0.64	0.166	-1.919	0.073	-2.290	1
16	40.20	39.64	0.56	0.166	1.653	0.055	1.840	16
17	39.60	39.64	-0.045	0.166	-0.133	0.000	-0.126	9
18	39.30	39.64	-0.34	0.166	-1.026	0.021	-1.029	3
19	40.00	39.64	0.36	0.166	1.058	0.022	1.065	17
20	39.80	39.64	0.16	0.166	0.462	0.004	0.443	4

Proceed to Diagnostic Plots (the next icon in progression). Be sure to look at the:

1) Normal probability plot of the studentized residuals to check for normality of residuals.
2) Studentized residuals versus predicted values to check for constant error.
3) Outlier t versus run order to look for outliers, i.e., influential values.
4) Box-Cox plot for power transformations.

If all the model statistics and diagnostic plots are OK, finish up with the Model Graphs icon.

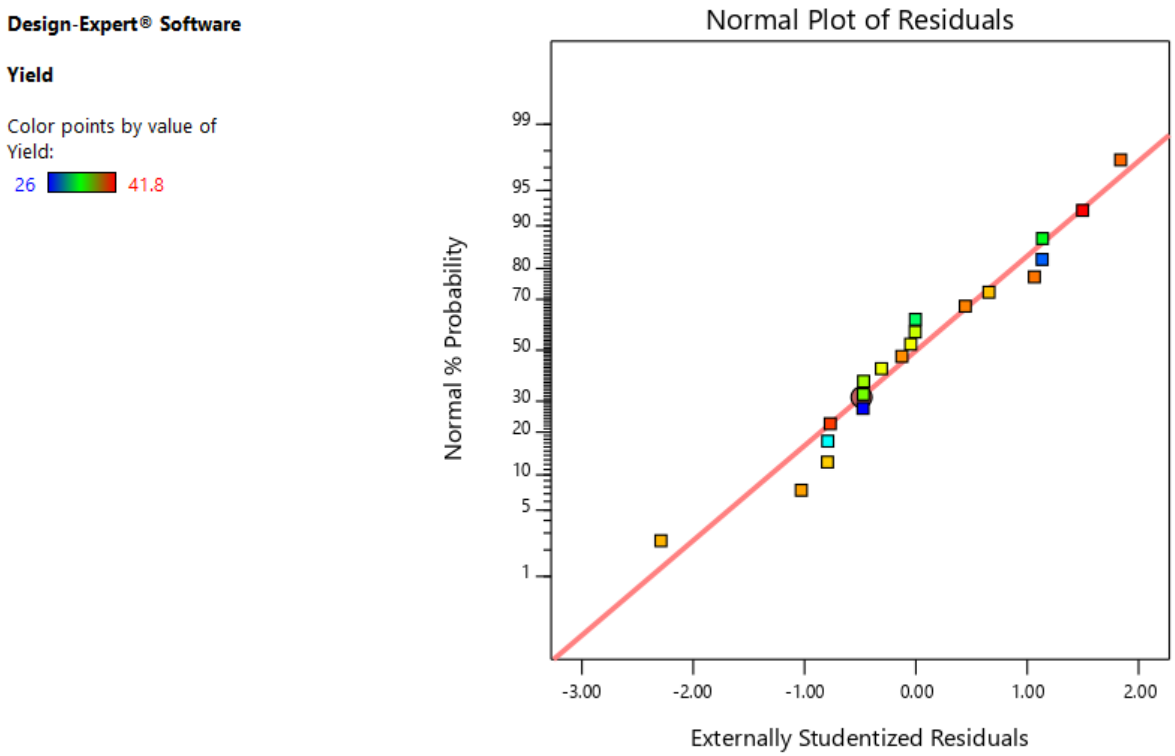

Figure C-1:Normal probability plot of the residuals

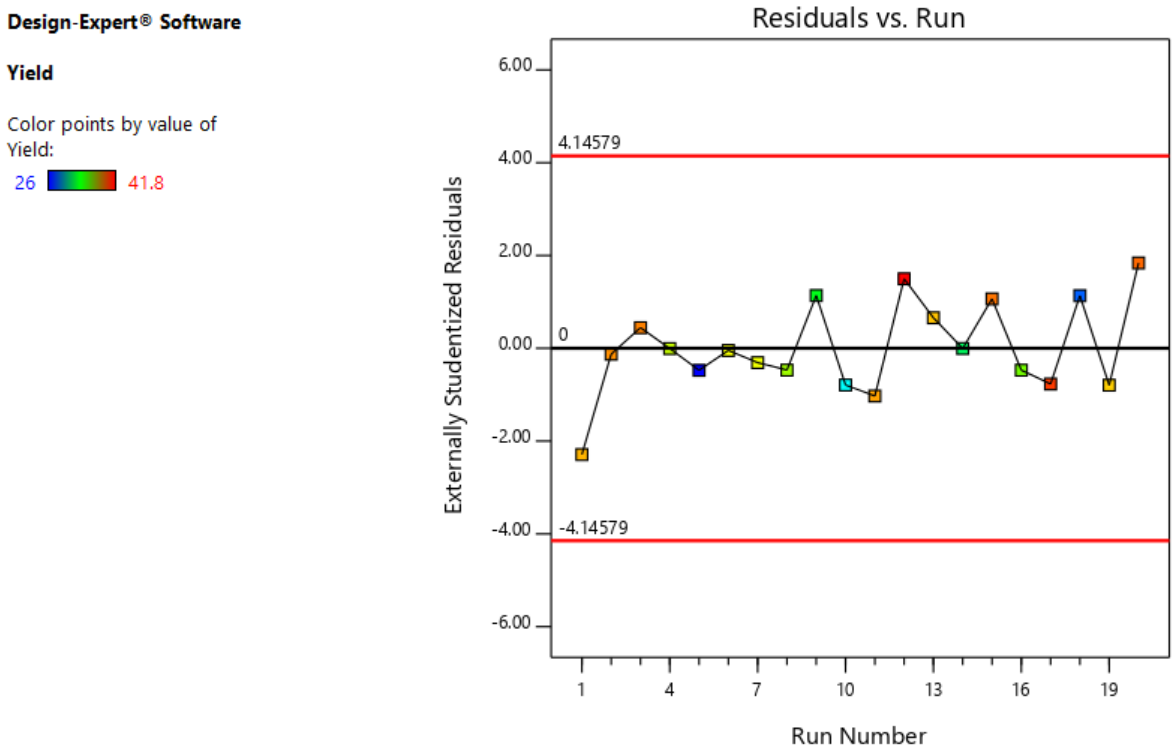

Figure C-2:Residual vs run plot

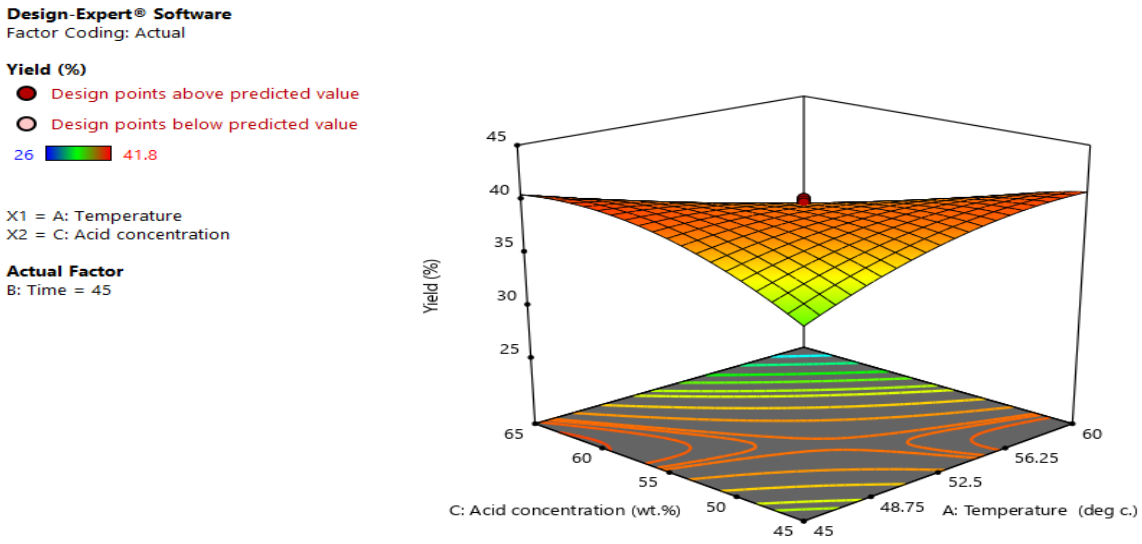

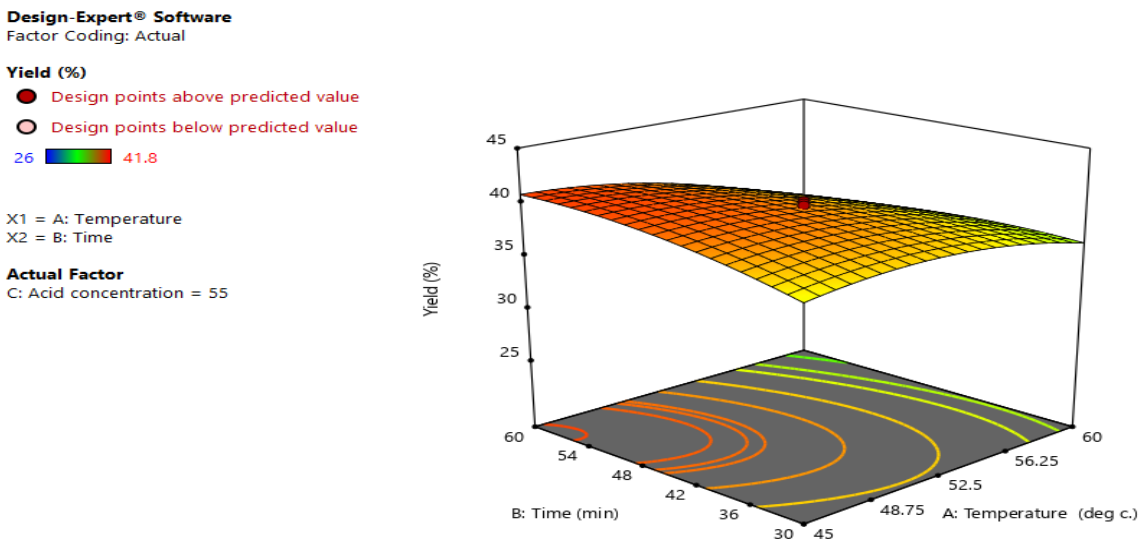

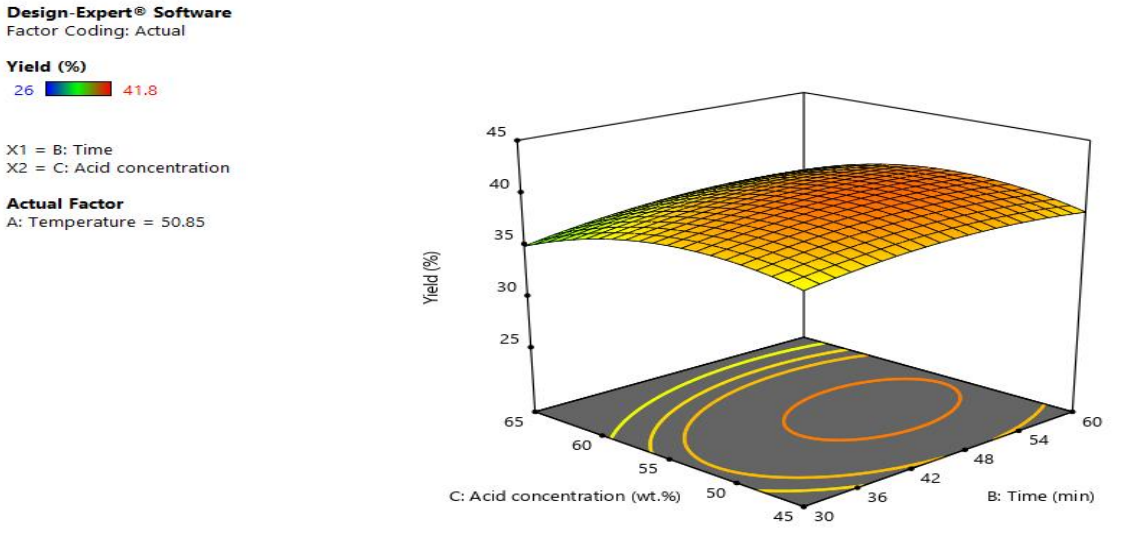

Figure C-3:Response surface plot interaction effect of parameters on the yield of CNCs

Table C-2: Solutions of numerical optimization with optimum process conditions and response

No.	Temperature	Time	Acid concentration	Yield	Desirability	
1	**45.000**	**59.896**	**61.663**	**41.740**	**0.996**	**Selected**
2	45.000	59.974	61.664	41.740	0.996	
3	45.000	59.832	61.649	41.740	0.996	
4	45.000	59.986	61.744	41.740	0.996	
5	45.000	59.656	61.663	41.740	0.996	
6	45.000	59.651	61.488	41.740	0.996	
7	45.000	59.512	61.486	41.739	0.996	
8	45.000	59.339	61.661	41.739	0.996	
9	45.000	59.394	61.475	41.739	0.996	
10	45.000	58.483	61.556	41.732	0.996	
11	45.000	59.999	60.754	41.723	0.995	
12	45.000	60.000	60.591	41.716	0.995	
13	45.000	57.006	61.717	41.706	0.994	
14	45.000	57.502	60.620	41.700	0.994	
15	45.000	56.728	62.187	41.691	0.993	
16	45.000	55.887	61.744	41.675	0.992	
17	45.000	55.361	61.133	41.657	0.991	
18	45.000	52.166	62.122	41.489	0.980	
19	45.000	52.790	58.659	41.391	0.974	
20	60.000	35.011	45.000	41.166	0.960	
21	60.000	34.857	45.000	41.166	0.960	
22	59.999	35.192	45.000	41.165	0.960	
23	60.000	35.354	45.000	41.165	0.960	
24	59.991	35.076	45.000	41.165	0.960	
25	60.000	34.418	45.000	41.164	0.960	
26	60.000	35.591	45.000	41.164	0.960	
27	60.000	36.003	45.000	41.161	0.960	
28	59.999	33.894	45.000	41.161	0.960	
29	59.999	36.168	45.000	41.160	0.959	
30	60.000	36.283	45.000	41.159	0.959	
31	60.000	36.687	45.000	41.154	0.959	

32	60.000	34.229	45.059	41.148	0.959
33	59.924	36.791	45.000	41.148	0.959
34	59.852	33.470	45.000	41.141	0.958
35	60.000	31.576	45.000	41.119	0.957
36	60.000	34.268	45.237	41.102	0.956
37	57.770	41.471	45.000	40.843	0.939

Appendix D: Images of an experiment during laboratory work

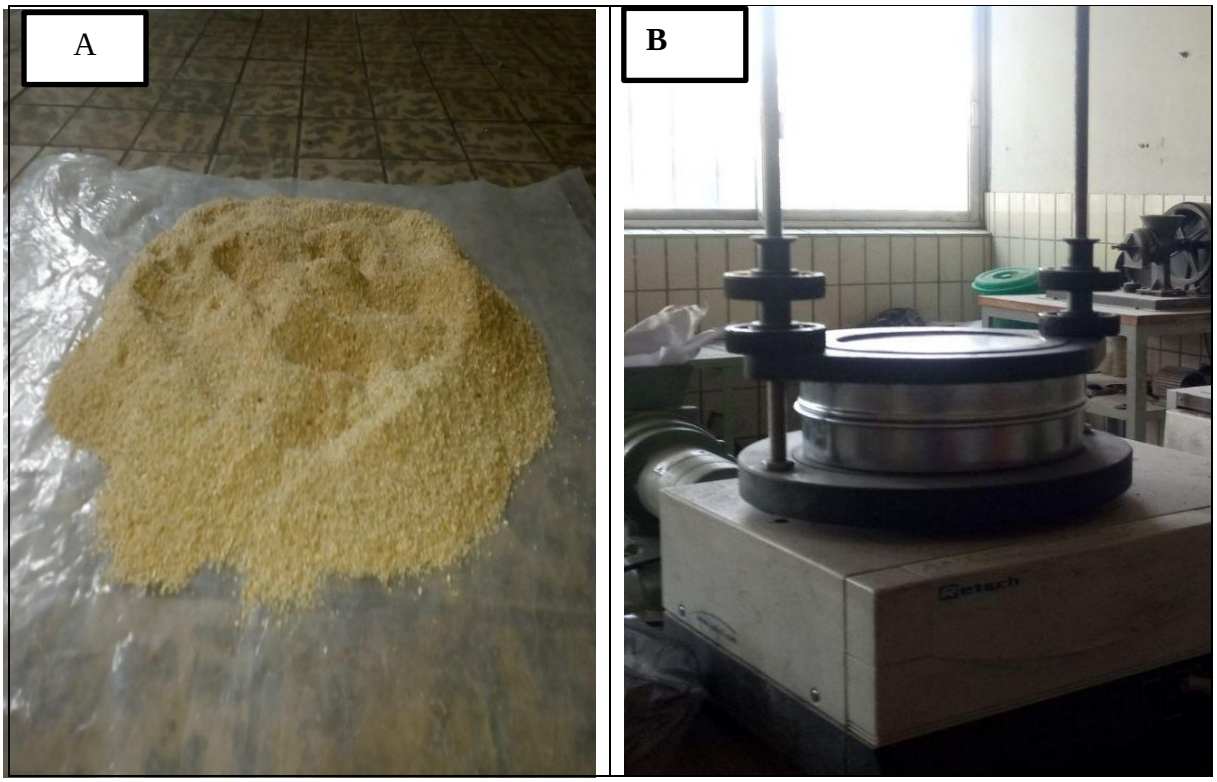

Figure D-1:(A) size reduced corncob and (B)sieve analysis of the corncob powder

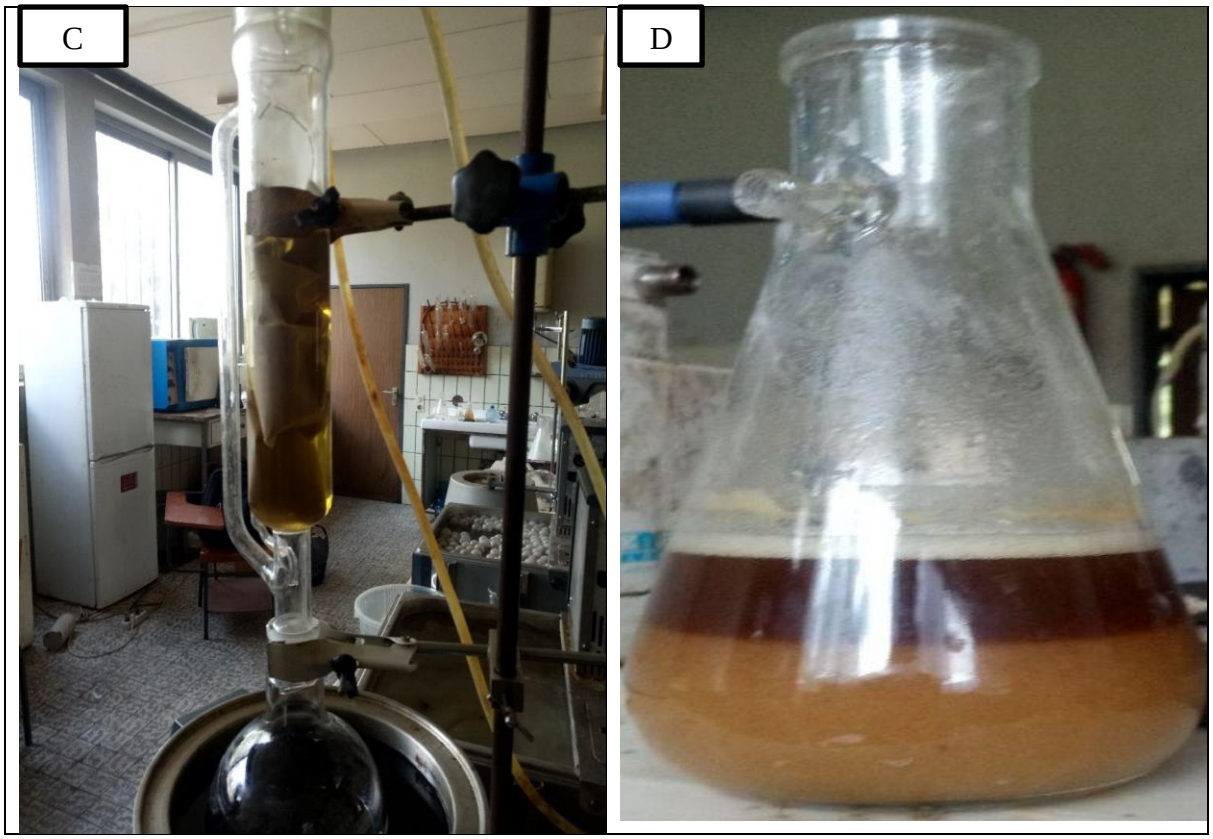

Figure D-2:(C) dewaxing of the sieved powder and (D)alkaline treated powder

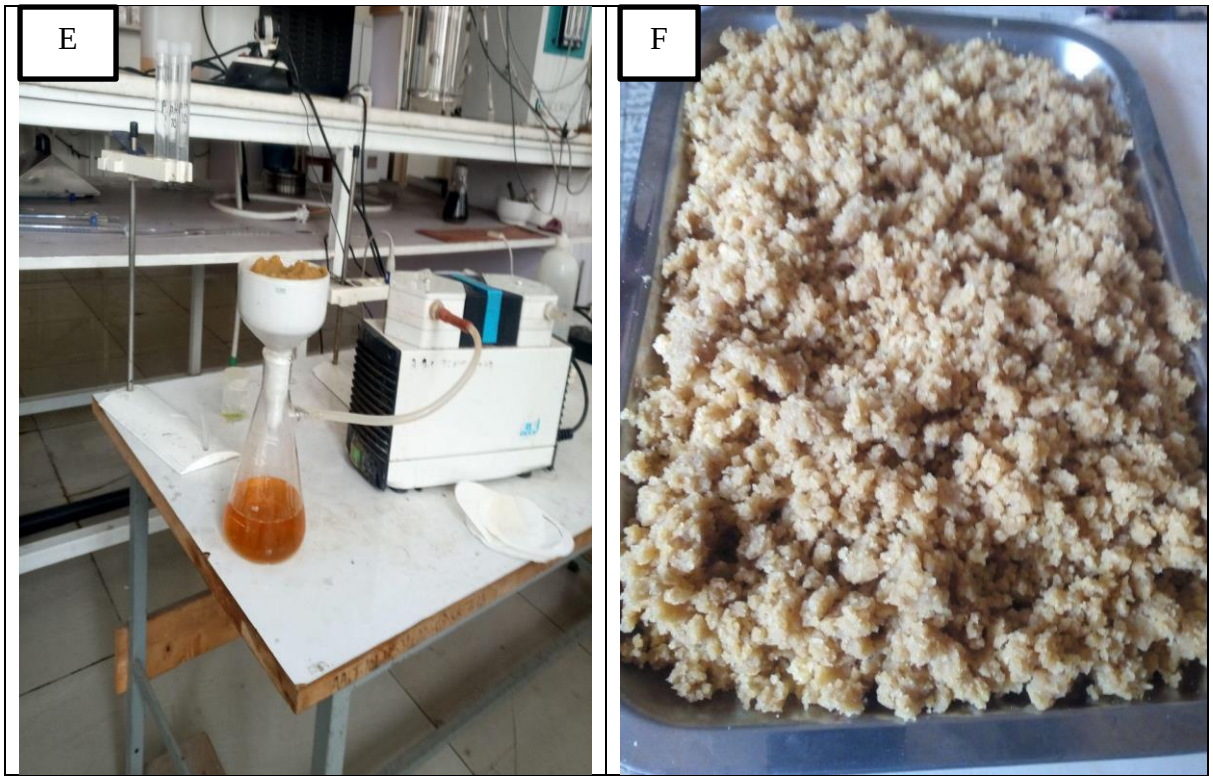

Figure D-3:(E)Vacuum filtered the suspension and (F)alkaline treated powder to dry

Figure D-4: (G)Bleached suspension and (H)bleached powder to dry

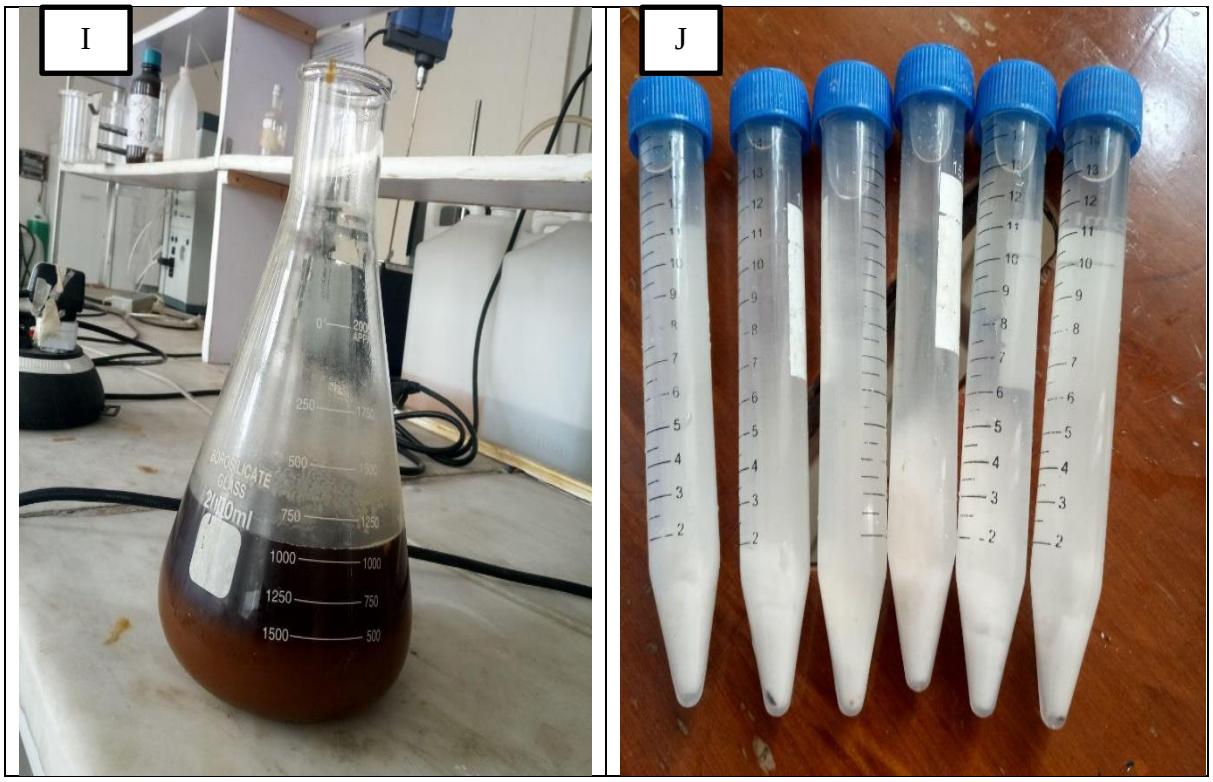

Figure D-5:(I) acid hydrolysis cellulose and (J) prepare a sample for centrifuging

Figure D-6:(K) centrifuge and (L)sonication of the centrifuged suspension